MOLECULAR LEVEL INVESTIGATIONS AND MATHEMATICAL MODELING OF IMMOBILIZED α-CHYMOTRYPSIN PREPARATION, UTILIZATION AND DEACTIVATION

Thesis by

Douglas S. Clark

In Partial Fulfillment of the Requirements

for the Degree of

Doctor of Philosophy

California Institute of Technology

Pasadena, California

1984

(Submitted December 7, 1983)

ACKNOWLEDGMENT

A successful Ph.D. project depends to a large extent on the proper juxtaposition of many people and events. This work was no exception, and the salient contributors to its completion merit special acknowledgment.

I would first like to express my deepest appreciation and admiration to Jay Bailey, whose consistent guidance and remarkable scientific acuity were, needless to say, indispensable to this research and to my own professional development. I also thank Sunney Chan and his group, especially Craig Martin, for their substantial and expert assistance with the EPR spectroscopy techniques that were central to this study. Special thanks are also deserved by April Olson for contributing her wizardly typing skills to the production of this thesis.

But my most heartfelt gratitude goes to my wife, Molly, for her unceasing support and understanding throughout my stay at Caltech. I have no doubt whatsoever that without her at my side this work would not have been possible.

ABSTRACT

Radiation-mediated grafting of polyacrolein onto polymethyl methacrylate microspheres activated the particles for chymotrypsin immobilization. Treatment of porous polystyrene/magnetite particles with polyacrolein produced very small enzyme loading enhancement and significantly increased substrate diffusional resistance. These results nonetheless demonstrate the feasibility of obtaining grafted materials and of utilizing this approach to improve the capacity of microspheres for protein immobilization.

Enzyme immobilization on a more conventional support material, CNBr-activated Sepharose 4B, was studied extensively. Specific activities and the amounts of active immobilized enzyme were determined for several different preparations of α-chymotrypsin immobilized on CNBr-activated Sepharose 4B. Electron paramagnetic resonance (EPR) spectroscopy of free and immobilized enzyme with a spin label coupled to the active site was used to probe the effects of different immobilization conditions on the immobilized enzyme active site configuration. Specific activity of active enzyme decreased and rotational correlation time of the spin label increased with increasing immobilized enzyme loading. Enzyme immobilized using an intermediate six-carbon spacer arm exhibited greater specific activity and spin label mobility than directly coupled enzyme. The observed activity changes due to immobilization were completely consistent with corresponding active site structure alterations revealed by EPR spectroscopy.

When EPR spectra were recorded in the presence of indole, direct evidence for the existence of two distinct forms of active

α-chymotrypsin immobilized on CNBr-activated Sepharose 4B was obtained. The indole EPR spectra of five different spin-labeled immobilized enzyme formulations were all resolved into the same two spectral components. Both subpopulation spectra were approximately identified experimentally, and the subpopulation exhibiting greatly restricted spin-label motion was shown also to be relatively inaccessible to solvent. Using overall specific activity data and subpopulation fractions from EPR spectral analysis, the specific activity of the more constricted immobilized enzyme active form was shown to be approximately fifteen times smaller than that of the other class of immobilized enzyme molecules with an indole EPR spectrum similar to that of chymotrypsin in solution. Variations in overall specific activity of formulations with different loadings and different supports result entirely from changes in the proportions of the same two subpopulations of immobilized enzyme molecules.

Deactivation in aliphatic alcohols of α-chymotrypsin and α-chymotrypsin-CNBr Sepharose 4B conjugates was also studied by several characterization methods. Active site titration measurements, which were used to determine the amount of catalytically active enzyme, revealed appreciable differences between the deactivation kinetics of free and immobilized chymotrypsin. In all cases for the immobilized enzyme, the kinetics of active enzyme disappearance differed significantly from first-order. Interestingly, the estimated intrinsic activity of immobilized chymotrypsin remaining active after different exposure times to 50% n-propanol solution increased somewhat as a result of exposure to alcohol. These findings were complemented

by direct information, provided by EPR spectroscopy, on the effects of alcohols on the active site configuration of spin-labeled chymotrypsin. EPR spectra of the free enzyme illustrated the appearance in different alcohol solutions of different enzyme forms with different active site structures. EPR experiments also showed that denaturation of immobilized chymotrypsin was accompanied by unfolding of the active site that followed similar multistep kinetics as the loss of active enzyme.

Further insight into the deactivation in 50% n-propanol of immobilized α-chymotrypsin was provided by analyses that focused on the behavior of the two distinct active forms of immobilized enzyme, designated here A and B, identified previously. Raw data provided by EPR spectroscopy clearly show that the relative quantities of active chymotrypsin-A and active chymotrypsin-B change as a result of exposure to alcohol, with the relative quantity of the B form increasing with time. These and additional results provide evidence that the distribution of A and B forms is a function of active enzyme loading but independent of the means used to obtain the loading. Different kinetic models in conjunction with experimental observations consistently indicate that the activity of enzyme form B, by far the more active enzyme form, does not change significantly during the initial 60 min. of catalyst deactivation but then decreases appreciably.

Finally, theoretical analyses of enzyme immobilization, more general in scope than the α-chymotrypsin work, were also performed. Enzymes are often immobilized on the internal surfaces of porous solid supports by immersing enzyme-free particles in a well-mixed solution

of enzyme. The ensuing impregnation process involves coupled transient mass transfer and surface attachment of enzyme. Mathematical models were employed to explore the influences of process parameters on the amount of enzyme loaded and the distribution of immobilized enzyme within the support particles. Nonuniform loading of the support occurs under some conditions, particularly when diffusion of unattached enzyme through the support is restricted by the large size of the enzyme relative to the accessible cross-sectional area of the support's pores. This is significant since the distribution of enzyme within the support particle influences the overall activity and stability of the immobilized enzyme catalyst. The models developed here may also be used to describe removal of reversibly immobilized enzyme during washing or utilization of the immobilized enzyme catalyst.

Table of Contents

INTRODUCTION

Immobilized enzymes, defined here as enzymes bound to or confined within a macroscopic support matrix, have been the focus of a great deal of research over the past two decades. Originally devised as model systems for membrane-bound enzymes in vivo, immobilized enzymes were quickly recognized for their potential as commercial catalysts. Since that time immobilized enzyme technology has grown rapidly and is now highlighted by successful applications of immobilized enzyme systems in large-scale processes, including isomerization of glucose with immobilized glucose isomerase and resolution of amino acids with immobilized aminoacylase. A comprehensive review of immobilized enzyme applications is not the objective of this work the interested reader should consult the monographs by Zaborsky[1] and Godfrey and Reichelt.[2] Although the current number of commercial applications for immobilized enzymes falls below initial expectations, the outlook for immobilized enzyme technology remains promising. In fact, with recognition that recombinant DNA technology and genetic engineering will soon enable naturally occurring enzymes and perhaps even "custom-made" enzymes to be produced more rapidly and more economically than ever before, current interest in immobilized enzyme catalysis is exceptionally high.

In many ways, however, enzyme immobilization and immobilized enzymes are very poorly understood. Despite prolonged research interest and despite the voluminous amount of published literature on various aspects of immobilized enzyme technology (protocols for immobilizing enzyme x on support y are particularly common), it is

still not possible to predict in advance the performance of an immobilized enzyme catalyst knowing the properties of the enzyme in solution and the immobilization method used. The expertise required to infer from such information the properties of an immobilized enzyme catalyst no doubt involves greater understanding of how the preparation and configuration of the catalyst's microstructure influence the apparent properties of the enzyme molecules, and of how the intrinsic properties; i.e., activity, selectivity, and stability, of the enzymes are affected by immobilization. The present work addresses these matters for selected model systems in order to obtain a greater fundamental understanding of enzyme immobilization and to establish guidelines and methodology for similar studies of additional systems by future investigators.

The format of this thesis eliminates the need for an elaborate and detailed introduction. The work is presented in three sections, each of which is comprised of chapters. Each chapter contains a separate introduction describing the motivation for part of the work and summarizing related studies.

The first section deals with intrinsic properties of immobilized α-chymotrypsin. Intrinsic properties include kinetic parameters and structural features of immobilized enzyme molecules determined under conditions where physicochemical events that disguise immobilized enzyme behavior; i.e., external and internal diffusion limitations, concentration and pH gradients, and so forth, are either absent or easily accounted for. This section also describes in detail the use of electron paramagnetic resonance (EPR) spectroscopy to study the configuration of immobilized enzyme active sites. More than any other

technique described, EPR spectroscopy has provided valuable insights at the molecular level into the structure and function of immobilized chymotrypsin, and warrants far greater attention in future studies of immobilized enzymes than it has received to date.

Section II applies the strategies and methods presented in Section I to examine deactivation in aliphatic alcohols of immobilized chymotrypsin preparations. Here again the level of understanding obtained significantly exceeds previous standards, and EPR spectroscopy has played an indispensable role. For the first time known to the author, deactivation of individual immobilized enzyme subpopulations has been studied and characterized, and in the process mechanisms that govern the overall behavior of immobilized enzyme catalysts in denaturing environments have been defined in considerable detail.

Finally, the third section addresses the theory of enzyme immobilization in porous materials. In order to immobilize enzymes in a controlled or predetermined fashion and formulate optimal catalysts that meet specific requirements, knowledge of how and why immobilization affects the intrinsic behavior of enzymes is essential. However, the overall activity of an immobilized enzyme catalyst often is a function of additional parameters, especially if the support is a porous matrix, which is often the case. For example, if very active enzymes are loaded uniformly throughout a porous support, conversion of substrate will be limited to the outer region of the catalyst and much of the attached protein will be wasted. It is therefore necessary for the enzyme engineer to be able to control the distribution of enzyme immobilized in a porous carrier, and it is to

this end that the mathematical models described in Section III are directed.

References

1. O. Zaborsky, Immobilized Enzymes (CRC, Cleveland OH, 1973).

2. T. Godfrey and J. Reichelt, Industrial Enzymology, The Application of Enzymes in Industry (Nature Press, New York NY, 1982).

PART I : INTRINSIC PROPERTIES OF IMMOBILIZED CHYMOTRYPSIN CATALYSTS

CHAPTER 1: ENZYME IMMOBILIZATION ON GRAFTED POLYMERIC MICROSPHERES

INTRODUCTION

Treatment of solids to render their exposed surfaces more suitable for enzyme and other biomolecule attachment is a strategy that dates from initial efforts to immobilize enzymes and prepare affinity adsorbents. Recently, this theme has been expanded by addition of a microscopic or molecular layer of carrier molecules to an insoluble core that serves as the mechanical carrier for the complex. Examples of this approach include the pellicular catalysts proposed and demonstrated by Horvath[1] and studied further by other investigators.[2-4] Also, several recent studies report grafting of various polymers onto other polymer carriers to formulate useful immobilization media with separately controlled and optimized bulk and surface properties.[5-7]

In this work, radiation-induced grafting of polyacrolein to various polymer microspheres, including magnetic carriers, is investigated. The purpose of this work is to explore the feasibility of obtaining such grafted materials and of utilizing this approach for improving the capacity of microspheres for protein immobilization.

METHODS

Radiation Grafting of Acrolein

Acrolein was grafted on polymeric spheres of various compositions and sized by means of ionizing rdiation. The radiation grafting resulted in hybrid spheres; i.e., small polyacrolein (PA) spheres on the surface of large spheres. The latter consisted of polystyrene or polymethyl methacrylate (PMMA). The size of the grafted PA spheres

depended on the amount of surfactant (sodium dodecyl sulfate) present in the reaction medium. An example of formation of hybrid spheres is as follows: Polymethyl methacrylate spheres of 10 μm diameter (50 mg) were suspended in distilled water (10 ml) containing freshly distilled acrolein (0.5 g) and sodium dodecyl sulfate (20 mg). The suspension was irradiated in a Co_γ source (0.2 Mr/hr) for 1/2 hour. For high density coverage the radiation was repeated several times. Preformed polymeric spheres with PA grafted on the surface were isolated by centrifugation (500xg for 10 min) and repeatedly washed with distilled water until the supernatant became clear. Transmission and scanning electron microscope studies of the surfaces of hybrid spheres revealed that PA microspheres grafted under these conditions were about 20-30 nm in diameter. For control experiments an equal amount of preformed spheres was irradiated in the absence of acrolein.

Preparation of Immobilized Enzymes

All enzyme immobilization reactions were performed at room temperature in 0.1 M $NaHCO_3$, 0.5 M in NaCl, pH 8.3.

Nonmagnetic Microspheres

5 ml of α-chymotrypsin (CT) solution (2 mg/ml) was added to a 15 ml Nalgene centrifuge tube containing a suspension of 105 mg polymer microspheres in 5 ml $NaHCO_3$ buffer. The reaction vessel was then rotated end-over-end on a Cole Parmer Heavy Duty Rotor for 3 hr. After this coupling reaction the reaction mixture was spun down for 10 min at speed 50 in an Adams Dynac centrifuge, and the enzyme

solution was decanted and replaced by 10 ml of coupling buffer. Following brief agitation on a Thermaline MaxiMix vortex mixer, the microspheres were again spun down in the centrifuge and the bicarbonate buffer decanted. This washing procedure was then repeated using 10 ml 0.1 M acetate buffer, 1 M NaCl, pH 5, after which Lowry's method[8] detected no residual enzyme in the supernatant. The final product was stored in 10 ml 0.1 M phosphate buffer, 1 M NaCl, pH 7.3, at 4°C.

Magnetic Microspheres

The immobilization and washing procedures were the same as above except that 2.5 ml enzyme solution (2 mg/ml) was added to a suspension of 50 mg microspheres in 2.5 ml buffer. The reaction time for samples K through N-1 was 3 hr. For N-2 the reaction time was 4 hr, and at 3 hr and 3.5 hr 1 mg $NaBH_7$ was added to the reaction mixture.

Determination of the Amount of Active Enzyme on the Support

The concentration of active immobilized α-chymotrypsin was determined by active site titration with MUTMAC. The procedure used for the nonmagnetic microspheres was identical to that described in Clark and Bailey,[9] while the magnetic microspheres required the following modifications: 200 µl of a well-stirred immobilized enzyme suspension (10.5 mg/ml) was added to a solution of MUTMAC in phosphate buffer. The reaction mixture was then shaken vigorously for 1 min and filtered through a Millipore Swinnex filter (0.3 µm cellulose ester filter), and the fluorescence of liberated product recorded. Controls were also run to determine the amounts of 4-methyl umbelliferone

adsorbed by the support materials, which for the magnetic microspheres proved to be significant (0.096-0.12 μmols/gm).

Determination of Immobilized Enzyme Activity

Activity measurements were carried out in a recirculation reactor of the type described elsewhere.[9] The nonmagnetic catalysts were assayed with 1 mM N-acetl-L-tyrosine ethyl ester (ATEE) in 0.1 M borate buffer, pH 8.6, at 39°C. The reaction rates of the magnetic catalysts were measured with 1 mM ATEE in 0.1 M phosphate buffer, 1 M NaCl, pH 7.3, at room temperature.

RESULTS

The general approach used here consists of grafting polyacrolein particles to larger polymer microspheres (1.2 μm, 6.5 μm, and 10.0 μm O.D.) to produce conjugate materials with reactive surfaces for enzyme immobilization. The polyacrolein particles contain surface aldehyde groups which react with the terminal α-amino group and/or exposed lysine residues on proteins. Depending on the pore structure of the support beads, two types of immobilized enzyme catalysts can be prepared. If the pores of the support polymer are smaller than the diameter of the polyacrolein particles, pellicular catalysts, with a thin coating of reactive material on top of an inert core, result from the grafting/enzyme-coupling sequence. Conversely, catalysts in which the polyacrolein-bound enzyme is distributed more uniformly throughout the support can be made by using polymer beads with larger pores. Both strategies have been employed in this work, the former using

nonmagnetic polymer supports and the latter using magnetic polymer beads.

Nonmagnetic Polymer Microspheres

Attempts were made to graft polyacrolein to polymethyl methacrylate (PMMA, diameter 1.2 μm and 6.5 μm), polystyrene (diameter 1.2 μm), and Sephadex G-25 microspheres (diameter ~ 20-80 μm, pore diameter ~ 40 Å). α-chymotrypsin (diameter ~ 40 A) was then coupled to each of the above polyacrolein-coated materials. Because polyacrolein-PMMA gave by far the largest activity per unit weight of solid, this system was chosen for further study.

Figure 1 shows SEM photographs (x20,000) of a 6.5 μm PMMA bead before and after treatment with polyacrolein. The pellet on the left has a relatively smooth surface, whereas the pellet on the right has extensive surface coverage of polyacrolein.

The effects of increasing exposure of PMMA beads to polyacrolein on the amounts of chymotrypsin immobilized are given in Table 1. These results illustrate that increasing the exposure period for polymer grafting increases the amount of enzyme that can be subsequently immobilized. The largest loading obtained, 1.1 mg active enzyme/g support, translates to an estimated total loading value of 1.8 mg total enzyme/g support, since active site titration of enzyme in solution revealed only 60% of the enzyme was active before immobilization. 1.8 mg/g is also the estimated monolayer coverage of a 25,000 dalton protein on a nonporous 6.5 μm sphere. These data indicate that the particle is completely saturated with immobilized

enzyme and that the immobilization process has not completely inactivated any of the chymotrypsin.

Porous Magnetic Materials

The applicability of the polyacrolein grafting technique to enzyme immobilization on porous magnetic material (polystyrene + magnetite) was investigated. Results given in Table 2 indicate that these particles adsorb enzyme without polyacrolein pretreatment, and that treatment with polyacrolein results in only modest increase in the amount of enzyme loaded (within experimental error). Unlike the PMMA spheres, the magnetic spheres have pores large enough for chymotrypsin and polyacrolein to penetrate. Higher enzyme loadings per unit weight of catalyst were thus possible with the magnetic beads than with the PMMA beads.

There are two particularly interesting results of Table 2. First, the enzyme loading after pretreatment with four thirty-minute exposures to polyacrolein (sample N-7) is lower than the loading after two thirty-minute exposures (M). This is possibly due to clogging of the magnetic material's pores by polyacrolein microspheres at longer exposure times, making the interior portion of the support particle less accessible to enzyme. This result indicates that there is an optimal pretreatment procedure to obtain the maximum enzyme loading. Second, treating the immobilized enzyme with $NaBH_4$ decreases the enzyme loading. Treatment with a mild reducing agent such as $NaBH_4$ should reduce, and stabilize, covalent bonds between lysine residues on the enzyme and aldehyde groups on the polyacrolein, i.e., Schiff's base linkages. Chymotrypsin removed from the support during this

process could well be enzyme that was only adsorbed, not covalently bound, to the surface.

Kinetic studies were conducted of preparation K, in which chymotrypsin is adsorbed on the polystyrene/magnetite microspheres, and immobilized chymotrypsin preparation M, in which the polymer microspheres were exposed to irradiation and acrolein prior to enzyme immobilization. The resulting data are plotted in Eadie-Hofstee form in Fig. 2. Kinetic data for the adsorbed chymotrypsin fall approximately on a straight line, from which the apparent kinetic parameters listed in Table 2 were evaluated. The data for chymotrypsin immobilized after polyacrolein pretreatment exhibit the curvature at small reaction rates expected for diffusion-limited systems. The portion of this data which is approximately described by a straight line, extrapolated by the dashed line for small v values, was used to evaluate the apparent kinetic parameters.

Using methods proposed previously by Kasche and Bergwall[10], the diffusion-influenced data for the covalently coupled system were used to estimate the effective diffusion coefficient for ATEE substrate in the chymotrypsin-acrolein-magnetic microsphere preparation. The resulting value, 5.6×10^{-7} $cm^2 s^{-1}$, is ten times smaller than the estimated diffusivity of substrate in solution (for comparison, the estimated[9] ATEE effective diffusivity in a chymotrypsin-Sepharose 4B conjugate is 3.8×10^{-6} cm^2/s). This finding is consistent with the earlier observation that total enzyme loading is reduced with prolonged exposure to polyacrolein for the porous, magnetite containing microsphere.

Acknowledgement: This work was supported by the Director's Discretionary Fund of the Jet Propulsion Laboratory.

REFERENCES

1. Horvath, C. Biochimica et Biophysica Acta 1974, **358**, 164-177

2. Horvath, C. and Engasser J. M. Ind. Eng. Chem. Fundam. 1973, **12**, 229-235

3. Lin, S. H. Chem. Eng. J. 1977, **14**, 129-136

4. Karanth, N. G. Chem. Eng. J. 1980, **19**, 167-169

5. D'Angiuro, L., Cremonesi, P., Mazzola, G., Focher, B., and Vecchio, G. Biotechnol. Bioeng. 1981, **22**, 2251-2272

6. D'Angiuro, L. and Cremonesi, P. Biotechnol. Bioeng. 1982, **24**, 207-216

7. Beddows, C., Gil, M. and Guthrie, J. Biotechnol. Bioeng. 1982, **24**, 1371-1387

8. Lowry, O. H., Rosebrough, N. J. , Farr, A. L. and Randall, R. J., J. Biol. Chem. 1951, **193** 265-275

9. Clark, D. S. and Bailey, J. E. Biotechnol. Bioeng. 1983, **25**, 1027-1047

10. Kasche, V. and Bergwall, M. in Insolubilized Enzymes (Salmona, M., Saranio, C., Garattini, S., eds) Raven, New York, pp.77-86, 1974

TABLE I

Results of Chymotrypsin Immobilization on PMMA
Activated by Varying Exposure to Polyacrolein Grafting

Polyacrolein exposure time of 6.5 μm PMMA	Active enzyme loading (μmol active CT/gm support)	Activity* $\left(\frac{\text{μmol ATEE}}{\text{s} \cdot \text{gm catalyst}}\right)$	Specific Activity* $\left(\frac{\text{μmol ATEE}}{\text{s} \cdot \text{μmol active enzyme}}\right)$
0 hr.	0	0	0
1/2 hr.	0.0219	0.35	16.0
2x1/2 hr.	0.0329	0.38	11.7
3x1/2 hr.	0.0432	0.67	15.5
4x1/2 hr.	0.0440	0.70	15.9

*1mM ATEE, 0.1 M borate buffer, pH 8.6, 39°C.

TABLE II

Immobilized Chymotrypsin Loadings and Apparent Kinetic Constants for Polystyrene-Magnetite Beads Grafted with Polyacrolein

Sample	Polyacrolein pretreatment	Active enzyme loading (μmol active CT/gm support)	v_{max} $\left(\frac{\mu mol\ ATEE}{gm\ catalyst\ s}\right)$	K_m (mM)
K	0 hr.	0.308 ± 0.016	47.4	1.3
L	1/2 hr.	0.336 ± 0.048		
M	2x1/2 hr.	0.376 ± 0.036	53.0	1.5
N-1	4x1/2 hr.	0.344 ± 0.024		
N-2	4x1/2 hr.*	0.284 ± 0.008		

*Enzyme immobilized on N-1 was reduced with $NaBH_4$.

Figure 1: Comparison of PMMA beads (6.5 μm diameter) before (top) and after (bottom) exposure to polyacrolein (4x1/2 hr., see Methods).

Figure 2: Eadie-Hofstee plot of kinetic data for chymotrypsin immobilized on polystyrene/magnetite microspheres with (Δ) and without (0) polyacrolein pretreatment.

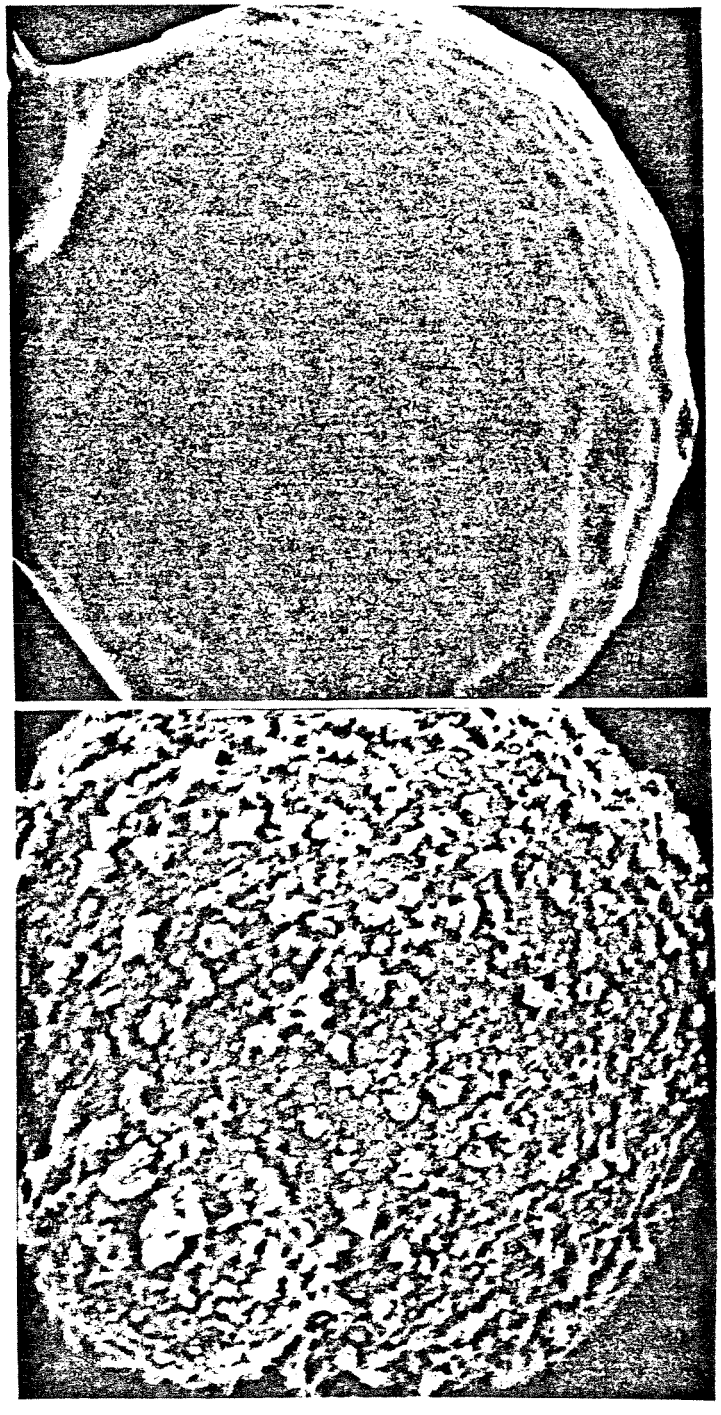

FIGURE 1

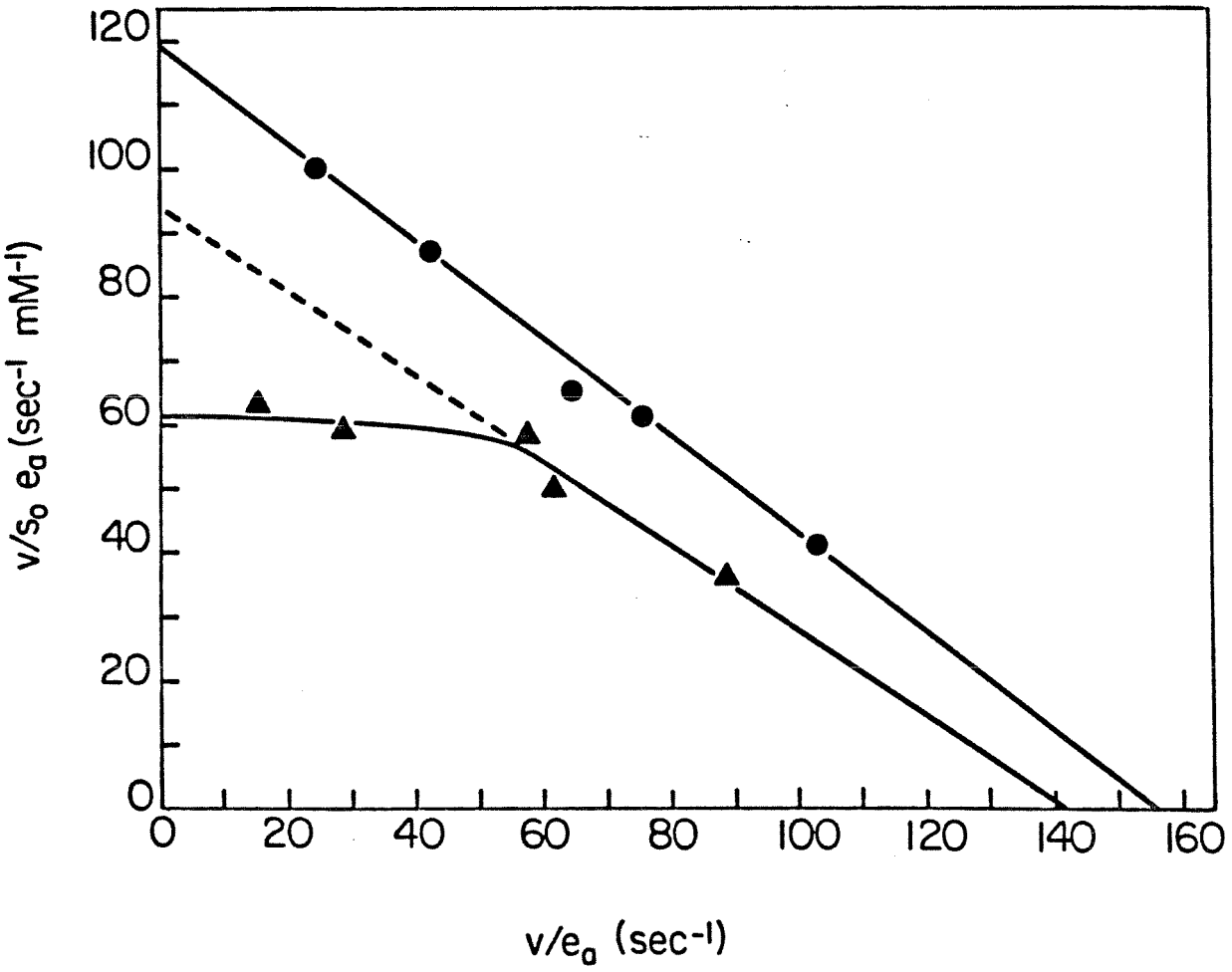
120
100
80
60
40
20
0
0
20
40
60
80
100
120
140
160
v/s$_o$ e$_a$ (sec^{-1} mM^{-1})
v/e$_a$ (sec^{-1})

FIGURE 2

CHAPTER 2 STRUCTURE FUNCTION RELATIONSHIPS IN IMMOBILIZED CHYMOTRYPSIN CATALYSIS

(The text of Chapter 2 consists of an article as it appears in Biotechnology and Bioengineering, 25, 1027, 1983.)

Structure-Function Relationships in Immobilized Chymotrypsin Catalysis

DOUGLAS S. CLARK and JAMES E. BAILEY, *Department of Chemical Engineering, California Institute of Technology, Pasadena, California 91125*

Summary

Specific activities and the amounts of active immobilized enzyme were determined for several different preparations of α-chymotrypsin immobilized on CNBr-activated Sepharose 4B. Electron paramagnetic resonance (EPR) spectroscopy of free and immobilized enzyme with a spin label coupled to the active site was used to probe the effects of different immobilization conditions on the immobilized enzyme active site configuration. Specific activity of active enzyme decreased and rotational correlation time of the spin label increased with increasing immobilized enzyme loading. Enzyme immobilized using an intermediate six-carbon spacer arm exhibited greater specific activity and spin label mobility than directly coupled enzyme. The observed activity changes due to immobilization were completely consistent with corresponding active site structure alterations revealed by EPR spectroscopy.

INTRODUCTION

The question of how immobilization can affect the physical and chemical properties of enzymes has received considerable attention in the past decade. Enhanced stability of enzymes to thermal denaturation upon immobilization has been reported in several cases,[1-4] and recently efforts have been made to understand further and optimize these effects by comparing the stabilities of enzymes immobilized by different methods to a wide variety of support materials.[5,6] In addition to studies of this nature, there are many articles, primarily theoretical, which describe possible influences of mass transfer of substrates and products on overall reaction rates of enzymes immobilized to solid supports. Graphical methods for extracting the intrinsic kinetic parameters of immobilized enzymes from diffusion-limited data have been outlined,[7,8] as well as solutions to the appropriate diffusion-reaction boundary value problems for various support geometries and reaction kinetics.[9-11]

Past works have not often addressed the fact that transport limitations and changes in the molecular properties of enzymes induced by immobilization can occur simultaneously and cause significant differences in the behavior of bound enzymes compared to enzyme characteristics in solution. In order to gain a greater understanding of how immobilized enzymes function and how enzymes are affected by the immobilization process, it is important to deter-

Biotechnology and Bioengineering, Vol. XXV, Pp. 1027-1047 (1983)
 CCC 0006-3592/83/041027-21$03.10

mine carefully intrinsic kinetics of immobilized enzymes and to probe more fully the influences of immobilization of enzyme structure and function. It is to these ends that this study is directed.

In this work the intrinsic activity and kinetic parameters of α-chymotrypsin (CT) covalently coupled to spherical Sepharose particles were determined. By varying the amount of enzyme present in the coupling solution, the enzyme loading of the particles was controlled to determine if the specific activity of the immobilized enzyme decreases as the protein content of the conjugate increases. This result was originally reported by Axén and Ernbach[12] and later by Koch-Schmit and Mosbach.[13] However, in the latter case the effects of increasing immobilized protein content and multipoint attachment were not clearly distinguished, and in neither case were diffusional limitations, which were found to be significant here under similar assay conditions, taken into account. Furthermore, in both of those studies the specific activity calculations were based on the total amount of bound protein instead of the total amount of active protein, which in the case of CT has been reported to be reduced by immobilization.[14] This research addresses all of these points.

Also undertaken was a comparison of the active site regions of enzyme conjugates of different specific activities. Direct physical methods are commonly used to study the structures of both crystalline and dissolved proteins but there are only a few examples of the application of such techniques to immobilized enzyme systems.[1,13,15-18] A spin-labeled sulfonyl fluoride developed by Wong et al.[19] has been employed to see if changes in the kinetic parameters of immobilized CT can be explained in terms of structural information provided by electron paramagnetic resonance (EPR) spectroscopy and the conformational dynamics exhibited by CT in its normal reaction sequence. Data which relate reduced activity to variations in the active site environments of immobilized CT preparations are reported. Finally, the effect of inserting a six-carbon spacer between the enzyme and the support surface was examined while taking into account the influence of transport limitations and protein loading on enzyme activity.

MATERIALS

The α-chymotrypsin (from bovine pancreas, three times recrystallized, salt-free), *N*-acetyl-L-tyrosine ethyl ester (ATEE), 4-methylumbelliferyl-*p*-trimethyl ammonium cinnamate chloride (MUTMAC), 1-ethyl-3-(3-dimethylaminopropyl) carbodiimide HCl, and fluorescein isothiocyanate isomer 1 (FITC) were obtained from Sigma. 6-aminocaproic acid, 2,2,6,6-tetramethyl-1-oxyl-4-aminopiperidine, *m*-fluorosulfonyl benzoyl chloride, and indole were purchased from Aldrich. Sepharose 4B preactivated with CNBr was a product of Pharmacia Fine Chemicals. Inorganic salts and all buffer solutions components were analytical grade reagents. Distilled water, deionized

by passage through two Research IonXchanger Model 2 columns supplied by Illinois Water Treatment Co., was used throughout.

METHODS

Preparation of Immobilized Enzymes

Covalent attachment to CNBr-Sepharose 4B

The α-chymotrypsin was covalently coupled to CNBr-Sepharose 4B as recommended by Pharmacia.[20] The freeze-dried gel (500 mg) was washed with 100 mL 1m*M* HCl. The activated gel was then transferred to a 25-mL scintillation vial and mixed with 5.0 mL 0.1*M* $NaHCO_3$ buffer solution, 0.5*M* in NaCl, containing the appropriate amount of enzyme. The weight/weight ratio of enzyme to gel was varied from 0.1 to 0.00125 to effect different active enzymne loadings. The reaction mixture was slowly rotated end-over-end on a Cole-Parmer Heavy Duty Rotor for two hours at room temperature. After completion of the coupling reaction, the conjugate was washed in a Millipore 13-mm ultrafiltration cell with three washing cycles. Each cycle consisted of a 6 mL/min wash at pH 5 (150 mL 0.1*M* acetate buffer containing 1*M* NaCl) followed by a similar wash at pH 8 (0.1*M* borate buffer containing 1*M* NaCl). The final product was stored overnight in mildly alkaline 0.1*M* phosphate buffer (pH 7.4) to hydrolyze any residual coupling groups on the gel surface, then transferred to acetate buffer, 1*M* NaCl, pH 5, for storage at 4°C.

Covalent coupling to ω-aminocaproyl-Sepharose 4B

Acid-washed CNBr Sepharose 4B (500 mg) was rotated end-over-end in a 1*M* solution of 6-aminocaproic acid in 0.1*M* $NaHCO_3$, 0.5*M* NaCl, pH 8, for three hours at room temperature. After overnight storage in the alkaline ligand solution to ensure deactivation of any remaining coupling groups, the ω-amino-caproyl-Sepharose (CNBr-6C) was washed with 200 mL coupling buffer and added to 5 mL H_2O (adjusted to pH 4.75 with HCl). Ninety-six milligrams 1-ethyl-3-(3-dimethyl aminopropyl) carbodiimide hydrochloride was then slowly added to give a final carbodiimide concentration of 0.1*M*. After 30 min of end-over-end rotation, the gel was washed quickly (1–2 min) with ice cold water, then rotated as above in 5 mL α-CT solution (10 mg enzyme/mL), pH 4.75, for 12 h at room temperature. After completion of the coupling reaction the conjugate was washed as previously described, then stored in acetate buffer at 4°C.

Determination of the Amount of Functional Enzyme Bound to the Support Matrix

The concentration of active immobilized enzyme was determined by active site titration with MUTMAC. Fluorescence measurements were carried out

in a Turner Model 430 Spectrofluorometer in 1-cm cuvettes. The samples were illuminated at 356 nm, and emission was recorded at 451 nm. The titration procedure reported by Gabel[14] was modified slightly by adding 250 μL 0.2m*M* MUTMAC solution in water to 3.0 mL potassium phosphate buffer (pH 7.3, 1*M* NaCl) to establish a baseline. 100–300 μL of a well-stirred immobilized enzyme suspension (20 mg/mL) was then added and the fluorescence of liberated 4-methylumbelliferone followed with time. At least two different amounts of conjugate were used for each titration, and the average difference in each determination was found to be ±4.4%. The amount of 4-methylumbelliferone liberated was independent of the concentration of MUTMAC and of pH in the range tested (7.3–8.5).

Determination of Enzyme Activity

Large (R = 60 μm) particles

The reaction rate v_{obs} of immobilized α-CT with ATEE was determined in a differential recirculation reactor of the type described by Ford et al.[21] equipped with a 10-cm water jacket for temperature control. In a typical assay, 5–10 mg of immobilized enzyme was retained in a Millipore 13-mm ultrafiltration cell by a stainless-steel screen and a cellulose ester filter with mean pore diameters of 8 μm. The substrate solution (1m*M* ATEE in 0.1*M* phosphate buffer, pH 7.3, 1*M* NaCl) was passed through the packed-bed reactor into an open reservoir and recirculated by a Cole-Parmer Masterflex variable speed pump through a 1-cm constant temperature flow-through cuvette where the change in substrate absorbance was recorded at 238 nm with a Bausch & Lomb Spectronic 21 UV-Visible spectrophotometer. The total volume of substrate solution ranged from 6.5 to 8.5 mL. The amount of immobilized enzyme used in the reactor ensured that the conversion never exceed 2% per pass, and the recirculation flow rate (usually 20 mL/min) was high enough to eliminate film diffusion resistance. Three different amounts of immobilized enzyme were used for each rate determination and the standard deviation of the results never exceeded 10%.

Small (R = 10 μm) particles

The large (R = 60 μm) support beads of a well-stirred immobilized enzyme suspension were ground up in a Thomas Teflon pestle tissue grinder, size B, packed in ice to eliminate heat effects. The pestle rod was inserted into the chuck of a Fisher Dyna-Mix mechanical stirrer and rotated in the grinding vessel at high speed for fifteen minutes to achieve adequate particle size reduction. The reaction rates of the small particles were determined as described above except that cellulose ester filters with smaller pore diameters (1.2 μm) were required to retain the catalyst in the reactor bed, and lower recirculation flow rates (6–15 mL/min) had to be employed in some cases.

Preparation of Spin-labeled Enzyme Derivatives and EPR Measurements

The procedures described by Wong et al.[19] were employed to prepare the spin-label *m*-IV, and to spin-label α-CT in solution. One hundred milligrams of the immobilized enzyme was spin-labeled at room temperature in 2-mL phosphate buffer, pH 7.3, containing a fivefold molar excess of an acetonitrile solution of *m*-IV. After 30 min a similar concentration of spin label was added and the reaction continued with gentle stirring for 30 min more. The final organic solvent concentration in the mixture was ca. 9% (v/v), as in the case of the free-enzyme labeling procedure referenced above. After completion of the labeling reaction the gel was washed exhaustively with 1m*M* acetic acid to remove excess spin label. A typical washing procedure consisted of a rinse with 200-mL acetic acid, followed by washes with 250 mL acetic acid in a recirculation system (6 mL/min) for successive 4-, 12-, and 2-h periods. The appropriate controls showed that no spin label remained adsorbed on the surfaces of the supports used in this study after such a treatment. The gel was then transferred via a syringe to a 1.5 × 90 mm capilary tube for immediate EPR analysis. For an indole experiment, the gel was rinsed briefly with a 12m*M* solution of indole in 1m*M* CH_3CO_2H before the spectrum was taken. The EPR spectra were recorded at the X band using a Varian E-Line Century Series EPR Spectrometer interfaced to a Digital Equipment Corp. PDP-8/A minicomputer.

Visualization of Internal Enzyme Distribution

The α-CT was coupled to CNBr-Sepharose 4B [0.1 (w/w) enzyme to gel ratio] and the product washed as described above. Five-hundred milligrams of the conjugate containing ca. 0.64 μmol active immobilized CT was then reacted at room temperature for 12 h with a tenfold molar excess of FITC dissolved in 20 mL 0.1*M* $NaHCO_3$, 0.5*M* NaCl, pH 8.5. The gel was then rinsed with 200 mL coupling buffer and washed in a recirculation system as follows: 2 × 200 mL coupling buffer for 2 h, 200 ml ethanol for 1 h, and 200 mL *t*-butanol for 2 h. The gel was then embedded in a 1 × 2 × 1 in. block of melted paraffin encased in aluminum foil, and stored at 4°C overnight. After solidifying, the block was cut into 10 μm thick slices with a microtome, then viewed with an Olympus BHB microscope equipped with a 100-W incident fluorescence illuminator. The sample was illuminated through an FITC barrier filter and viewed at wavelengths greater than 515 nm. Similar methods have been employed for examination of entire immobilized enzyme particles.[22]

INTRINSIC KINETICS STUDIES

Because of mass transport resistances, the measured overall kinetic properties of an immobilized enzyme catalyst pellet may differ from the true kinetics of the immobilized enzyme.[7,8,22,23] The latter, called here intrinsic

kinetics, characterizes the local relationship between catalytic activity of the enzyme and the substrate concentration in the enzyme's immediate environment. It is important to determine intrinsic kinetic properties for several reasons. First, these reflect directly the effects of immobilization upon catalytic activity of the enzyme. Also, once the intrinsic kinetics are known, the effects on the overall reaction rate of changes in external substrate concentration, use of different catalyst particle sizes, and changes in flow field around the particle may be calculated with some confidence.

One way to identify the existence of mass transport effects on measured rates is nonlinearity in Eadie-Hofstee or Lineweaver-Burk plots.[7,24-26] As shown in Figure 1, kinetic data for immobilized CT obtained in this study clearly manifests such behavior. Intrinsic kinetic data may be determined in such cases by reducing the catalyst particle size sufficiently. A series of experiments was conducted with Sepharose particles after different degrees of grinding until the observed reaction rate was independent of particle size.

Artifacts can arise in use of this procedure if the distribution of enzyme within the porous particles is spatially nonuniform. Direct justification of immobilized enzyme spatial uniformity was obtained by photographing, under fluorescent light, thin (10 μm) slices of CNBr-Sepharose to which FITC-labeled CT was attached. This method reveals directly the approximate distribution of immobilized enzyme within the porous support. The enzyme functional groups most likely to react with the carboimidoesters of the sup-

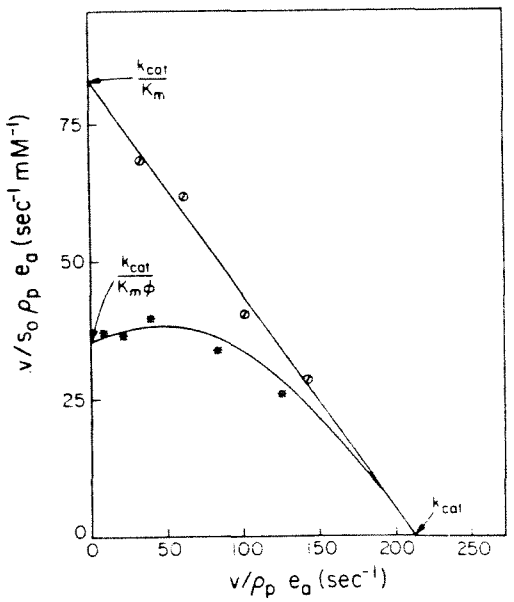

Fig. 1. Experimental determination of K_m, k_{cat}, and ϕ: (•) large catalyst particles and (○) small catalyst particles).

TABLE I
Intrinsic Kinetic Properties of Chymotrypsin in Solution and Immobilized in Sepharose 4B

Sample	$\left(\frac{q_E}{\frac{\mu\text{mol ATEE}}{\mu\text{mol active CT s}}}\right)$	K_m (mM)	k_{cat} (s^{-1})	k_f (mM^{-1} s^{-1})
Free CT	163 ± 6.2	0.73 ± 0.03	311 ± 17	426 ± 41
CNBr-1	115 ± 12	...	...	...
CNBr-6C	68.7 ± 9.3	2.6 ± 0.5	213 ± 29	82 ± 27
CNBr-5	31.0 ± 3.2	1.7 ± 0.07	82 ± 5	48 ± 4.9

port surface are also among those most likely to complex with the FITC, so conceivably the loading distribution of FITC-labeled CT may differ from that of unlabeled CT. Consequently, the CT was labeled after the immobilization was complete in order to preserve the enzyme's full complement of potential coupling groups during its reaction with the support. Control experiments with enzyme-free support demonstrated that nonspecific labeling of the support by FITC does not occur. All labeled immobilized enzyme sections produced uniform fluorescence, confirming uniform distribution of immobilized CT throughout the porous Sepharose particles.

Intrinsic kinetic parameters determined using ground particles are listed in Table 1 along with kinetic parameters for the enzyme in solution. These results clearly show that the intrinsic specific activity of *active* enzyme (recall that the amount of active enzyme was determined in separate active site titration experiments) decreases upon immobilization. This decrease is less when a spacer arm is used between the solid and the immobilized enzyme. Probes of the molecular basis for these results will be described below.

Experiments with these ground particles were inconvenient. The small particle size of the ground particles made it difficult to achieve sufficiently high flow rates through the packed bed to eliminate external mass transfer resistances; clogging of the filter supporting the catalyst bed was a frequent problem. As a result, an alternate approach for determination of intrinsic activities of the immobilized enzyme was applied for these and other catalyst preparations.

Using the mathematical description of simultaneous diffusion and reaction within an immobilized enzyme pellet, methods have been proposed for estimating intrinsic activities from overall kinetic data.[27-29] While the equations involved are well known, they will be summarized briefly here so that the assumptions and parameters involved are explicitly displayed. Since CT in solution with ATEE substrate exhibits Michaelis-Menten kinetics, it will be assumed here that the same form applies for immobilized CT so that the rate v per unit volume of catalyst (μmol ATEE cm^{-3} s^{-1}) is given by

$$v(s) = \frac{v_{max}s}{K_m + s} \tag{1}$$

The maximum velocity parameter v_{max} may be expressed as the product of the active enzyme loading e_a (μmol active CT/g Sepharose), the particle density ρ_p (g Sepharose/cm^3 Sepharose), and the active enzyme specific activity q_E (μmol ATEE s^{-1} μmol active CT^{-1}):

$$v_{max} = e_a \rho_p q_E. \tag{2}$$

Obviously, the support used and the immobilization method can influence e_a and thus v_{max}. However, data presented in Table I clearly show that immobilization can also alter the intrinsic specific activity of active enzyme q_E and the intrinsic Michaelis constant K_m of the immobilized enzyme.

The dimensionless steady-state material balance of a single rate-limiting substrate in a spherical particle of radius R is given by

$$\frac{d^2\bar{s}}{d\bar{r}^2} + \frac{2}{\bar{r}}\frac{d\bar{s}}{d\bar{r}} = \frac{vR^2}{D_{eff}s_0} = \frac{9\phi^2\bar{s}}{1 + \beta\bar{s}} \tag{3}$$

where $\bar{s}$, $\bar{r}$, and β are defined by

$$\bar{s} = s/s_0 \qquad \bar{r} = r/R \qquad \beta = s_0/K_m \tag{4}$$

s_0 is the substrate concentration in the bulk liquid surrounding the sphere, and the Thiele modulus ϕ is defined by

$$\phi = \frac{R}{3}\left(\frac{v_{max}}{K_m D_{eff}}\right)^{1/2} \tag{5}$$

As mentioned in the Methods section, external film diffusion does not significantly influence the observed reaction rates under the conditions of these experiments so that appropriate boundary conditions for eq. (3) are:

$$\bar{s}|_{\bar{r}=1} = 1; \qquad \left.\frac{d\bar{s}}{d\bar{r}}\right|_{\bar{r}=0} = 0 \tag{6}$$

The observed overall reaction rate v_{obs} per unit volume of immobilized enzyme is given by

$$v_{obs} = 3\int_0^1 \bar{r}^2 \frac{v_{max}\bar{s}(\bar{r})}{\bar{s}(\bar{r}) + \beta^{-1}}\, d\bar{r} \tag{7}$$

This rate is traditionally presented in dimensionless terms using the effectiveness factor η defined by

$$\eta \triangleq \frac{\text{(observed rate)}}{\text{(rate evaluated under bulk fluid conditions)}} = \frac{v_{obs}}{v(s_o)} \tag{8}$$

Explicit relationships for overall rates in terms of Michaelis-Menten intrinsic kinetic parameters are provided for slab geometry by the correlations of Atkinson and Davies[30]:

$$\eta(\phi,\beta) \triangleq \begin{cases} 1 - \dfrac{\tanh\phi}{\phi}\left[\dfrac{1/\eta_D}{\tanh(1/\eta_D)} - 1\right]; & \dfrac{1}{\eta_D} \le 1 \\ \eta_D - \dfrac{\tanh\phi}{\phi}\left[\dfrac{1}{\tanh(1/\eta_D)} - 1\right]; & \dfrac{1}{\eta_D} > 1 \end{cases} \tag{9}$$

where

$$\eta_D = \sqrt{2}\left(\frac{1+\beta}{\phi\beta}\right)[\beta - \ln(1+\beta)]^{1/2}. \tag{10}$$

Since effectiveness factor/Thiele modulus relationships are known to be quite insensitive to particle geometry provided that appropriate definitions of ϕ are employed,[9,10] eqs. (9) and (10) will closely approximate the exact relationships for spherical particles.

It is appropriate at this point to review the following assumptions that have been made in the preceding treatment of internal diffusion effects on the overall rate of reaction within the particles: 1) the immobilized enzyme is uniformly distributed throughout the particle, 2) the transport of substrate through the support is described by a Fick's law form relating the diffusive flux to the substrate concentration gradient, and the effective diffusivity D_{eff} of substrate in the pores of the support is a constant, 3) the reaction occurs at uniform temperature and pH throughout the catalyst pellet, and 4) pressure and electrostatic effects are negligible. The hydrolysis of ATEE by immobilized chymotrypsin in an aqueous solution of high buffering capacity and high ionic strength makes assumptions 3 and 4 reasonable, and immobilized enzyme spatial distribution visualizations mentioned earlier confirm assumption 1 for this immobilized enzyme system.

Consistency of assumption 2 and indeed the complete mathematical modeling framework given above can be demonstrated by comparing calculated and measured quantities for several different reaction conditions. Such comparisons have been undertaken previously, confirming the suitability of the diffusion-reaction model above for relating intrinsic and overall kinetic properties of those immobilized enzyme catalysts.[31,32] Especially noteworthy in this regard are the studies of Atkinson et al.[31] in which the centerline pH was also measured and shown to be consistent with model simulations. The success of the diffusion-reaction model for interpreting experimental data in this study will be considered next.

Using eqs. (3), (5), and (8), an independent equation may be derived relating η, ϕ, β, and the observable modulus Φ:

$$\eta(\phi, \beta, \Phi) = \frac{\Phi(1+\beta)}{\phi^2} \tag{11}$$

The observable modulus Φ, defined for spherical pellet geometry as

$$\Phi \triangleq \frac{v_{obs}}{D_{eff} s_0} \left(\frac{R}{3}\right)^2, \tag{12}$$

is so named because it contains only the measured overall rate and not intrinsic rate parameters.

Equations (9)-(12) provide the basis for estimating intrinsic immobilized enzyme activity based upon overall rate measurements: after estimating D_{eff}, evaluate Φ using the known R and measured s_0 and v_{obs} values. It is known that η is much more sensitive to a ϕ value than to a β value.[33] Consequently, assume a reasonable β value by use of a K_m value in the general range given for free and immobilized CT in Table I. Substitute this β value in eqs. (9) and (11) and the Φ value in eq. (11) and equate the results, giving a single equation that can be solved for ϕ numerically. Then, evaluate η using eq. (11), and determine the intrinsic rate at the bulk substrate concentration using eq. (8). Combining this with active site titration results allows evaluation of the active immobilized enzyme specific activity q_e at the bulk fluid substrate concentration.

An essential element of the above procedure is determination of the parameter D_{eff}. The value of D_{eff} was estimated using eq. (5) and the value of ϕ obtained for one immobilized CT preparation from the intercepts of the Eadie-Hofstee plots in Figure 1.[8] From these data a value of 3.8×10^{-6} cm^2/s for the effective diffusivity of ATEE in Sepharose 4B was obtained. This value was employed for intrinsic activity estimates of all the immobilized CT catalysts considered in this work.

For comparison, the bulk diffusivity of ATEE in aqueous solution was determined from an empirical modification of Stoke's equation based on the data reported by Longsworth.[34] The relationship given by Longsworth in his report:

$$D_s\,(cm^2/s) \times 10^6 = 24.182/(V^{1/3} - 1.280), \tag{13}$$

where V is the molal volume (cm^3/mol), represents with an average deviation of 2% the data obtained for various peptides and amino acids, but does not apply well to aromatic and heterocyclic amino acids. However, the following modified expression

$$D_s\,(cm^2/s) \times 10^6 = 25.414/(V^{1/3} - 1.364) \tag{14}$$

fits Longsworth's experimental diffusivities of amino acids of this type with an average deviation of 1.4%, and gives a diffusion coefficient for tyrosine of 7.03×10^{-6} cm^2/s.

The apparent molal volume of ATEE was calculated from that of tyrosine (123.6 cm^3/mol[35]) by making the appropriate corrections for additional atoms and the absence of electrostriction.[35] The diffusivity of ATEE thus calculated by eq. (14) is 5.7×10^{-6} cm^2/s. The use of this value presupposes that the diffusion coefficient is relatively insensitive to moderate changes in

the amino acid and NaCl concentrations of the bulk solution, an assumption supported by the results of Sherrill and Albright.[36]

Combining this result with the estimated value of D_{eff} yields a ratio for the diffusion coefficient of ATEE in Sepharose 4B to that in aqueous solution of 0.67. This ratio lies in the range 0.6-0.7 obtained by Horowitz and Fenichel[37] for the diffusion of molecules of molecular weight less than 100 in Sephadex G-34, and compares favorably with the data reported by Nakanishi et al.[38] for the diffusion of saccharides and amino acids in dextran gels of similar gel concentration as Sepharose 4B.

The results of intrinsic activity determinations by the above method for all of the immobilized enzyme preparations considered in this study are listed in Table II. Since Michaelis constants (i.e., β values) were not known for some of these catalysts, intrinsic activities were calculated for different K_m values spanning the range indicated in Table I. As already noted, the activity estimates are not very sensitive to the K_m value employed in the procedure. Intrinsic activities given in Table II estimated from diffusion-influenced data (note all of the estimated effectiveness factors are less than unity) agree reasonably well with the direct activity measurements for three preparations listed in Table I. This supports the applicability of the diffusion-reaction model to these catalysts and the suitability of the estimated D_{eff} for ATEE.

The values listed in Table II indicate a clear sequence of specific intrinsic activities for the catalysts CNBr-1 through CNBr-5 in which enzyme is immobilized directly to the Sepharose by CNBr-mediated attachment. Thus, the specific intrinsic activity of the immobilized CT decreases as the protein content of the conjugate increases. Also of interest is the higher activity of the

TABLE II
Estimated Intrinsic Specific Activities and Diffusion-Reaction Parameters for Different Immobilized Chymotrypsin Catalysts

Sample	e_u (μmol active CT/g)	Φ	η		q_E ($\frac{\mu\text{mol ATEE}}{\mu\text{mol active CT} \cdot \text{s}}$)	
			K_m		K_m	
			1.7	0.73	1.7	0.73
CNBr-1	0.0105 ± 0.000283	0.45	0.89	0.91	113	111
CNBr-2	0.0525 ± 0.00395	1.4	0.66	0.73	94.0	85.7
CNBr-3	0.192 ± 0.00529	2.1	0.52	0.57	49.2	44.8
CNBr-4	0.541 ± 0.00850	3.3	0.35	0.38	41.2	37.2
CNBr-5	1.27 ± 0.09610	4.5	0.26	0.28	32.2	29.0
-			2.6	0.73	2.6	0.73
CNBr-6C	0.184 ± 0.00772	2.6	0.42	0.48	88.7	77.3

preparation with spacer arm compared to a directly coupled immobilized enzyme catalyst at similar enzyme loading. An investigation of how the activity differences of these samples may be related to variations in their active site environments is described in the next section.

EPR STUDIES OF IMMOBILIZED ENZYME ACTIVE-SITE ENVIRONMENT

While most physical-chemical techniques for studying the structure of proteins (x-ray diffraction, circular dichroism, UV absorption) are not applicable to the study of enzymes attached to insoluble supports, EPR spectroscopy exhibits enormous potential in this area. Unlike optical techniques which require a transparent solution, EPR spectroscopy can be used equally well with optically transparent or opaque samples, and is not limited to enzymes immobilized on the external surface of a carrier. The "spin-labeling" technique consists of attaching a small paramagnetic molecule (the label), generally a stable nitroxide, to a particular region of the protein to obtain information on the surrounding environment. The EPR spectrum reflects the environment of the nitroxide radical. The method is extremely sensitive and can be used when only a small amount of labeling sites are available. If the spin-labeled protein is immobilized, the EPR spectrum is a composite of interactions among the nitroxide ring, the protein, and the support surface. Despite these advantageous characteristics, with the exception of a few limited cases (see, for example, refs. 15-17), EPR spectroscopy has been virtually ignored as a tool for studying immobilized enzymes.

Berliner et al.[15] were the first to spin-label an immobilized enzyme and compare the spectral results with those of the enzyme in solution. They found in their study of trypsin immobilized on porous glass that the EPR spectrum of the immobilized enzyme's active site region was the same regardless of whether the enzyme was labeled before immobilization or after immobilization. Subtle differences between the spectra of the free and immobilized enzymes were observed, but these were attributed to the elimination of the enzyme's rotational movement upon immobilization. No activity data were presented, and possible effects of the immobilization process on the active site configuration were not considered.

Dimicoli et al.[16] have used a spin-labeled phosphophonofluorodate to examine the active site of porcine pancreatic elastase crosslinked via glutaraldehyde to polyacrylamide beads. The EPR spectra of free and immobilized elastase spin-labeled at serine 195 were measured at various pH and temperature values. The lineshape, pH dependence, and temperature dependence of the EPR signals were similar for the free and immobilized spin-labeled proteins. The ability of Cu^{2+}, a known noncompetitive inhibitor of elastase, to bind in the active site region and quench the EPR signal was also compared for the free and immobilized enzyme. The kinetics of immobilized elastase inhibition by copper were not analyzed quantitatively, however,

because of diffusional limitations. It is interesting to note, in contrast to the case of trypsin, that elastase could not be spin-labeled after it was immobilized, indicating that attachment to the support greatly reduced the accessibility of its target serine residues. No activity data or enzyme loadings were reported, and different immobilization schemes were not compared.

One of the spin labels first introduced by Berliner and Wong[39], 4-(2,2,6,6-tetramethylpiperidine-1-oxyl)-*m*-fluorosulfonylbenzamide (*m*-IV), has been employed in this research to study the active site regions of immobilized CT preparations.

m-IV

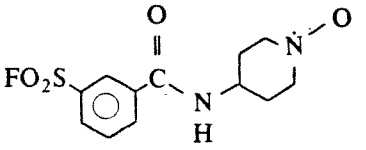

This label is an irreversible inhibitor of CT which reacts specifically with serine 195 of the active site. Berliner and Wong's work[39] indicates that *m*-IV does not react with inactive CT. The labeling of CT is therefore limited to the same enzyme population that reacts with the active site titrant (MUTMAC) and ester substrate (ATEE). When attached to free CT in solution, *m*-IV produces a "mobile" spectrum, making it a likely candidate to determine if the enzyme's active site is compressed, or constricted, by the immobilization process.

The EPR spectra of four spin-labeled CT derivatives shown in Figure 2 are direct evidence of modification in enzyme active site structure caused by immobilization. Spectrum 2(a) (in Fig. 2) for spin-labeled CT in solution is a baseline to which the other spectra can be compared. Line broadening relative to spectrum 2(a) is evident in spectrum 2(b) which was obtained from spin-labeled CT attached to the support through a six-carbon spacer. This broadening, indicating less label mobility, could be due to a conformational change in the active site, to elimination of the macromolecular contribution to spin label overall motion (that is, the contribution of rotation of the entire enzyme molecule in solution) or to a combination of these factors.

Spectrum 2(c) (in Fig. 2) is of Sepharose particles with the same immobilized enzyme content as sample 2(b), but here the spin-labeled CT is coupled directly to the support surface instead of through an intervening spacer. Further peak broadening has occurred, indicating that the overall motion of the label has become more restricted. Since there is no macromolecular contribution to either spectrum 2(b) or 2(c), differences between these two conjugates are attributable entirely to differences in the active site environment.

A surface of aliphatic carbon chains, like that presented by the support CNBr-6C, should conform to the molecular topography of CT more readily than the original, less yielding surface of CNBr-Sepharose. It is therefore expected that the enzyme must incur more conformational stress in order to bind directly to the support surface rather than through a spacer, and this is

manifested here by more extensive changes in the configuration of its active site. Spectrum 2d for a directly coupled CT catalyst with more immobilized protein than the previous case shows even further spin-label restriction.

The overall effect of increased immobilized enzyme structural modification is evidenced in these spectra by the increasing broadness of the low-field peak and the decreasing curvature of the center peak. Any alteration of the molecular geometry of CT's active site region could reduce the efficiency of complexation, and subsequent reaction, between enzyme and substrate. Consequently, it is not surprising that there is a direct corresondence between the degree of restriction of spin label mobility observed and the extent of reduction of immobilized enzyme specific activity.

In order to examine this relationship more carefully, it is useful to characterize the spin label mobility in these different CT catalysts quantitatively using the rotational correlation time τ. A simplified definition of τ is the average time required for a nitroxide molecule to move through a significant arc, and usually ranges from 0.05 ns (very fast rotation) to 50 ns (very slow rotation).[40] The value of τ is thus inversely related to the overall mobility of the spin label. The rotational correlation times for four spin-labeled CT derivatives were determined from spectra 2(a)-2(d) using the theoretical relations of Kivelson[41] and Stone et al.[42] assuming that the motion of the nitroxide label is isotropic. Smith[43] states that the assumptions of Kivelson are reasonable for systems in which $\tau < 5$ ns. Assuming isotropic motion for all of the systems considered (a simplification which greatly facilitates analysis of these spectra) yields τ values well below this upper limit. It is doubtful that more involved spectral simulation techniques would significantly improve the accuracy of these results.

The calculated rotational correlation times are indicated in the inserts in Figures 2(a)-2(d). In Figure 3, the τ values for each CT catalyst are plotted versus the corresponding specific activities of active enzyme (e_a) for these

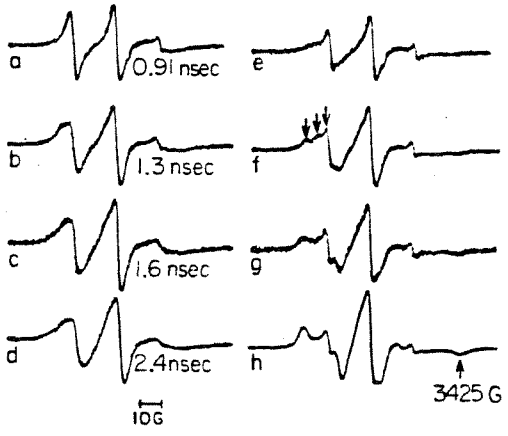

Fig. 2. The EPR spectra and rotational correlation times, taken in 1 mM acetic acid (a-d) and 1mM acetic acid with 12mM indole (e-h), of spin-labeled α-chymotrypsin in aqueous solution (a, e), immobilized on CNBr-6C (b, f), immobilized on CNBr-3 (c, g), immobilized on CNBr-5 (d, h). All spectra were taken at room temperature.

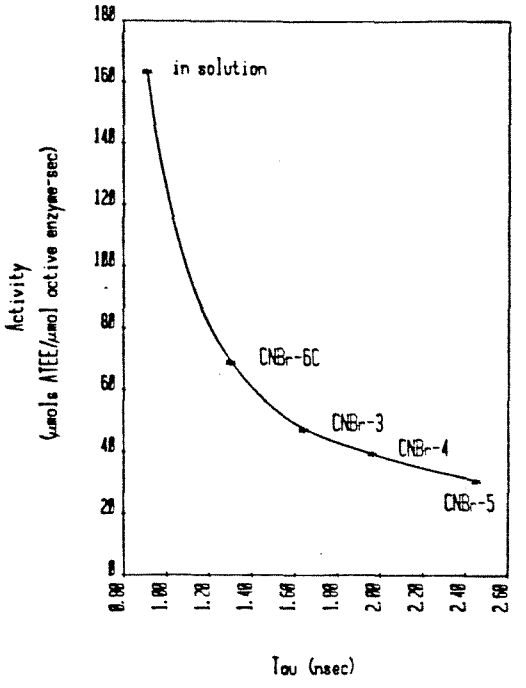

Fig. 3. Specific activity (e_a) of uninhibited α-chymotrypsin (measured with 1m*M* ATEE, 1*M* NaCl, pH 7.3) versus the corresponding rotational correlation time (τ) of *m*-IV attached to serine 195 of the enzyme's active site.

four systems. Noting that larger τ values imply more restricted spin label and thus a more modified active site structure, the decline in specific activity with increasing τ is completely consistent with the expected connection between enzyme structure and catalytic activity.

Indole Effects on EPR Spectra of Spin-Labelled Immobilized Chymotrypsin

Indole, a substrate analog and competitive inhibitor of CT, was used by Berliner and Wong to obtain additional insights into the active site structures of CT and trypsin in solution. Indole can occupy the tosyl hole (also called the binding pocket, the hydrophobic cleft, or the specificity pocket) of CT, a narrow slit defined by CT residues 184–191 and 214–227 which has dimensions suitable to accommodate one precise orientation of a molecule about the size of tryptophan.[44] By competing with the aromatic portion of *m*-IV for the binding pocket, indole can shift the average location of spin label from the immediate vicinity of the tosyl hole to an alternative site.

Berliner and Wong found in their studies of CT and trypsin in solution that, after exposure to saturated indole, many spin-labeled CT derivatives (including that labeled with *m*-IV) exhibited EPR spectra closely resembling the spectrum of spin-labeled trypsin which does not possess a tosyl hole. An equilibrium between three primary orientations of spin label relative to the tosyl hole, represented below by A, B, and C, was proposed to account for this observation:

$$A \rightleftharpoons B \rightleftharpoons C \qquad (15)$$

where A is the label completely inserted in the tosyl hole; B is the label located just outside the tosyl hole; C is the label occupying area removed from tosyl hole, common to both CT and trypsin. Displacement of label from *A* or *B* to *C* can apparently occur if indole can compete favorably with *m*-IV for the tosyl binding pocket.

The effects of indole (12m*M*) on the EPR spectra of different spin-labeled chymotrypsin catalysts are dramatic and distinctive as shown in Figures 2(e)—2(h). Comparison of these spectra with the corresponding τ values and spectra in the absence of indole shows that, as the mobility of the enzyme-bound spin label decreases, its spectrum is more dramatically affected by indole. The low-field peak in the presence of indole becomes increasingly bimodal as immobilized enzyme specific activity decreases, until finally in spectrum 2h the low-field (less mobile) side dominates. Note also in Figure 2 the appearance of a dip at 3425 G, giving an outer hyperfine separation of 62.6 G, indicative of highly hindered motion. Clearly, indole affects the label's mobility more extensively in the less active samples than in the more active samples. The extent of the indole effect is significantly greater on the immobilized enzyme than on the free enzyme in solution.

The eight spectra of Figure 2 illustrate that the spin-label can experience several different environments when attached to immobilized CT. Spectrum 2(f) may contain three distinct spin-label populations, as evidenced by the trimodal character of the low-field peak (see arrows). Spectra 2(g) and 2(h) are each comprised of two major components, one of which (the narrow line component) is significantly less restricted than the other. The remaining spectra, on the other hand, are apparently each composed of one dominant component, although it is possible that the broadening observed in 2(b)-2(d) is the contribution of more hindered subpopulations of spin-label.

Composite spectra are known to occur whenever the spin-label partitions between two or more environments.[45] For example, composite spectra are often observed in studies where spin probes are intercalated in biological membranes (e.g. ref. 46), and have also resulted when spin-labels have been attached to human carbonic anhydrase in solution[47] and to Ca^{2+}-transport ATPase in sarcoplasmic reticulum membranes.[17]

In immobilized enzyme catalysts, heterogeneity in the local structure of the support surface, as well as that of the enzyme's surface, no doubt combine to produce heterogeneity in the orientation, conformation, and extent of attachment (i.e., the number of bonds between enzyme and support) of the immobilized protein.[6,13] Assorted immobilized enzyme states may result, each with its own free energy, activity, and stability, where here stability is defined as the resistance to loss of catalytic activity. For each immobilized enzyme preparation the sum total of bound protein consists of different immobilized enzyme subpopulations, each of which may have a different active site configuration which contributes a characteristic component to the overall EPR spectrum. It is not readily apparent at this point to what extent the spectral results can be attributed to the label moving among several different positions in the same active site as indicated in Reaction (15) or to label fixed in

different positions in different immobilized enzyme subpopulations. Current research in this laboratory is seeking clarification of the basis for the observed heterogeneity in these immobilized enzyme systems.

DISCUSSION

The structural information obtained from EPR measurements provides insight into the observed activity differences summarized in Table I. Higher loading of directly-attached protein and lower enzyme activity are accompanied by changes in the interaction between *m*-IV and the specificity pocket of immobilized CT. When CT is bound to the support through a six-carbon spacer, the effects of immobilization on the enzyme's activity and active site configuration are less pronounced than in a directly-attached preparation of comparable loading.

The interactions between *m*-IV and the active site areas of free and immobilized CT should resemble those of a similar-sized substrate (i.e., ATEE) during its reaction sequence with the enzyme. Since substrate binding in the active site is believed to be of paramount importance in reducing the activation energy of CT-catalyzed reactions, it is not surprising that changes in the nature of spin label-active site interaction revealed by the EPR data are correlated with changes in the enzyme catalytic activity.

It is helpful to consider these results in conjunction with the normal reaction sequence of CT

$$E + S \overset{K_s}{\rightleftharpoons} ES \tag{16a}$$

$$ES \overset{k_2}{\rightarrow} EP_2 + P_1 \tag{16b}$$

$$EP_2 \overset{k_3}{\rightarrow} E + P_2 \tag{16c}$$

where EP_2 is the acyl-enzyme intermediate and, in the hydrolysis of ATEE, step (16c) is rate-limiting. It has been shown that if equilibrium is established in step (16a) much more rapidly than acylation occurs, the Michaelis constant for this system can be expressed as

$$K_m = \frac{k_3 K_s}{k_2 + k_3} \tag{17}$$

and that

$$v_{max} = k_{cat} e_0 \tag{18}$$

where

$$k_{cat} = \frac{k_2 k_3}{k_2 + k_3}. \tag{19}$$

Therefore the first-order rate constant when $s \ll K_m$ is

$$k_f = \frac{k_{cat}}{K_m} = \frac{k_2}{K_s}. \tag{20}$$

The covalent coupling between CT and spin label *m*-IV, as well as the latter's structural homologies with *N*-acetyl tyrosine, indicate that spin-labeled CT should closely resemble reaction intermediate EP_2 in the CT-catalyzed hydrolysis of ATEE. Therefore, it is worthwhile to consider the EPR results as they relate to both acylation (rate constant k_2) and deacylation (k_3), as EP_2 represents the transition between these two processes. Because these two reactions occur in the vicinity of the bond being cleaved, their rates are highly dependent on the orientation the substrate adopts in the active site relative to the enzyme's catalytically important residues. In the free enzyme, this positioning is extremely precise. Wright[48] reports that during normal catalysis there are at least four hydrogen bonds formed between residues of the active site (His 57, Ser 214, Ser 195, Gly 193) and a substrate such as ATEE. It is clear that should the normal binding pattern between CT and substrate be disturbed, both rate constants k_2 and k_3 are likely to be affected.

While neither of these kinetic parameters was measured directly for any of the immobilized enzyme preparations of this study, how they are affected by increasingly "abnormal" spin label (or substrate) binding can be approximated from data in Table I. For the reaction of free enzyme with ATEE at pH 8.0, $k_2/k_3 = 27$.[49] Under these conditions, eq. (19) indicates that k_{cat} becomes approximately

$$k_{cat} \approx k_3 \tag{21}$$

Assuming that this equation also applies for the immobilized enzyme. Table I shows that k_{cat} (ca. k_3) decreases as enzyme loading increases. The EPR studies show that the motion of enzyme bound spin label also become more restricted as k_{cat} decreases.

Evaluation of the effects of immobilization on k_2 is more difficult. It is not immediately clear whether an increase in K_s (which depends on the binding energy between enzyme and substrate), or a decrease in k_2 (which depends on the orientation of substrate relative to the enzyme), or both, is responsible for the observed decrease in k_f (Table I). Equation (20) implies that comparisons of k_2 for these systems can be made only if K_s is assumed to be a constant. This study contains no direct evidence in support of this assumption. However, previous investigators[49-51] have shown that K_s is less sensitive than k_2 to pH and temperature, both of which affect the configuration of CT, and that changes in K_s are often accompanied by larger changes in k_2. If similar trends obtain for immobilized enzyme, it can be suggested that immobilization has reduced k_2, a result consistent with the active site structural aberrations, revealed by EPR spectra, which have resulted from immobilization of the enzyme.

Additional spin labels of various geometries would provide more informa-

tion about the active site configurations of these immobilized CT preparations. Such EPR data would serve to further characterize, on a molecular level, the associated interactions between substrates and the binding pocket of immobilized CT. Information of this kind would assist in gaining a more complete mechanistic understanding of the immobilized enzyme's catalytic behavior. More detailed kinetic studies, in which the active enzyme is isolated by active site titration, are also needed to reveal further the manner in which the catalytic sequence of CT and other enzymes is affected by immobilization to a solid support.

The fact that immobilization can affect the reaction sequence of CT-catalyzed hydrolysis reactions, particularly the steps which require precise orientation of substrate relative to enzyme, may have additional implications in this and other immobilized enzyme systems. It is possible that when the specificity pocket of the enzyme is altered, the selectivity of the enzyme may change accordingly. Doel et al.[52] have recently reported direct evidence of a change in CT's selectivity caused by immobilization to Sepharose 4B. They observed that while soluble CT did not digest to any degree the repeating dipeptide poly(aspartyl-phenylalanine), some degree of digestion was achieved with the immobilized enzyme. The present work provides direct evidence that chemical and structural interactions which regulate CT-substrate binding were altered by immobilization; i.e., the protein lost some of its fine tuning. This may have significant consequences for separation processes employing immobilized enzymes and other biological macromolecules to effect affinity association with specific substrates, inhibitors, antigens, antibodies, or other molecules in a liquid mixture.

Once such effects are more fully understood, it may be possible through careful selection of the immobilization technique and use of protein-modifying reactions to alter a protein's binding equilibria and selectivity in a predetermined fashion. The sensitivity of enzyme activity to immobilization conditions described here also suggests that attachment of enzymes to membranes may be a natural mechanism of enzyme regulation in biological systems. Future studies which detail the effect that immobilization can have on the structure and function of enzymes will undoubtedly contribute to the design and development of biocatalysts with optimal activity, selectivity, and stability.

The authors are indebted to Joseph Schuh and Sunney Chan for assistance with EPR spectroscopy experiments and their interpretation. This work was supported by the National Science Foundation.

Nomenclature

D_{eff}	effective diffusivity
D_s	bulk diffusivity
e_a -	active enzyme loading
e_0	total enzyme concentration
k_2	rate constant for acylation

k_3 rate constant for deacylation
k_{cat} defined in eq. (19)
k_f defined in eq. (20)
K_m Michaelis constant, defined in eq. (17)
K_s dissociation constant of enzyme-substrate complex
q_e active enzyme specific activity
r radial coordinate
$\bar{r}$ nondimensional radial coordinate
R particle radius
s substrate concentration
$\bar{s}$ nondimensional substrate concentration, defined in eq. (4)
s_0 substrate concentration at particle surface
v reaction rate per unit volume of catalyst, defined in eq. (1)
v_{max} maximum reaction rate, defined in eqs. (2) and (18)
v_{obs} observed overall reaction rate, defined in eq. (7)
V molal volume

Greek symbols

β defined in eq. (4)
η effectiveness factor, defined in eq. (8)
η_D defined in eq. (10)
ρ_p particle density
τ rotational correlation time
ϕ Thiele modulus, defined in eq. (5)
Φ observable modulus, defined in eq. (12)

References

1. D. Gabel, I. Z. Steinberg, and E. Katchalski, *Biochemistry*, **10,** 4661 (1971).
2. D. Gabel, *Eur. J. Biochem.*, **33,** 348 (1973).
3. K. Martinek, A. M. Klibanov, V. S. Goldmacher, and I. V. Berezin, *Biochim. Biophys. Acta*, **485,** 1 (1977).
4. O. Zaborsky, *Immobilized Enzymes* (CRC, Cleveland, OH, 1973), pp. 57-60.
5. A. Flynn and D. B. Johnson, *Biotechnol. Bioeng.*, **20,** 1445 (1978).
6. Y. Kawamura, K. Nakanishi, R. Matsuno, and T. Kamikubo, *Biotechnol. Bioeng.*, **23,** 1219 (1981).
7. J. M. Engasser and C. Horvath, *J. Theor. Biol.*, **42,** 137 (1973).
8. V. Kasche and M. Bergwall, in *Insolubilized Enzymes*, M. Salmona, C. Saranio, and S. Garattini, Eds. (Raven, New York, 1974), p. 77.
9. R. Aris, *The Mathematical Theory of Diffusion and Reaction in Permeable Catalysts. Volume 1: The Theory of the Steady State* (Oxford University Press, London, 1975).
10. E. E. Peterson, *Chemical Reaction Analysis* (Prentice-Hall, Englewood Cliffs, NJ, 1965).
11. M. Moo-Young and T. Kobayashi, *Can. J. Chem. Eng.*, **50,** 162 (1972).
12. R. Axén and S. Ernback, *Eur. J. Biochem.*, **18,** 351 (1971).
13. A.-L. Koch-Schmidt and K. Mosbach, *Biochemistry*, **16,** 2105 (1977).
14. D. Gabel, *FEBS Lett.*, **49,** 280 (1974).
15. L. J. Berliner, S. T. Miller, R. Uy, and G. P. Royer, *Biochim. Biophys. Acta*, **315,** 195 (1973).
16. J. L. Dimicoli, M. Nakache, and J. M. Lhoste, *Biochim. Biophys. Acta*, **571,** 294 (1979).
17. H. Nakamura and A. N. Martonosi, *J. Biochem.*, **87,** 525 (1980).
18. J. Lasch, *Eur. J. Biochem.*, **63,** 591 (1976).
19. S. S. Wong, K. Quiggle, C. Triplett, and L. J. Berliner, *J. Biol. Chem.*, **249,** 1678 (1974).
20. "Affinity Chromatography: Principles and Methods," Pharmacia Fine Chemicals Publication, 1979.

21. J. R. Ford, A. H. Lambert, W. Cohen, and R. P. Chambers, *Biotechnol. Bioeng. Symp.*, **3,** 267 (1972).

22. P. F. Greenfield and R. L. Laurence, in *Enzyme Engineering. Volume 4* (Plenum, New York, 1978), p. 381.

23. T. Kobayashi and K. J. Laidler, *Biochim. Biophys. Acta*, **302,** 1 (1973).

24. W. K. Shieh, *Biotechnol. Bioeng.*, **21,** 503 (1979).

25. B. K. Hamilton, C. R. Gardner, and C. K. Colton, *AIChE. J.*, **20,** 503 (1974).

26. I. A. Webster, *Biotechnol. Bioeng.*, **22,** 2455 (1981).

27. T. Yamane, *Biotechnol. Bioeng.*, **19,** 749 (1977).

28. S. B. Lee and D. D. Y. Ryu, *Biotechnol. Bioeng.*, **21,** 1499 (1979).

29. G. K. Lee, R. A. Lesch, and P. J. Reilly, *Biotechnol. Bioeng.*, **23,** 487 (1981).

30. B. Atkinson and I. J. Davies, *Trans. Inst. Chem. Eng.*, **52,** 248 (1974).

31. B. Atkinson, J. Rott, and I. Rousseau, *Biotechnol. Bioeng.*, **19,** 1037 (1977).

32. V. Kasche, *DECHEMA Monogr.* **84,** 224 (1979).

33. J. E. Bailey and D. F. Ollis, *Biochemical Engineering Fundamentals* (McGraw-Hill, New York, 1977).

34. L. G. Longsworth, *J. Am. Chem. Soc.*, **75,** 5705 (1953).

35. E. J. Cohn and J. T. Edsall, *Proteins. Amino Acids and Peptides as Ions and Dipolar Ions* (Holt Reinhold. New York, 1943), p. 372.

36. B. C. Sherrill and J. G. Albright, *J. Solution Chem.*, **8,** 217 (1979).

37. S. B. Horowitz and I. R. Fenichel, *J. Phys. Chem.*, **68,** 3378 (1964).

38. K. Nakanishi, S. Adachi, S. Yamamoto, R. Matsuno, A. Tanaka, and T. Kamikubo, *Agric. Biol. Chem.*, **41,** 2455 (1977).

39. L. J. Berliner and S. S. Wong, *J. Biol. Chem.*, **249,** 1668 (1974).

40. O. H. Griffith and A. S. Waggoner, *Acc. Chem. Res.*, **2,** 17 (1969).

41. D. Kivelson, *J. Chem. Phys.*, **33,** 1094 (1960).

42. T. J. Stone, T. Buchman, P. L. Nordio, and H. M. McConnell, *Proc. Natl. Acad. Sci. US*, **54,** 1010 (1965).

43. I. C. P. Smith, in *Biological Applications of Electron Spin Resonance Spectroscopy*, J. R. Bolton, D. Borg, and H. Schwartz, Eds. (Wiley, New York, 1972), pp. 483-589.

44. J. J. Birktoft, P. M. Blow, R. Henderson, and T. A. Steitz, *Phil. Trans. Roy. Soc. Ser. B.* **257,** 67 (1970).

45. P. Jost and O. H. Griffith, in *Spin Labeling: Theory and Applications*, L. J. Berliner, Ed. (Academic, New York, 1976), p. 268.

46. I. K. Moules, E. K. Rooney, and A. G. Lee, *FEBS Lett.*, **138,** 95 (1982).

47. V. T. Wee, R. J. Feldman, R. J. Tanis, and C. F. Chignell, *Mol. Pharmcol.*, **12,** 832 (1976).

48. H. T. Wright, *J. Mol. Biol.*, **79,** 1 (1973).

49. J. McConn, E. Ku, A. Himoe, K. G. Brandt, and G. P. Hess, *J. Biol. Chem.*, **246,** 2918 (1971).

50. B. Zerner and M. L. Bender, *J. Am. Chem. Soc.*, **86,** 3669 (1964).

51. M. L. Bender, G. E. Clement, F. J. Kézdy, and H. D'A. Heck, *J. Am. Chem. Soc.*, **86,** 3680 (1964).

52. M. T. Doel, M. Eaton, E. A. Cook, H. Lewis, T. Patel, and N. H. Carey, *Nucl. Acid Res.*, **8,** 4575 (1980).

Accepted for Publication October 6, 1982

CHAPTER 3 CHARACTERIZATION OF HETEROGENEOUS IMMOBILIZED ENZYME SUBPOPULATIONS USING EPR SPECTROSCOPY

INTRODUCTION

Determination of the effects on enzyme properties of covalent enzyme attachment to a solid support has long been a major objective of immobilized enzyme research. Measurements of enzyme activity and enzyme stability at elevated temperatures and/or in the presence of chemical denaturants are standard means used to characterize and evaluate immobilized enzyme preparations. Often the measured properties of immobilized enzymes differ to some extent from soluble enzyme properties, and elucidation of the fundamental causes for such differences has been the objective of several recent studies.

Implicit in most analyses of immobilized enzymes is the assumption that the immobilized enzyme population is homogeneous. This assumption is justified within the domain of enzyme catalysis applications if the population of immobilized enzyme molecules is essentially homogeneous with respect to functional properties. This in turn will be true, one expects, either if the immobilized enzyme molecules have essentially the same state and environment or if the functional characteristics of the enzyme are insensitive to the existing extent of heterogeneity in bound enzyme molecular state.

Heterogeneity within immobilized enzyme systems has been investigated and demonstrated in relatively few previous studies. Lasch and Koelsch[1] found evidence of two primary subpopulations in leucine amino peptidase attached through a single bond to thiol-Sepharose 6B (CNBr-Sepharose that has been treated with L-glutathione): one class of immobilized enzyme that leaks exponentially with time from the support surface in 1 M hydroxylamine, and one that is stable to such treatment throughout the time range studied (~5 hr.). When multipoint attachment of the enzyme to CNBr-activated Sepharose was studied, similar behavior was

observed, but over a much longer time period. At least two different populations of immobilized enzyme molecules were also observed by Lasch *et al.* for α-chymotrypsin immobilized on CNBr-activated dextran 500.[2] In this system the unfolding of immobilized enzyme at elevated temperatures, followed by activity and fluorescence measurements, was a two-phase process. This was attributed to differences in the number of surface attachment points for each subpopulation of immobilized chymotrypsin.

Similarly, heterogeneity in the bonding between α-chymotrypsin and CNBr-activated Sepharose CL-4B was suggested by the stability studies of Kawamura *et al.*[3] They found thermal deactivation of immobilized chymotrypsin could not be described by a single, first-order reaction. Rather, the measured time course of thermal deactivation could be simulated by assuming a normal Gaussian distribution of activation energies for denaturation, and treating both the standard deviation of the distribution and the initial deactivation rate of immobilized enzyme as adjustable parameters. In the analysis of Kawamura *et al.* it was assumed that each of the heterogeneous enzymes had the same catalytic activity.

In the present work, α-chymotrypsin immobilized on CNBr-activated Sepharose 4B is used as a model system to investigate heterogeneity within immobilized enzyme preparations. EPR spectroscopy of spin-labeled immobilized enzyme provides direct evidence of significant heterogeneity in active site structure. The degree of such heterogeneity and its implications for overall catalytic activity of the immobilized chymotrypsin population is subsequently quantified based upon spectral deconvolution and activity data.

MATERIALS

α-chymotrypsin (from bovine pancrease, three times recrystallized, salt-free), N-acetyl-L-tyrosine ethyl ester (ATEE), and 4-methylumbelliferyl-p-

trimethyl ammonium cinnamate chloride (MUTMAC) were obtained from Sigma. Potassium ferricyanide, 2,2,6,6-tetramethyl-1-oxyl-4-aminopiperidine, m-fluorosulfonyl benzoyl chloride, and indole were purchased from Aldrich. Sepharose 4B preactivated with CNBr was a product of Pharmacia Fine Chemicals. Two different batches of this material, designated Supports I and II, were employed in this research. As noted below, these supports were different in loading capacities and in other properties. Inorganic salts and all buffer solution components were analytical grade reagents. Distilled water, deionized by passage through two Research IonXchanger Model 2 columns supplied by Illinois Water Treatment Co., was used throughout.

METHODS

Covalent Attachment of α-Chymotrypsin to CNBr-Sepharose 4B

α-Chymotrypsin was covalently coupled to CNBr-Sepharose 4B, and the resulting catalysts washed and stored, as described in Clark and Bailey.[4] The (wt/wt) ratio of enzyme to gel in the immobilization vessel was varied from 0.0178 to 0.1 to effect different active enzyme loadings.

Determination of the Amount of Functional Enzyme Bound to the Support Matrix

The concentration of active immobilized enzyme was determined by active site titration with MUTMAC. Fluorescence measurements were carried out in a Turner Model 430 Spectrofluorometer in 1 cm cuvettes. The titration procedure followed is the same as described elsewhere.[4] For a few immobilized chymotrypsin catalysts prepared in similar fashion to those considered in

this investigation, amino acid analysis was used to determine the total amount of bound protein. It was found that the fractions of completely inactive immobilized enzyme present in the samples investigated were at most only 7% greater than the fraction of inactive enzyme present in the immobilizing solution (~40%), determined by UV absorption and active site titration. Thus, although immobilization does not cause any significant increase in inactive enzyme fraction, the immobilized enzyme preparation includes a significant subpopulation of inactive enzyme.

Determination of Immobilized Enzyme Activity

The reaction rate of immobilized α-chymotrypsin with ATEE was determined in a differential recirculation reactor of the type described by Ford *et al.*[5] equipped with a water jacket for temperature control. The details of this procedure for large (R = 60 μm) and small (R ≲ 10 μm) Sepharose particles, obtained by grinding the large particles in a Potter-Elvehjelm tissue grinder, can be found in Clark and Bailey.[4] As discussed there, large particles exhibit intraparticle diffusion disguises that can be corrected by effectiveness factor calculations. This approach was used to determine intrinsic specific activities from diffusion-limited rate data for catalysts prepared with Support I.

Preparation of Spin-Labelled Enzyme Derivatives and EPR Measurements

The procedures described by Wong *et al.*[6] were employed to prepare the nitroxide spin label (m-IV), and to spin label α-chymotrypsin in solution. The immobilized enzyme was spin labeled and prepared for EPR analysis, and the EPR spectra recorded in 12 mM indole with or without $K_3Fe(CN)_6$, according

to Reference 4. EPR spectra were recorded at the X band using a Varian E-Line Century Series EPR Spectrometer equipped with temperature regulation by nitrogen gas flow. The spectra were digitized using a Digital Equipment Corp. PDP-8/A minicomputer interfaced to the EPR spectrometer.

RESULTS

Subpopulation Quantitation by EPR Spectra Decomposition

The specific activity of α-chymotrypsin immobilized on CNBr-activated Sepharose 4B (Support I) decreases as the loading of active enzyme increases (Table 1). To determine the extent to which this result coincides with conformational changes at or near the enzyme's active site, the EPR spectra of immobilized chymotrypsin labelled at serine 195 with a nitroxide spin label (4-(2,2,6,6-tetramethylpiperidine-1-oxyl)-m-fluorosulfonylbenzamide) were recorded. As described in Clark and Bailey,[4] the decrease in specific activity is accompanied by a decrease in the overall mobility of the attached spin label. This relationship is completely consistent with the established sensitivity of chymotrypsin's catalytic activity to the configuration of its active site region.

When the EPR spectra of spin-labelled immobilized chymotrypsin are recorded in the presence of indole, a substrate analog and competitive inhibitor of the enzyme, two distinct spectral components are observed. Each of these components corresponds to spin label with a certain degree of mobility. Because the spin label used here binds to only one site on the enzyme,[7] the two overlapping EPR signals indicate the existence of two subpopulations of immo-

bilized enzyme with active site regions that, in the presence of indole, provide the attached spin label with significantly different degrees of motional freedom.

For future reference, each set of characteristic spectral components has been assigned to an enzyme subpopulation as shown in Fig. 1. As evidenced by the positions and lineshapes of the indicated peaks, the mobility of spin label in enzyme subpopulation A is much more restricted than spin label in enzyme subpopulation B. In order to obtain more insight into the nature and origin of these two subpopulations, and to determine how their catalytic activities may differ, it is necessary to resolve each overall spectrum into the contributions provided by enzyme subpopulations A and B. As a working model, the following relationship is assumed relating the overall normalized spectrum f(G) to the normalized spectra $f_A(G)$ and $f_B(G)$ corresponding to immobilized enzyme with states A and B, respectively:

$$f(G) = \alpha f_A(G) + (1 - \alpha) f_B(G) \quad . \tag{1}$$

Next, the suitability of this representation and identification of the subpopulation spectra are considered.

Figure 2 shows a sequence of indole spectra with the result for chymotrypsin in solution in the rear and data for three immobilized enzyme catalysts arranged from back to front in order of active enzyme loading. Distinctive modes noted in the solution indole spectrum are clearly evident in the overall immobilized enzyme spectra, and the prominence of these features declines as enzyme loading increases. This suggests that the indole spectrum for enzyme in solution may be a reasonable approximation to the indole spectrum for subpopulation B and

that α, the fraction of active immobilized enzyme comprised of state A, increases with enzyme loading. Both of these points will be reexamined after discussion of independent investigations on direct determination of $f_A(G)$.

Since spin label in immobilized enzyme subpopulation A exhibits relatively restricted motion, it is reasonable to presume that such label is relatively inaccessible to the surrounding solvent. Consequently, a reagent which selectively removes the spectral component contributed by more accessible spin label should permit direct measurement of a spectrum approximating $f_A(G)$. The paramagnetic molecule $K_3Fe(CN)_6$ has been employed for this purpose in this work. Sufficiently close contact between this paramagnetic species and the nitroxide group on the spin label causes line-broadening interactions that quench the EPR signal from the affected nitroxide. Physiochemical interactions of this kind have been utilized previously in analyses of complex EPR spectra obtained in studies of the internal viscosity of red blood cells[8] and of the active site environment of hepatic membrane-bound cytochrome P-450 of the endoplasmic reticulum.[9]

Figure 3 shows the effect of various concentrations of $K_3Fe(CN)_6$ on a typical composite spectrum of immobilized chymotrypsin in indole. These spectra show that the characteristic features contributed by spin label in subpopulation B can be eliminated from the total spectrum by 150 mM $K_3Fe(CN)_6$. This indicates that the active site region of subpopulation B is more accessible to the surrounding solvent than the active site of subpopulation A.

Validity of the composite spectrum representation proposed in Eqn. (1) and of the f_A and f_B estimates just described can be tested by comparing composite experimental spectra with results calculated from Eqn. (1) after adjusting α to maximize the correspondence. The resolution of this test can be maximized by

using a measured composite indole spectrum and one of the estimated subpopulation spectra to estimate both the relative content of the two immobilized enzyme forms (α) and the other subpopulation spectrum. Suppose, for example, that the indole spectrum of enzyme in solution is employed as $f_B(G)$. This spectrum is multiplied by a weighting factor between zero and unity (i.e., $1 - \alpha$) and subtracted from a composite indole spectrum. The weighting factor is increased until the following two criteria are satisfied: (i) the residual spectrum does not contain features indicative of two components, and (ii) the residual spectrum does not contain any physically unreasonable features. While this procedure may seem to involve significant subjectivity in evaluation of the weighting factor, the stated simultaneous criteria provide very clear and sensitive constraints for the search for the appropriate weighting factor value for a particular immobilized chymotrypsin formulation. A similar approach was employed by Marsh *et al.* in analysis of lipid-protein interactions in membranes.[10]

A representative spectral decomposition is shown in Fig. 4. The middle spectrum is that which results when the optimally weighted digitized indole spectrum of chymotrypsin in solution, shown below, is subtracted from the indole spectrum of catalyst CNBr-5. As illustrated in Fig. 5, the residual indole spectrum so obtained is nearly identical to the indole spectrum measured for the same immobilized enzyme preparation in 150 mM $K_3Fe(CN)_6$. The slight mismatch is likely due to slight line broadening in the measured spectrum -- an "overshoot" in the attempt at chemical isolation of the subpopulation A spectrum.

Such excellent consistency is not restricted to a single case. Figure 6 compares the residual indole spectra obtained by spectral subtraction analysis of two immobilized chymotrypsin preparations with different loadings and overall specific activities. These are virtually identical and both are extremely similar to the direct experimental estimate of $f_A(G)$.

These results imply that overall indole spectra of the immobilized chymotrypsin catalysts considered in this research can be closely approximated by Eqn. (1) where $f_B(G)$ is the indole spectrum of enzyme in solution and where $f_A(G)$ is the same function in each case. The close correspondence between the $f_A(G)$ estimates by spectral subtraction and indole spectra in the presence of a paramagnetic molecule strongly supports the previous hypothesis equating relative label mobility and relative solvent accessibility of immobilized chymotrypsin active sites. The overall consistency of this set of indole spectra analyses indicates that the weighting factors obtained in the spectral decomposition calculations are physically meaningful parameters which should be valuable in characterizing and describing biocatalyst function. This theme is elaborated next.

Determination of Subpopulation Specific Activities

Both active enzyme subpopulations identified above have distinctive and very different indole spectra, which in turn indicates different active site structures in the two populations. Since active site structure is likely directly related to catalytic function of the immobilized enzyme, it is reasonable to propose that the catalytic activities of the two subpopulations are different. Extending this structure-function argument a step further, it appears that the activity of each subpopulation may be the same in all of the immobilized chymotrypsin catalysts studied since the indole spectrum of each catalyst can be decomposed into essentially the same two subpopulation indole spectra.

These hypotheses imply that changes in overall specific activity (q_E) which result from differences in enzyme loading are due entirely to alterations in the distribution of active immobilized enzyme molecules between states A and

B. Restated in equation form,

$$q_{Ei} = \alpha_i q_A + (1 - \alpha_i) q_B \quad . \qquad (2)$$

The i subscript denotes different formulations of immobilized enzyme. It is very important to recognize that, apart from the subscript added to the notation at this point, the α value in Eqn. (2) is identical to the α value in the EPR indole spectrum representation in Eqn. (1). Thus, once the overall indole spectrum decomposition analysis has been done for immobilized enzyme catalyst i, the α_i value for that catalyst is known. Also, it is significant that the specific activities q_A and q_B of subpopulations A and B, respectively, are *independent of i: these properties are invariant from one chymotrypsin-CNBr Sepharose conjugate to the next.*

The validity of Eqn. (2) has been tested using experimental data for five different immobilized chymotrypsin biocatalysts. First, data on the three preparations listed in Table 1 were employed to estimate q_A and q_B. The corresponding fractions of A and B immobilized enzyme states determined by indole spectral decomposition are given in Table 2. Using overall activities (q_{Ei}, q_{Ej}) and distribution parameters (α_i, α_j) from any pair of these systems gives, in conjunction with Eqn. (2), two linear equations in unknowns q_A and q_B. Table 2 presents the results of such calculations. The catalysts used to obtain each set of specific activities q_A and q_B are given in the last column of Table 2.

For example, when samples CNBr-3 and CNBr-4 are used, a specific activity of 8.4 μmols ATEE/(μmol active chymotrypsin-sec) is calculated for subpopulation A, and 127.8 μmols ATEE/(μmol active chymotrypsin-sec) is the corresponding subpopulation B specific activity. Similarly, CNBr-4 and CNBr-5 give 8.2 and and 128.2, and CNBr-3 and CNBr-5 give 8.3 and 128.5 for q_A and q_B, respectively.

The remarkable consistency of these results strongly supports the hypothesized existence of two subpopulations of immobilized enzyme with distinct specific activities that differ by more than a factor of ten. The higher percentage of less active enzyme is responsible for the lower overall specific activity of the catalysts with higher enzyme loadings.

The last two immobilized chymotrypsin conjugates considered, designated CNBr-3.5' and CNBr-4.5', were prepared from a different batch (denoted Support II) of Pharmacia CNBr-Sepharose 4B than used in formulation of catalysts CNBr-3 through CNBr-5 (denoted Support I). Several differences were observed in catalyst formulation and characterization experiments that were essentially identical except for the support batch employed. Equal initial immobilizing solution enzyme concentrations gave different final immobilized enzyme loadings (e.g., e_a = 1.27 and 0.75 μmoles CT/gm catalyst for Supports I and II, respectively, with e_{b0} = 0.4 μmol/ml). While the trend of decreased specific activity with increased loading is also observed for Support II (see Table 3), chymotrypsin immobilized on Support II exhibits higher loadings for given specific activity than observed for Support I. Small (≈10 μm radius) particles were used for Support II activity assays to eliminate possible diffusion limitations.

Indole spectra for preparations CNBr-3.5' and CNBr-4.5' could be very well approximated by a linear combination (Eqn. (1)) of the same subpopulation indole spectra identified and applied in studies of the first three catalysts. Using the subpopulation fractions estimated from EPR data on Support II formulations (Table 3) and the means of the subpopulation A and B activities determined from the CNBr-3, 4, and 5 analysis, activities were calculated using Eqn. (2) for immobilized enzyme catalysts CNBr-3.5' and CNBr-4.5'. These calculated values, listed in the last column of Table 3, agree within experimental error with the measured specific activities of these catalysts.

DISCUSSION

The data interpretation presented above is based on a two-state model for active immobilized enzyme. It is important to consider alternative models and their consistency with experiment. This is aided by examination of a more general formalism for the heterogeneous immobilized enzyme population and its properties. In the Appendix, an alternative model is developed and shown to be less consistent with all available experimental information for these catalysts than is the two-state model.

When one considers the heterogeneity of gel structure, possible enzyme attachment orientations and number of covalent linkages, and other potential sources for heterogeneity in immobilized enzyme structure and function, it is not surprising that heterogeneity occurs. It is, however, perhaps unexpected to find that, to a very high level of approximation, the heterogeneity in these immobilized enzyme systems is manifested only in two very distinct forms of active immobilized enzymes. Why are there only two forms? What is the underlying mechanism which determines these molecular states and their relative numbers in a particular catalyst formulation? While answers to these questions are not presently available, some speculations are possible.

Previous studies have established that α-chymotrypsin in aqueous solution can equilibrate between a number of different conformational substates.[11,12] Steady-state fluorescence and optical rotary dispersion measurements indicate that at 25° C and pH 8 - conditions very similar to those under which chymotrypsin was immobilized in the present study - two substates with different catalytic activities predominate.[13] The transition between these two substates is characterized by large enthalpy and entropy changes consistent with a significant change in the enzyme's conformation. Given this information, it might be expected *a priori* that covalent attachment to an insoluble support would result in two separate configurations of immobilized enzyme similar or identical

to those that characterize chymotrypsin in solution. This hypothesis is supported by the Sepharose-bound chymotrypsin results to the extent that two subpopulations of immobilized enzyme are observed. Why the relative amounts of each enzyme subpopulation vary with the total enzyme loading; i.e., the concentration of enzyme in the immobilizing solution, remains unclear, unless the equilibrium composition of the immobilizing solution is a function of the total enzyme concentration. No evidence known to the authors indicates this is the case. Nonetheless, the results of the present study are consistent with the reported coexistence of two stable configurations of α-chymotrypsin in an aqueous environment, and there are a number of factors, in addition to conformational heterogeneity of the preimmobilized enzyme, that may contribute to the presence of two forms of immobilized enzyme. The most likely of these possibilities are discussed in turn below.

Recent evidence suggests that CNBr-activated Sepharose does not offer a single population of homogeneous binding sites for the attachment of ligands and proteins. Kohn and Wilchek reported that CNBr activation results in the formation of two types of reactive groups on the surface of Sepharose: imidocarbonates and cyanate esters.[14] Acid washing reduces the amount of imidocarbonates, which react with ligands more slowly than cyanide esters. It is currently unknown how much of each type of binding group was present in the CNBr-Sepharose samples used in this work, and such measurements are not possible in retrospect since the entire supply of the original support material has now been exhausted.

Binding site inhomogeneity was demonstrated in a different manner by Aplin and Hall, who labeled Pharmacia CNBr-Sepharose 4B with spin labels directly and also through oligoglycines and ω-amino-carboxylic acids of varying lengths.[15] It was found using computer simulation techniques that none of the EPR spectra obtained from directly-labeled Sepharose samples could be simulated

by assuming a homogeneous population of isotropically reorienting spins. Site variations arising from the nature of the gel structure, causing heterogeneity in the population of immobilized nitroxides, were proposed as a possible explanation for the EPR spectra observed in that work. Similar gel structure variations could influence heterogeneities observed here in immobilized enzyme molecular state.

The influence of total enzyme loading on the relative proportions of the two active forms of immobilized chymotrypsin also suggests that protein-protein interactions may be involved. The number of neighboring proteins in the immediate vicinity of a given immobilized enzyme molecule will clearly increase with increasing enzyme loading, possibly causing steric crowding or otherwise influencing the conformation of the immobilized enzyme molecules. Evidence for immobilized enzyme inhibition as a result of protein-protein interactions has been suggested in at least one naturally occurring immobilized enzyme system, Ca^{+2}-transport ATPase in native and reconstituted sarcoplasmic reticulum membranes.[16] It was found with this system that replacement of membrane phospholipids with dipalmitoylphosphatidylcholine reduced the mobility of spin labels covalently attached to the transport ATPase polypeptide. The authors suggested that this result may be due to a redistribution of ATPase molecules in the membrane, with the formation of ATPase aggregates, accompanied by reduction of ATPase activity and a restriction of spin label mobility due to protein-protein interactions. The possibility that interactions of this type reduce enzyme activity in both natural and manmade immobilized enzyme systems is reasonable, but remains unproven.

It is not clear from available data on immobilized chymotrypsin on CNBr-Sepharose whether the observed heterogeneity is due to *a priori* heterogeneity

in the physical and chemical properties of the support or to induced heterogeneity caused by interactions among immobilized enzyme molecules. Clarification of the relative contributions of these two causes of heterogeneity would aid in determining the extent to which and in what direction the results of this work could be extrapolated to other immobilized enzyme systems. Further research on this question is in progress.

It is possible that only two subpopulations of active immobilized enzymes were observed because the methods employed were not sufficiently sensitive to determine finer scale molecular differences in the immobilized protein molecules. A variety of additional immobilized enzyme characteristics could be considered in characterizing immobilized enzyme molecular state including other spin labels, NMR spectroscopy, and analysis of the number of bonds between the enzyme molecule and the support matrix. However, it is significant that, from the point of view of immobilized enzyme catalyst characterization and formulation, the optimal measure of the enzyme molecular state is one that relates directly to catalytic functional properties of the protein. The indole EPR measurements have clearly met this requirement for this system. Active site environmental differences revealed by EPR spectroscopy of immobilized chymotrypsin in the presence of indole has identified two subpopulations and their relative contributions which correlate quantitatively and directly with enzyme activity.

CONCLUSIONS

The preceding analyses of EPR spectral data and catalytic activity measurements for five different immobilized chymotrypsin biocatalysts clearly indicate the existence of two distinct forms of active immobilized enzyme. All EPR indole spectra for these systems may be accurately approximated by a convex combination of the same two subpopulation spectra. Each subpopulation spectrum has been directly measured in a separate experiment.

Furthermore, the presumed correlation between active site state as revealed by EPR measurement and catalytic activity of the immobilized enzyme is clearly supported by the data and the analysis described above. Each characteristic subpopulation, originally identified on the basis of EPR measurements, can be associated with a well-defined specific activity, and the overall specific activities of each catalyst are equal to the weighted sum of these specific subpopulation activities. These conclusions hold for different enzyme loadings on two different CNBr-Sepharose supports.

These results substantially clarify the underlying structure of the previously reported phenomenon of reduced specific activity with increasing immobilized enzyme loading. For the present system, at least, the effect of increasing loading is to increase the proportion of the active enzyme in the relatively inactive form. Changing loading does not change the types of active immobilized enzyme present or their active site structure as revealed by EPR spectroscopy. The well established structure-function connection for enzymes in solution has been shown, as expected, to apply to immobilized enzyme molecules. The enzyme subpopulation displaying greatly restricted spin label mobility in the active site has been determined to possess an order of magnitude smaller specific activity than exhibited by the immobilized enzyme form characterized by an EPR spectrum almost identical to that of enzyme in solution.

An important question that has not yet been sufficiently addressed is the possibility that the stability of the two active immobilized enzyme forms may differ substantially. As mentioned above, Kawamura *et al.*[3] obtained evidence that chymotrypsin immobilized on CNBr-activated Sepharose consists of multiple subpopulations of immobilized enzyme with different thermal deactivation rates. Preliminary results in studies in this laboratory using high concentrations of n-propanol to induce denaturation support this observation .

It was found that the activity decay of immobilized chymotrypsin differs significantly from simple first order kinetics, and the observed pattern of decay may be resolvable into a combination of simpler kinetics corresponding to different subpopulations. However, further research, now in progress, is required to fully address this class of questions. It is presently unknown whether the characterization of enzyme molecular state afforded by EPR spectroscopy possesses the resolution and information content necessary to characterize the denaturation properties of the immobilized protein. An answer to this question for the particular immobilized enzyme system addressed in this work is expected in the near future.

In order to optimize the formulation of an immobilized enzyme catalyst, it is necessary to know as much as possible about the influences of protein properties, support characteristics, and immobilization process conditions on the important properties of the enzyme. The clear demonstration of multiple subpopulations of immobilized enzyme with greatly different activities should motivate further detailed study of structure-function relationships in immobilized enzyme populations. The present work has demonstrated that changes in the support and changes in immobilization conditions, namely the initial enzyme concentration in the immobilizing solution, can influence the overall specific activity and the distribution of different active enzyme molecular states in the catalyst.

As opportunities increase for applications of immobilized enzymes in unnatural environments, it is critical to understand at a fundamental level the available strategies to manipulate and optimize immobilized enzyme structure and function. Further studies are thus required to determine when and why multiple subpopulations of immobilized enzyme occur and how subpopulation properties differ. Such information will help to transform immobilized enzyme catalyst formulation and optimization from a trial and error art to more of a science, and should ultimately greatly expand the efficiency and utility of immobilized enzyme catalysts.

REFERENCES

1. J. Lasch and R. Koelsch, *Eur. J. Biochem.*, 82, 181 (1978).

2. J. Lasch, L. Bessmertnaya, L. V. Kozlov, and V. K. Antonov, *Eur. J. Biochem.*, 63, 591 (1976).

3. Y. Kawamura, K. Nakanishi, R. Matsuno, and T. Kamikubo, *Biotechnol. Bioeng.*, 23, 1219 (1981).

4. D. S. Clark and J. E. Bailey, *Biotechnol. Bioeng.*, in press (1983).

5. J. R. Ford, A. H. Lambert, W. Cohen, and R. P. Chambers, *Biotechnol. Bioeng. Symp. 3*, 267 (1972).

6. S. S. Wong, K. Quiggle, C. Triplett, and L. J. Berliner, *J. Biol. Chem.*, 249, 1678 (1974).

7. L. J. Berliner and S. S. Wong, *J. Biol. Chem.*, 249, 1668 (1974).

8. A. D. Keith, W. Snipes, and D. Chapman, *Biochemistry*, 16, 635 (1977).

9. D. Schwarz, J. Pirrwitz, H. Rein, and K. Ruckpaul, *J. Magn. Res.*, 47, 375 (1982).

10. D. Marsh, A. Watts, R. D. Pates, R. Uhl, P. F. Knowles, and M. Esmann, *Biophys. J.*, 37, 265 (1982).

11. R. Lumry and R. Biltonen, in *Structure and Stability of Biological Macromolecules*, S. Timasheff and G. Fasman, Eds., Marcel Dekker, New York, 1969, p. 65.

12. R. P. Taylor, J. B. Vatz, and R. Lumry, *Biochemistry*, 12, 2933 (1973).

13. Y. D. Kim and R. Lumry, *JACS*, 93, 1003 (1971).

14. J. Kohn and M. Wilchek, *Enzyme Microb. Technol.*, 4, 161 (1982).

15. J. D. Aplin and L. D. Hall, *Eur. J. Biochem.*, 110, 295 (1980).

16. H. Nakamura and A. N. Martonosi, *J. Biochem.*, 87, 525 (1980).

APPENDIX: ALTERNATIVE MODELS OF HETEROGENEOUS IMMOBILIZED ENZYME POPULATIONS

Suppose that the immobilization state of a catalytically active immobilized enzyme molecule can be indexed by a nonnegative scalar x, and let $f_E(x)dx$ denote the fraction of the immobilized enzyme molecules with states between x and x+dx. (It would obviously be more accurate to represent the immobilization state in a higher dimensional space, but such an elaborate representation would not be of any greater utility in the following considerations.) The molecular intrinsic specific activity of a molecule of state x will be written q(x). Then, the overall intrinsic specific activity

$$q_E = \int_0^\infty q(x) f_E(x) dx \qquad \text{(A1)}$$

Viewed from this perspective, changes in intrinsic catalytic properties of enzymes caused by immobilization are the result of redistribution of enzyme molecular states; i.e., modification of f_E, such that a different mix of molecular intrinsic activities is produced. In a similar fashion, the EPR spectrum of a spin-labeled immobilized enzyme catalyst is a summation of contributions from individual labeled immobilized enzyme molecules. Letting $f_e(x;G)$ denote the EPR spectrum (G is field strength) of labeled enzyme of state x, the measured overall spectrum may be written

$$f(G) = \int_0^\infty f_e(x;G) f_E(x) dx \qquad \text{(A2)}$$

Because $f_e(x;G)$ here denotes an intrinsic property of immobilization state x, observed alterations in f(G) for a given environmental state are direct manifestations of changes in f_E.

The discussion above is based on the presumption that $f_E(x)$ is well approximated as a convex combination ($0 \leq \alpha \leq 1$) of impulse functions:

$$f_E(x) = \alpha\delta(x) + (1-\alpha)\delta(1-x) \qquad \text{(A3)}$$

where here x = 0 and x = 1 have been assigned to enzyme states denoted A and B above, respectively. It is interesting to note that an alternative model exists which leads to the same equation forms as Eqns. (1) and (2) above. Suppose that the EPR spectrum of labeled enzyme of state x is the following linear function of x:

$$f_e(x;G) = f^0(G) + x[f^1(G) - f^0(G)] \tag{A4}$$

and that the specific immobilized enzyme activity depends on x in a similar fashion

$$q(x) = q^0 + x(q^1 - q^0) \quad . \tag{A5}$$

Substituting Eqns. (A4) and (A5) into Eqns. (A2) and (A1) yields

$$f(G) = \bar{x} f^1(G) + (1 - \bar{x}) f^0(G) \tag{A6}$$

and

$$q_E = \bar{x} q^1 + (1 - \bar{x}) q^0 \quad , \tag{A7}$$

respectively, where $\bar{x}$ is the mean of the f_E density function:

$$\bar{x} = \int_0^\infty x\, f_E(x)\,dx \quad . \tag{A8}$$

Clearly, so long as $\bar{x} \leq 1$, Eqns. (A6) and (A7) are formally equivalent to Eqns. (1) and (2).

However, the physical interpretation of the model just presented may be significantly different from that of the two-state model. Provided that relationships (A4) and (A5) are valid, Eqns. (A6) and (A7) hold independent of the form of $f_E(x)$. Then, the applicability of Eqns. (A6) and (A7) (or, equivalently, (1) and (2)) to the data does not necessarily imply a two-state distribution of states for active immobilized enzyme. The enzyme states may be continuously distributed instead.

While the alternative model just described (called now the continuum-state model) is mathematically equivalent to the two-state model, it is not necessarily equivalent from the viewpoint of chemical and spectroscopic feasibility. It is possible to dispel the continuum model by contradiction: suppose it is true. If $f_E(x)$ has significantly nonzero values for x values significantly removed from zero and unity, enzyme states possessing EPR spectra given by Eqn. (A4) are implied. Remembering that $f^0(G)$ and $f^1(G)$ correspond to $f_B(G)$ and $f_A(G)$, respectively, identified above, this implies a multiple peak spectrum for enzyme with this intermediate state.

Such a spectrum for a particular enzyme state is physically unreasonable. It would occur only if the spin label oscillated back and forth between two domains of the active site at a rate slower than the EPR spectrometer is capable of detecting: specifically, based on the sensitivity limits of conventional EPR spectroscopy, two overlapping spectra of the kind that characterize each indole spectrum would result only if the spin label occupied each domain for longer than 10^{-8} sec. Such a long residence time does not seem consistent with an equilibrium between one spin label orientation and another. Similar arguments can be constructed based on the $K_3Fe(CN)_6$ EPR indole spectra experiments. For the paramagnetic molecule to eliminate one spectral component only, the label would have to move into a position accessible to solvent, be quenched, then move to a second environment away from solvent and regain its EPR signal. Such a scenario is very unlikely given the expected rapid motion of the label under these experimental conditions.

FIGURE CAPTIONS

Figure 1. EPR spectrum of spin-labeled immobilized chymotrypsin, recorded in 12 mM indole (indole spectrum), showing characteristic features of spectra from immobilized enzyme subpopulation A and subpopulation B.

Figure 2. EPR indole spectra of (from rear): spin-labeled chymotrypsin in solution and immobilized chymotrypsin preparations CNBr-3,-4, and -5. Arrows above rear spectrum indicate spectral features of subpopulation B that are present in each spectrum. The amount of active enzyme immobilized on the support and the relative amount of subpopulation A present in each sample increase in the direction of the arrow at lower left.

Figure 3. Indole spectra of CNBr-5 in various concentrations of $K_3Fe(CN)_6$. The portion of the spectrum contributed by subpopulation B becomes progressively smaller as the concentration of $K_3Fe(CN)_6$ increases. In 150 mM $K_3Fe(CN)_6$ (bottom), only the spectrum of subpopulation A is evident. The instrument gain used for recording the bottom spectrum was 1.6 times the gain setting for the other three measurements. $K_3Fe(CN)_6$ at 150 mM concentration affects the magnitude but does not significantly alter lineshape of the subpopulation A spectrum.

Figure 4. Decomposition of the indole spectrum of catalyst CNBr-5. The middle spectrum is that which results when optimally weighted indole spectrum of chymotrypsin in solution (below) is subtracted from the indole spectrum of CNBr-5 (top). Weighting factors of each spectrum are shown at left.

Figure 5. Comparison of the indole spectrum of subpopulation A isolated in 150 mM $K_3Fe(CN)_6$ (line with circles), and the spectrum obtained by subtracting the optimally weighted indole spectrum of chymotrypsin in solution from the indole spectrum of CNBr-5.

Figure 6. Residual indole spectra obtained by subtracting the optimally weighted indole spectrum of chymotrypsin in solution from the spectra of CNBr-4 and CNBr-5.

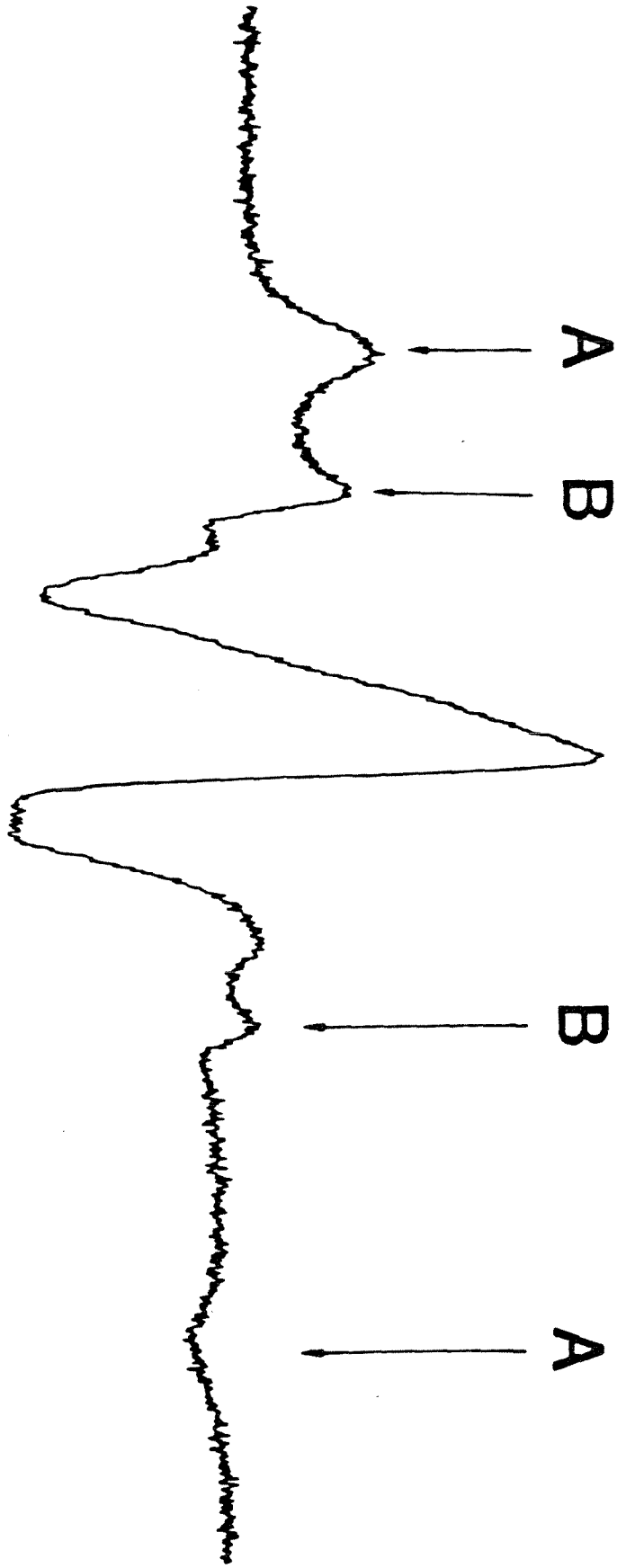

FIGURE 1

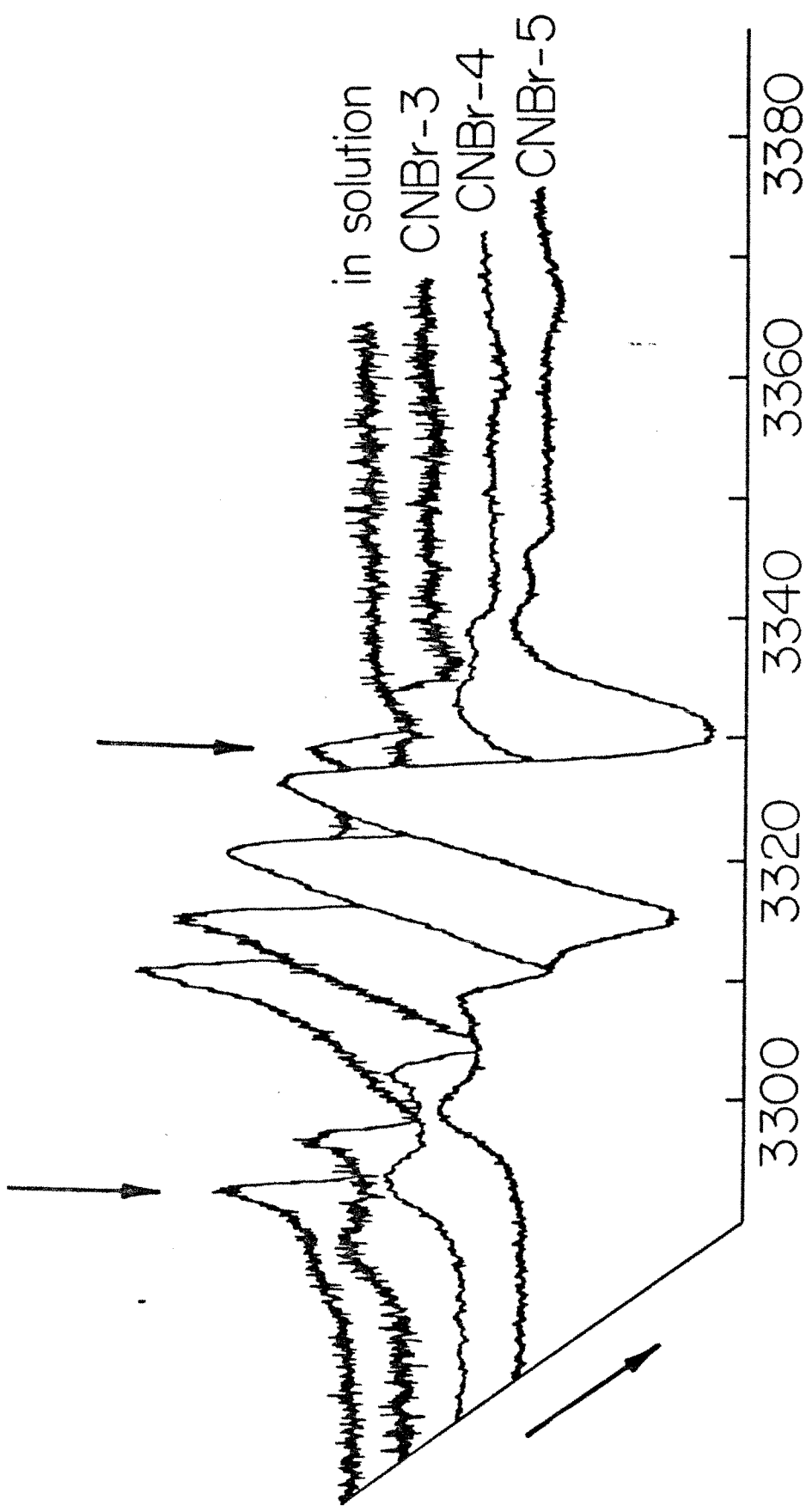
in solution
CNBr-3
CNBr-4
CNBr-5
3300
3320
3340
3360
3380
GAUSS

FIGURE 2

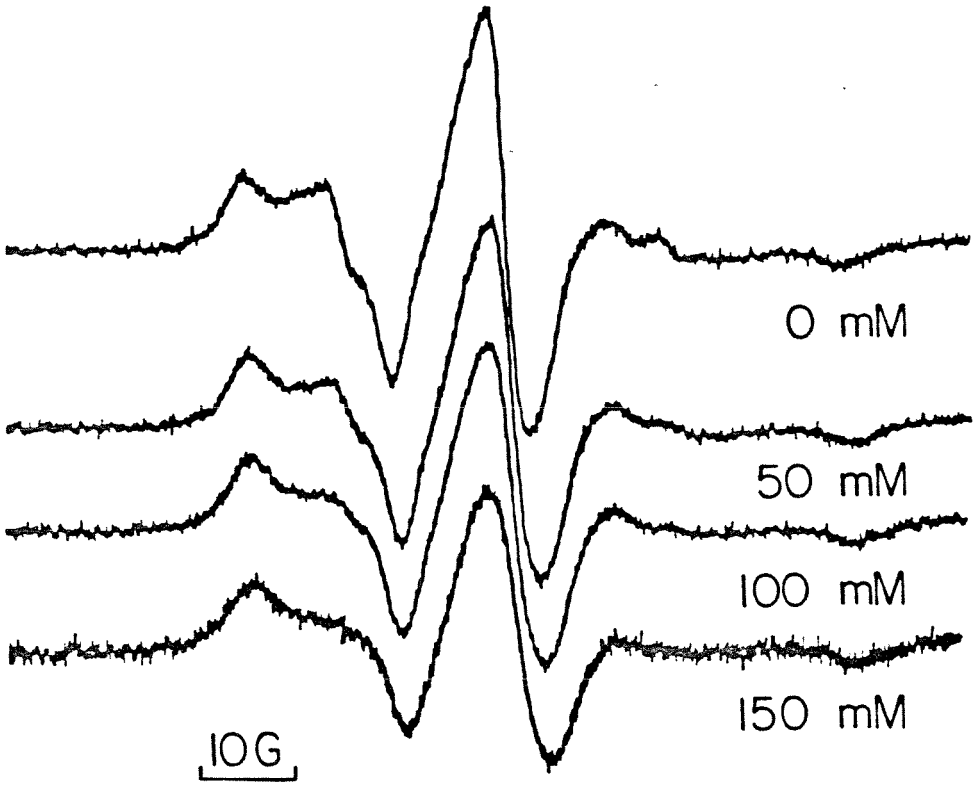

FIGURE 3

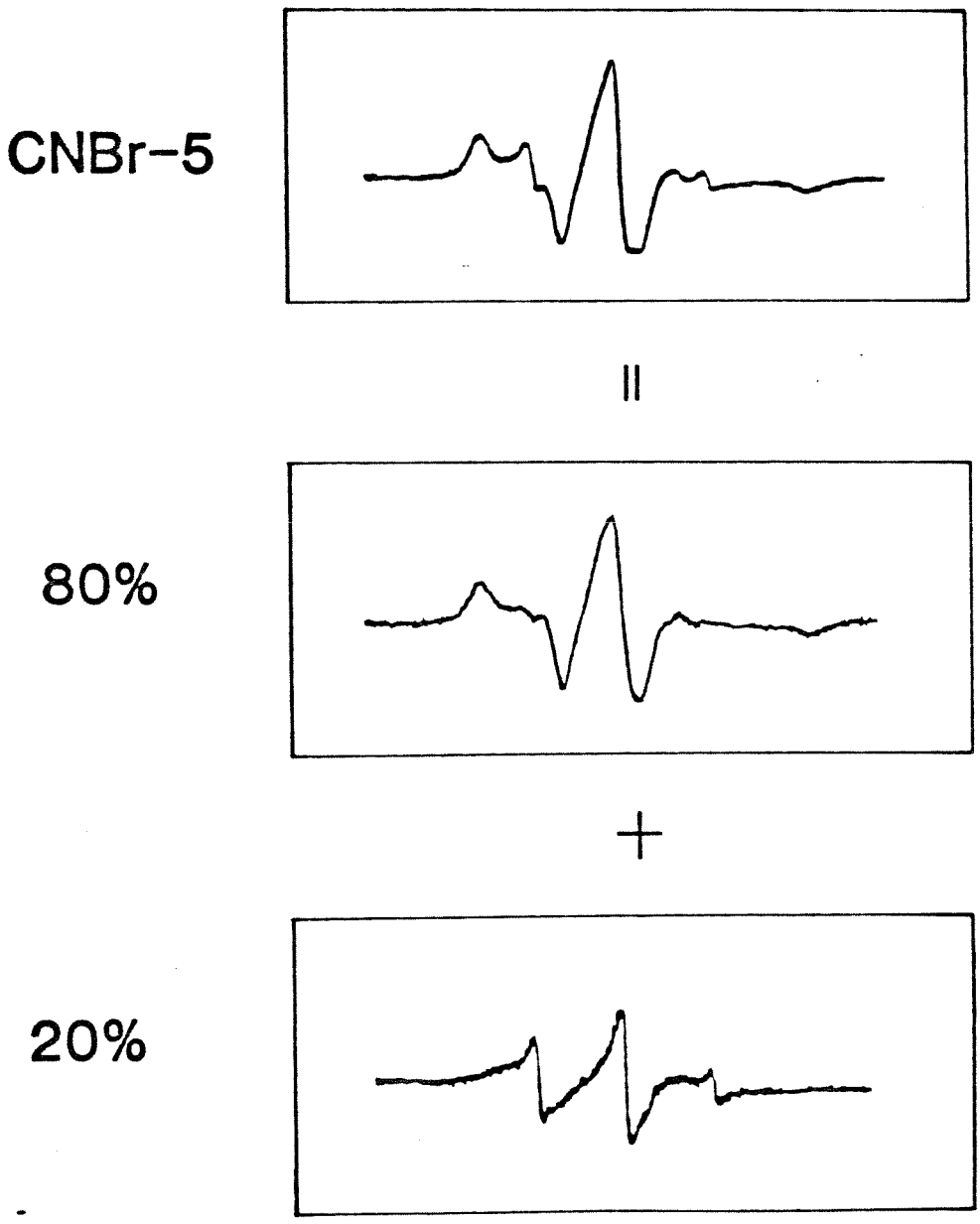

FIGURE 4

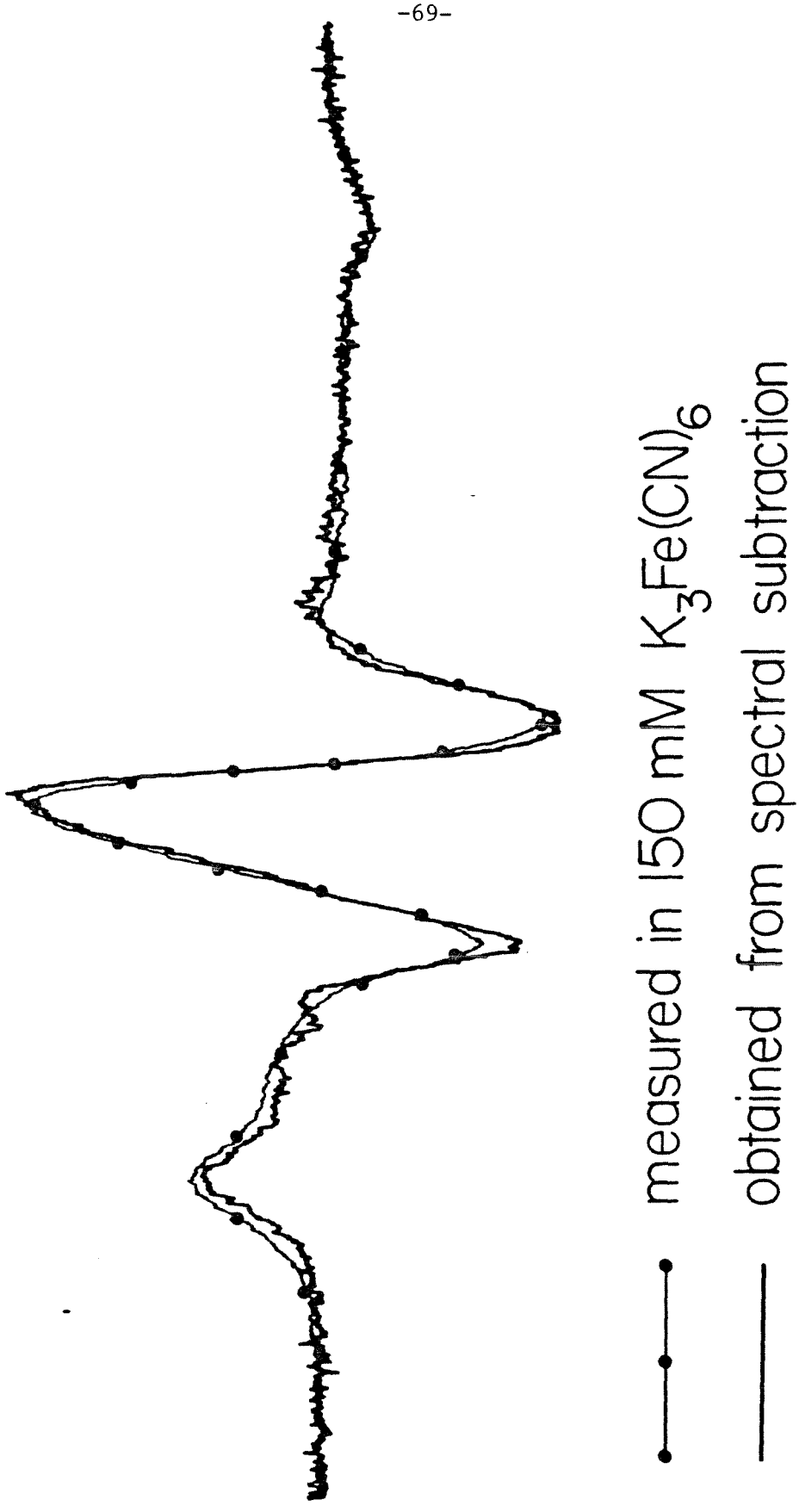
measured in 150 mM $K_3Fe(CN)_6$
obtained from spectral subtraction

FIGURE 5

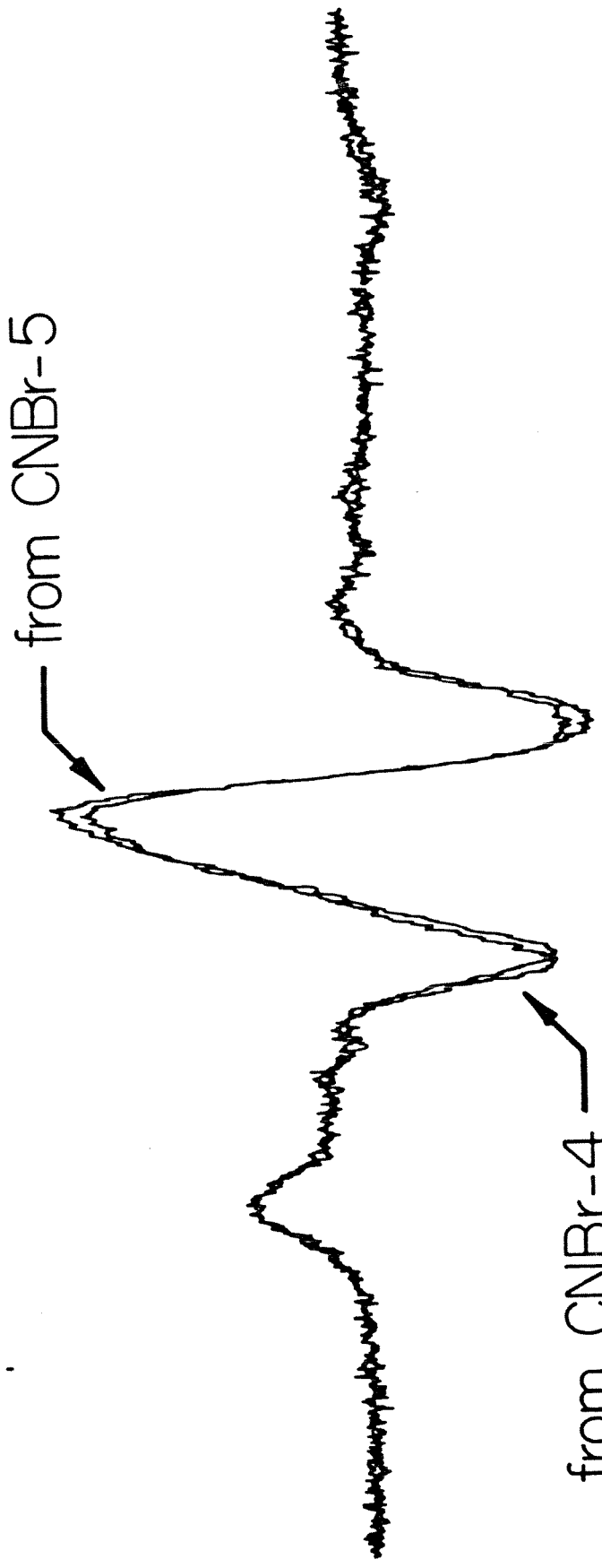

FIGURE 6

PART II: DETAILED ANALYSIS OF IMMOBILIZED CHYMOTRYPSIN DEACTIVATION IN ORGANIC SOLVENTS

CHAPTER 4: DEACTIVATION OF α-CHYMOTRYPSIN AND α-CHYMOTRYPSIN-CNBr SEPHAROSE 4B CONJUGATES IN ALIPHATIC ALCOHOLS

INTRODUCTION

Enzyme structure and function are profoundly influenced by the molecular environment of the protein. This environment is dictated by the aqueous solution in the case of enzymes in solution and by the combination of the solution milieu and nearby support structure in the case of immobilized enzymes. Also, in the latter situation, the immobilization event may perturb the native structure of the protein and also modify its molecular dynamics. While this view of immobilized protein structure and function is intuitively plausible, relatively little data exist which directly support these hypotheses.

In this work a combination of characterization methods including relatively recent EPR spectroscopy methods are applied to investigate and to characterize the molecular structure and catalytic activity of a particular enzyme, αchymotrypsin, in solution and in immobilized form. Previous investigations of αchymotrypsin covalently attached to CNBr Sepharose 4B have shown that the immobilized conjugate contains multiple enzyme forms[1,2]. First, an inactive form exists in approximately the same proportion to total immobilized enzyme as existed in the immobilizing solution. Second, it has been shown by EPR spectroscopy of spin-labeled α-chymotrypsin that immobilization alters the average active site structrure of the immobilized enzyme and also alters the intrinsic specific activity. Here similar methods are applied to investigate α-chymotrypsin in solution and in covalently immobilized form in solutions of aliphatic alcohols.

Previous studies have already shown that the activities of proteolytic enzymes such as α-chymotrypsin are particularly sensitive to the presence of aliphatic alcohols [3,4]. Several possible

mechanisms for loss of hydrolytic activity have been identified, although the extent to which each mechanism will contribute in a given situation remains somewhat difficult to predict. Transesterification, in which the alcohol competes with water in the nucleophilic deacylation of the enzyme-substrate intermediate, has been observed in a variety of cases [5-7]. Also important is competitive inhibition of protease activity caused by binding of alcohols to hydrophobic portions of the enzyme's surface; i.e., those regions that normally serve as secondary binding sites for polypeptide segments. This phenomenon, which has been studied with a number of proteases [8-10] including α-chymotrypsin [11,12], probably does not involve significant conformational changes of the enzyme molecule. If the alcohol concentration is sufficiently high, however, denaturation due to gross conformational changes and breakdown of tertiary structure can occur as a result of disorganization by the alcohol of the protein's hydrophobic interior [13,14]. Based on available data it appears that increasing chain length and hydrocarbon content generally correspond to increasing effectiveness of alcohols as protease inhibitors [3,4] and/or protein denaturants [15,16].

MATERIALS

The α-chymotrypsin (bovine pancreas, three times recrystallized, salt free), N-acetyl-L-tyrosine ethyl ester (ATEE), and 4-methylumbelliferyl-p-trimethyl ammonium cinnamate chloride (MUTMAC) were obtained from Sigma. 1-oxyl-2,2,6,6-tetramethyl-4-piperidinol was purchased from Aldrich. Methylphosphonic difluoride was obtained from Alfa. CNBr-Sepharose 4B was a product of Pharmacia Fine

Chemicals. Inorganic salts and all buffer solution components were analytical grade reagents. Distilled water, deionized by passage through two Research IonXchanger Model 2 columns supplied by Illinois Water Treatment Co., was used throughout.

METHODS

Immobilization procedure

α-Chymotrypsin was immobilized on CNBr-Sepharose 4B as described in Clark and Bailey [1].

Enzyme assays

Catalytic activity of the immobilized enzyme was assayed by measuring hydrolysis rates of ATEE. A detailed decription of the procedure has been presented elsewhere [1]. The quantity of catalytically active enzyme was determined by active site titration with MUTMAC. Active enzyme loadings before exposure of the catalysts to alcohol solutions were measured as described in [1].

Slightly different titration procedures were employed to determine the amount of active enzyme remaining after contact with the alcohols. In the case of the free enzyme, 0.1 ml of enzyme-alcohol solution was added at various times to 3.25 ml potassium phosphate buffer (pH 7.3, 1 M NaCl) containing 250 0.2 mM MUTMAC. For the immobilized enzyme, 0.1-0.2 ml of the immobilized enzyme-alcohol slurry was removed from the main reaction vessel at various times and added to a Millipore 13-mm ultrafiltration cell (cellulose ester filter, 8 μm mean pore diameter). Following filtration of the alcohol solution, 3.25 ml MUTMAC solution were passed through the filtration cell containing the catalyst (flow rate 8 ml/min) two times, then

transferred to the spectrofluorometer where the fluorescence of liberated product was measured. Appropriate controls showed that the total contact time between MUTMAC solution and catalyst under these conditions was more than sufficient for all of the enzyme to react.

Preparation of spin-labeled enzyme and EPR measurements

The spin label used in this study, 1-oxyl-2,2,6,6-tetramethyl-4-piperidynl methylphosphonofluoridate, was synthesized according to Morrisett, et al. [17]. α-Chymotrypsin in its soluble form was spin labeled by the procedure of Morrisett and Broomfield [18], except that acetonitrile was used in place of benzene. The immobilized enzyme was spin labeled in similar fashion: to 250 mg enzyme-Sepharose conjugate, in 5 ml .pa 0.1 M acetate buffer (pH 5) was added 0.5 ml acetonitrile containing a 100-fold molar excess of spin label. After two hours of gentle stirring at room temperature, the conjugate was washed and prepared for EPR analysis as described previously [1]. The EPR spectra were recorded in 1 mM acetic acid (pH 3.5) or in mixtures of 1 mM acetic acid (pH 3.5) and alcohol. All spectra were taken at room temperature at the X band using a Varian E-Line Century Series EPR Spectrometer interfaced to a Digital Equipment Corp. PDP-8/A minicomputer.

Deactivation conditions

To examine deactivation of the free enzyme, 2.5 ml n-propanol were added to 2.5 ml aqueous enzyme solution (4 mg α-chymotrypsin/ml), and at various times aliquots were removed for active site titration. Deactivation of the immobilized enzyme was studied by first isolating a quantity of immobilized enzyme from its aqueous storage solution

with the Millipore filtration cell, then transferring the conjugate into a scintillation vial containing the alcohol solution of interest (alcohol solutions consisted of the analytical grade alcohol and distilled, deionized water, pH 4.7, except for those used in the EPR measurements, as mentioned). The resulting slurry (20 mg catalyst/ml) was then stirred gently at room temperature with a magnetic stirrer and samples removed at given times for analysis.

RESULTS: α-CHYMOTRYPSIN IN SOLUTION

In order to establish a baseline for later immobilized enzyme studies, α-chymotrypsin in solution was exposed to a 50% n-propanol solution (final enzyme concentration: 0.95 mg active chymotrypsin/ml solution). Deactivation kinetics were almost impossible to measure because reduction in the quantity of active enzyme occurred so rapidly. The two data points obtained were as follows at 1 and 5 minutes after exposure to alcohol solution, the fraction of remaining active enzyme was 39% and 0.17%, respectively. These data show clearly that this environment is extremely active in denaturing the native form of the enzyme.

In order to gain further insights on the influence of alcohols on α-chymotrypsin deactivation in solution, spin-labeled enzyme was exposed to alcohol solution and the EPR spectrum of the preparation measured. Fig. 1 illustrates the spectra obtained in three different experiments. The top spectrum for the spin-labeled enzyme before exposure to n-propanol solutions provides a reference frame for the other spectra. The second frame shows the spin-labeled enzyme's EPR spectrum recorded in 50% n-propanol solution. Great sharpening in the

spectrum clearly indicates less restricted label motion which results from unfolding of the protein molecule. The EPR spectrum for spin-labeled enzyme in 90% n-propanol, shown at the bottom of Fig. 1, illustrates new modes indicative of appearance of a different class of enzyme forms with modified active-site structures. Interestingly, under these conditions, the enzyme is beginning to precipitate. This experiment suggests that EPR spectroscopy may be useful in studying modification of protein structure which results from intermolecular interactions which accompany aggregation.

RESULTS: α-CHYMOTRYPSIN-CNBr SEPHAROSE 4B CONJUGATES

Quantity of active enzyme

The influence of exposure to alcohol on the remaining amount of catalytically active immobilized chymotrypsin is determined by active site titration. The effects of different alcohols and of alcohol concentration on the kinetics of disappearance of active enzyme is illustrated in Fig. 2. These measurements clearly demonstrate that immobilization stabilizes α-chymotrypsin significantly. This result is consistent with the appreciable hydrolytic and synthetic activities in ethanol-glycerol solutions of immobilized chymotrypsin reported by Ingalls *et al*. [19] and with the stabilization effects of immobilization observed previously for the protease trypsin [20,21].

The kinetics of loss of active enzyme are very much different than observed for the enzyme in solution (shown for comparison in Fig. 2). Deactivation rates are significantly greater in n-propanol than in t-butanol. In all cases for the immobilized enzyme, the kinetics of active enzyme disappearance differ significantly from

first order. For each of the immobilized enzyme deactivation experiments, a fraction of the initially active enzyme remains active at the end of the indicated intervals of alcohol exposure. This implies that an enzyme subpopulation exists that is not deactivated by exposure on this time scale to these alcohols. The residual activity after two-hour exposure to alcohol depends upon the alcohol used and its concentration.

Experimental data plotted in Fig. 3 shows the time trajectory of active enzyme following exposure of immobilized enzyme catalyst formulations which differ in their initial content of active enzyme and initial specific activity to solutions of 50% n-propanol and 90% n-propanol. The deactivation kinetics have the general features just summarized. Interestingly, the loss of active enzyme kinetics are quite similar for the same alcohol solution for different preparations, although some differences are apparent.

Quantity of immobilized enzyme

The amount of enzyme associated with the α-chymotrypsin-CNBr Sepharose conjugate and the amount of enzyme and possible proteolysis products released into solution were measured by amino acid analysis after different exposure times to 50% n-propanol. The results are summarized in Table I. Also shown there for comparison is the quantity of active enzyme retained with the conjugate at the same exposure times. These data show some protein loss from the support. Examination of the amino acid profile of protein in solution (data not shown) provides some evidence of proteolysis. The amino acid distribution of the soluble protein is slightly different from that

characteristic of native α-chymotrypsin. The information in Table I clearly shows that the total loss of active enzyme is much greater than total loss of protein, indicating that exposure to alcohol solution inactivates significant quantities of immobilized enzyme. It is inactivation of the enzyme retained in the conjugate rather than enzyme removal from the conjugate that is the dominant deactivation process.

Catalytic activity

An α-chymotrypsin-CNBr Sepharose 4B conjugate containing initially 0.88 μmol active CT/g support was exposed to a 50% n-propanol solution in a gently agitated slurry. Samples were withdrawn intermittently, and the catalytic activity of the preparation for ATEE hydrolysis determined. The results are listed in Table II in terms of the observed activity per unit amount of catalyst preparation, in terms of the observed activity per unit amount of active enzyme (determined by parallel active site titration experiments) and diffusion-corrected intrinsic specific activities of active enzyme. The latter numbers are obtained by applying the procedure for extracting intrinsic activity information from diffusion-disguised activity data previously described [1].

These data illustrate several important points. First, the overall activity per unit amount of support, the quantity typically reported in enzyme deactivation studies, declines as expected as a result of exposure to alcohol. However, with the additional measurement of the quantity of enzyme which is active, the specific activity of what remains may be examined. The observed specific

activity increases dramatically. Here, however, caution must be exercised in interpretation because of diffusional effects. If the measured activity for the initial preparation is significantly influenced by diffusion limitations, as the amount of active enzyme in the preparation declines, the relative significance of diffusion relative to reaction limitations will decline. In other words, the effectiveness factor for the catalyst will increase. Such an effectiveness factor increase is expected to result in an increase in the observed specific activity. Consequently, it is important to decouple the substrate diffusion effects on measured overall activities from the intrinsic catalytic activity of the enzyme. The results of application of such a procedure, shown in the right-hand column in Table I, indicate that the intrinsic specific activity of active enzyme does not change nearly so much as the overall observed specific activity, clearly demonstrating a decline in the influence of diffusion resistance during the deactivation process. Much of the increase in specific activity shown in the observed specific activity column is due to this effect.

However, it is extremely interesting to note that the estimated intrinsic catalytic activity of the enzyme remaining active after different exposure times to 50% n-propanol solution increases somewhat as a result of exposure to alcohol. This indicates that much of the overall loss of catalytic activity of the immobilized enzyme conjugate is due to complete deactivation of some of the enzyme. Explanation of the increase in intrinsic specific activity during deactivation depends upon a detailed analysis of active enzyme subpopulations in

this catalyst which have been previously identified [2]. This analysis will be reported in a subsequent publication.

EPR observation of spin-labeled enzyme deactivation

The time sequence of EPR spectra for spin-labeled chymotrypsin-Sepharose exposed to 50% n-propanol is presented in Fig. 4. The front spectrum corresponds to spin-labeled chymotrypsin on Sepharose 4B before alcohol solution addition. The successive spectra shown were obtained at 4 minute intervals after addition of 50% n-propanol. Time increases in the direction indicated by the arrow.

The sharp, large-amplitude modes correspond to highly mobile label in substantially unfolded enzyme molecules. In this experiment, the effect of denaturation on the active-site local environment is shown directly. One unknown prior to these experiments was the extent to which exposure to alcohol might cause detachment of spin label from its attachment site in the enzyme active site. Such label detachment would limit the application of EPR spectroscopy for studying this kind of deactivation process. Significantly, the spectra shown here manifest no significant evidence of detached spin label. Consequently, EPR spectroscopy should be of quite general applicability in studying enzyme deactivation in alcohols provided that suitable active-site labels and labeling methods can be identified for the enzyme system of interest.

It was observed that the peak heights of the sharp modes which develop over time in these experiments might be used to indicate the kinetics of enzyme unfolding. Plotted in Fig. 5 is the time trajectory of the normalized reciprocal height of the first sharp mode

in the spectra shown in Fig. 4 as well as the analogous mode heights for a number of other successively measured spectra. Shown for comparison in Fig. 5 is the amount of active enzyme versus time as measured by active site titration. Interestingly, both types of experiments give similar behavior: an initial extremely rapid change, followed by a transition to a plateau with kinetic behavior clearly different from first order. These data demonstrate the possibility of using EPR data directly to determine deactivation kinetics.

These deactivation kinetics should be quite useful in understanding overall deactivation mechanisms which can depend upon a combination of changes in the molecule, with corresponding manifestations in catalytic activity. The interesting feature of deactivation kinetics monitored by EPR spectroscopy is direct access to information on active site structure so that one can determine the time course of structural modifications. Fig. 5 can be viewed as a confirmation of expected structure-function relationships since, as the quantity of enzyme with significantly unfolded active sites increases, so too is the quantity of catalytically active enzyme expected to decline.

DISCUSSION

The data presented above clearly illustrate the power of simultaneous application of complementary analytical and physical methods to the study of enzyme deactivation. Key measurements are active site titrations, which allow direct determination of the quantity of catalytically active enzyme, and EPR spectroscopy, which provides direct information on the conformation of the population of

protein molecules considered. The EPR spectrum for enzyme in solution with 90% n-propanol is consistent with multiple forms which can be tentatively identified as soluble and aggregated, precipitating enzyme. This indicates significant potential in a more general sense for EPR spectroscopy in investigating changes in protein configuration and consequently potential inactivation caused by aggregation in other systems. This may be of significance, for example, in the study of protein aggregation, solubilization, and reactivation encountered in the production of eucaryotic proteins in genetically engineered bacteria.

It was shown that the kinetics of enzyme unfolding can be monitored directly by EPR spectroscopy and that such measurements correlate closely with a functional assay based upon activity towards a suicide inhibitor (the active site titrant MUTMAC). The kinetics are clearly distinct from first order. An immobilized enzyme subpopulation exists which resists dectivation during 120 min. exposure to aliphatic alcohols. Qualitatively similar deactivation kinetics were observed for five different experiments involving two different immobilized chymotrypsin conjuates and three different alcohol solutions. By contrast, chymotrypsin in solution is rapidly deactivated under these conditions.

Acknowledgements. This work was supported by the National Science Foundation.

REFERENCES

1. Clark, D. S. and Bailey, J. E. (1983) Biotechnol. Bioeng. **25**, 1027-1047.

2. Clark, D. S. and Bailey, J. E. (1983) Biotechnol. Bioeng., in press.

3. Svendsen, I. (1971) C. R. Trav. Lab. Carlsberg **38**, 385-397.

4. Ralston, G. B. (1972) C. R. Trav. Lab. Carlsberg **39**, 25-31.

5. McDonald, C. E. and Balls, A. K. (1956) J. Biol. Chem. **221**, 993-1003.

6. Glazer, A. N. (1966) J. Biol. Chem. **241**, 635-638.

7. Klibanov, A. M., Samokhin, G. P., Martinek, K., and Berezin, I. V. (1977) Biotechnol. Bioeng. **19**, 1351-1361.

8. Hill, R. L. and Smith, E. L. (1957) J. Biol. Chem. **224**, 209-223.

9. Tang J. (1965) J. Biol. Chem. **240**, 3810-3815.

10. Sluyterman, L. A. E. (1967) Biochim. Biophys. Acta. **139**, 418-429.

11. Stein, B. R. and Laidler, K. J. (1959) Can. J. Chem. **37**, 1272-1277.

12. Clement, G. E. and Bender, M. L. (1963) Biochemistry **2**, 836-843.

13. Herskovits, T. T. and Jaillet, H. (1968) Fed. Proc. **27**, 771.

14. Herskovits, T. T., Gadegbeku, B., and Jaillet, H. (1970) J. Biol. Chem. **245**, 2588-2598.

15. Herskovits, T. T. and Jaillet, H. (1969) Science **163**, 282-285.

16. Parodi, R. M., Bianchi, E., and Cifferri, A. (1973) J. Biol. Chem. **248**, 4047-4051.

17. Morrisett, J. D., Broomfield, C. A., and Hackley, B. E., Jr. (1969) J. Biol. Chem. **244**, 5758-5761.

18. Morrisett, J. D. and Broomfield, C. A. (1972) J. Biol. Chem. **247**, 7224-7231.

19. Ingalls, R. G., Squires, R. G., and Butler, L. G. (1975) Biotechnol. Bioeng. **17**, 1627-1637.

20. Horvath, C. (1974) Biochim. Biophys. Acta. **358**, 164-177.

21. Weetall, H. H. and Vann, W. P. (1976) Biotechnol. Bioeng. **18**, 105-118.

TABLE CAPTIONS

Table I. Measured reaction rates and estimated intrinsic specific activities of immobilized chymotrypsin after different exposure times to 50% n-propanol. Parameters used in the calculation of intrinsic specific activities are: average radius R of the support particles, 60 μm effective diffusivity D_{eff} of ATEE through CNBr-Sepharose 4B, $3.8 \times 10^{-6} cm^2\ s^{-1}$; Michaelis constant K_m of immobilized enzyme, 1.7 mM [1].

Table II. Comparisons at different exposure times of the residual loading of active chymotrypsin with the amount of protein released into solution and remaining on the support.

Table I

Exposure time (min)	Overall Activity ($\frac{\mu mol\ ATEE}{g\ catalyst \cdot s}$)	Active Enzyme Content ($\frac{\mu mol\ active\ CT}{g\ catalyst}$)	Overall Specific Activity ($\frac{\mu mol\ ATEE}{\mu mol\ active\ CT \cdot s}$)	Intrinsic* Specific Activity ($\frac{\mu mol\ ATEE}{\mu mol\ active\ CT \cdot s}$)
0	9.12	0.875	10.4	35.5
5	7.43	0.519	14.3	39.7
65	4.89	0.249	19.6	38.4
120	4.39	0.199	22.1	39.8

*Measured at room temperature with 1mM ATEE in 0.1 M phosphate buffer, pH 7.3, 1 M NaCl.

Table II

Exposure time to 50% n-propanol (min)	Protein content in alcohol solution (mg/ml)	Total protein loading (mg/g catalyst)	Active enzyme loading (mg/g catalyst)
0	-	48.7	21.9
5	0.074	43.6	11.2
120	0.112	43.1*	4.50

*Calculated from mass balance and direct measurements of initial protein loading and protein content in alcohol solution.

FIGURE CAPTIONS

Figure 1: EPR spectra recorded at room temperature of spin-labeled α-chymotrypsin in 1 mM acetic acid solution, pH 3.5, mixed with n-propanol in proportions (v/v) as marked. Gain and power settings for each spectrum are (from top): 1.6, 5 mW; 2.5, 5 mW; 4.0, 30 mV.

Figure 2: Fraction of enzyme remaining active, determined by active site titration, versus exposure time to various alcohol solutions. Initial loadings of active immobilized chymotrypsin: -▽-, 0.922 μmols g^{-1}; -●-, average of runs with 1.09 and 0.967 μmols g^{-1}; -□-, 1.09 μmols g^{-1}. Free enzyme concentration in alcohol solution: -▲-, 0.474 mg ml^{-1}.

Figure 3: Active enzyme content as a function of exposure time to different alcohol solutions for various α-chymotrypsin-CNBr Sepharose conjugates. Initial active enzyme loadings: -△-, average of runs with 1.09 and 0.967 μmols g^{-1}; -●- average of two runs with 0.567 μmols g^{-1}; -○-, 0.623 μmols g^{-1}; -■-, 1.09 μmols g^{-1}.

Figure 4: EPR spectra of spin-labeled α-chymotrypsin-CNBr Sepharose (0.967 μmols active chymotrypsin g^{-1}) in 50% n-propanol. Front spectrum is of spin-labeled chymotrypsin on Sepharose 4B before addition of n-propanol. Successive spectra obtained at four minute intervals following addition of n-

propanol. Time increases in direction of arrow. All spectra were recorded at the same instrument settings.

Figure 5: Immobilized enzyme deactivation kinetics from EPR spectroscopy. Lower curve shows time sequence of denatured enzyme inverse EPR peak heights (see Fig. 4) of spin-labeled immobilized enzyme in 50% n-propanol. Shown for comparison is the amount of active enzyme versus time as measured by active site titration.

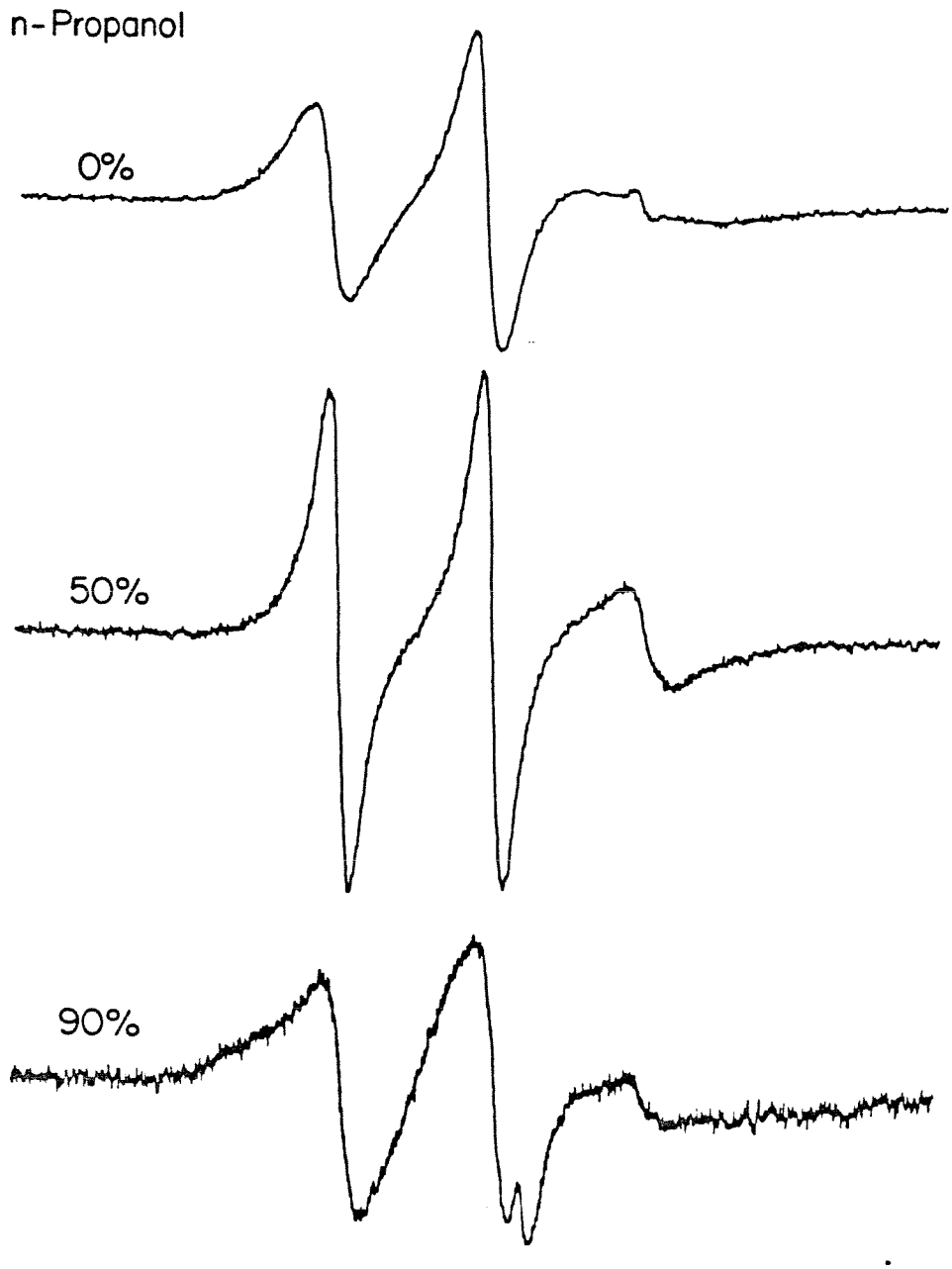

FIGURE 1

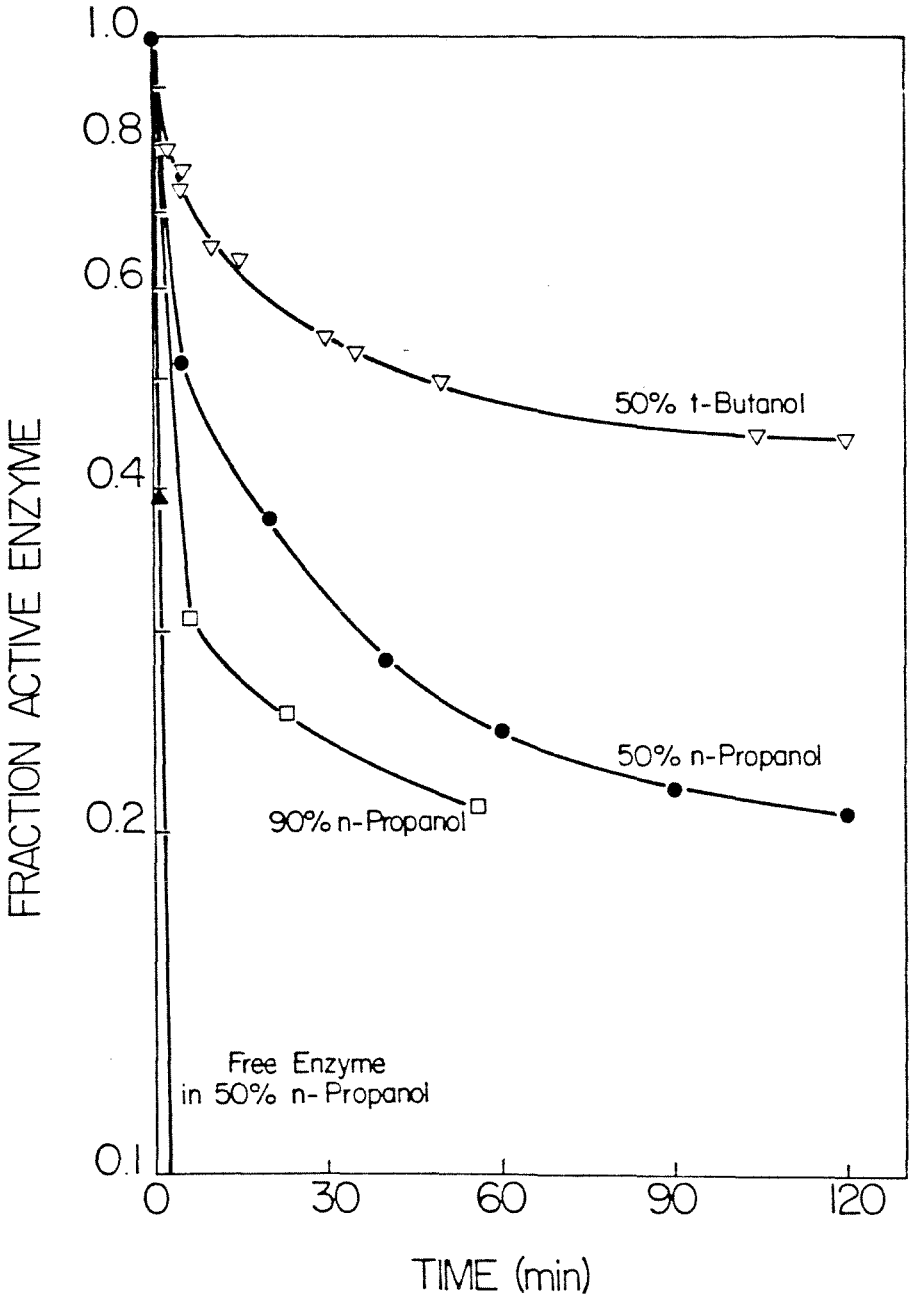
1.0
0.8
0.6
0.4
0.2
0.1
FRACTION ACTIVE ENZYME
50% t-Butanol
50% n-Propanol
90% n-Propanol
Free Enzyme
in 50% n-Propanol
0
30
60
90
120
TIME (min)

FIGURE 2

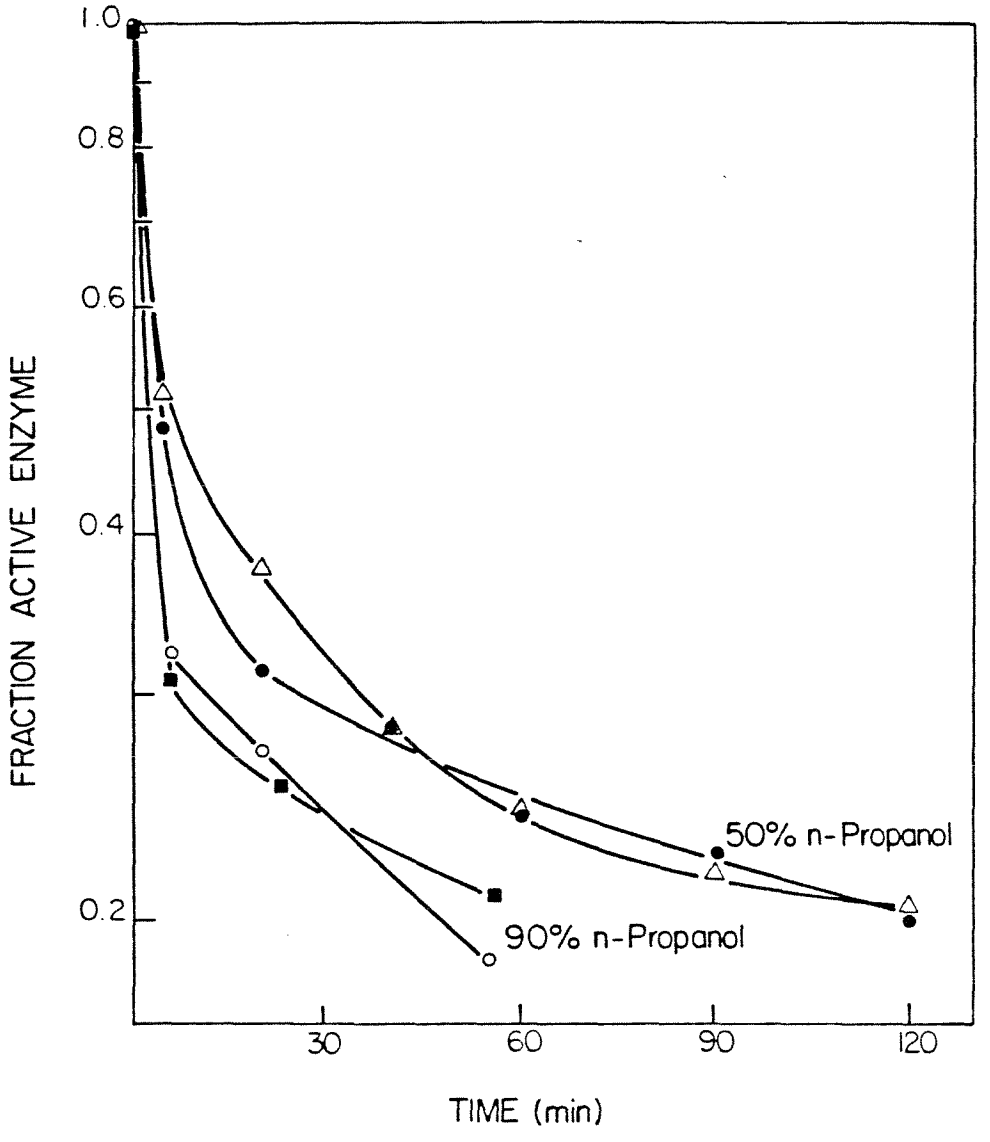
1.0
0.8
0.6
0.4
0.2
FRACTION ACTIVE ENZYME
50% n-Propanol
90% n-Propanol
30
60
90
120
TIME (min)

FIGURE 3

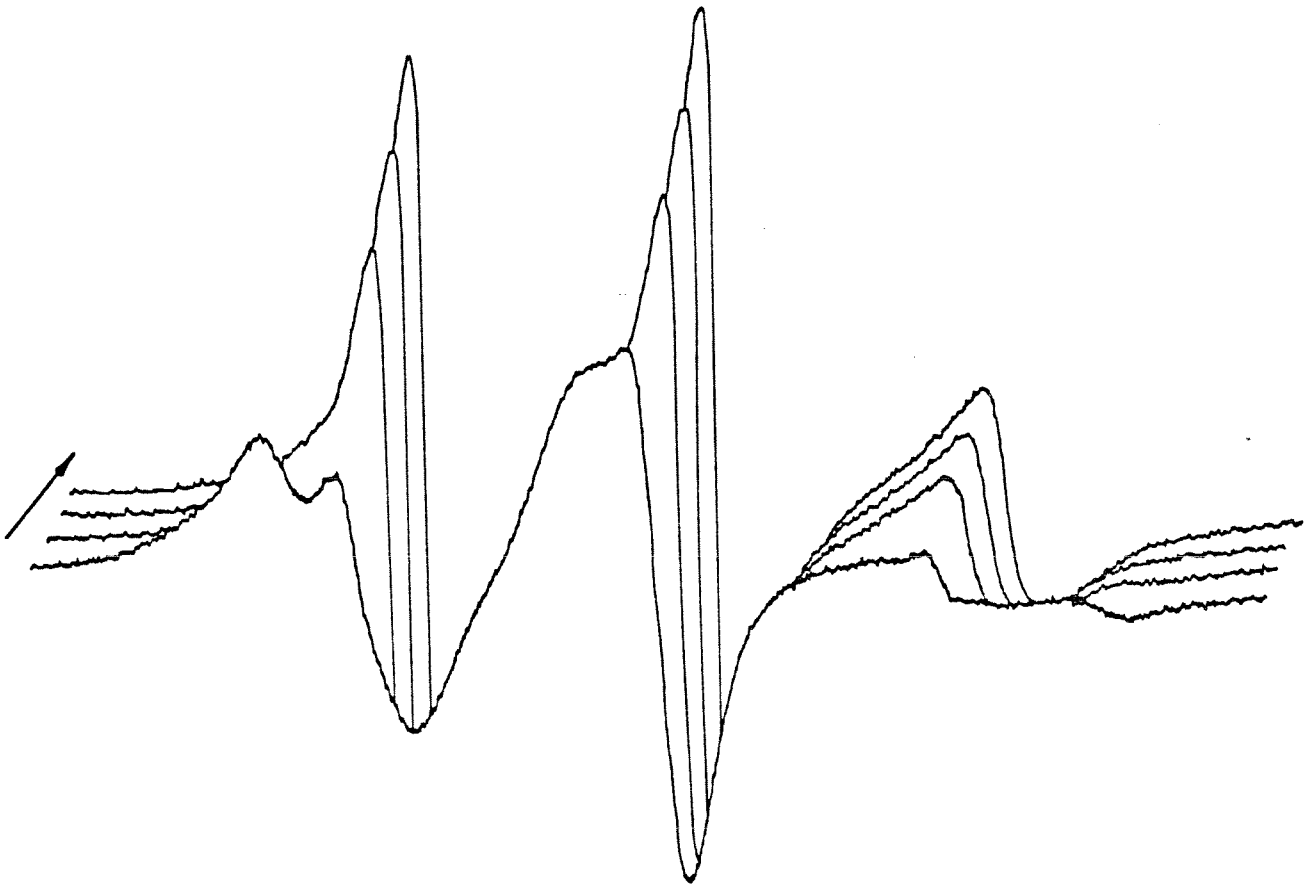

FIGURE 4

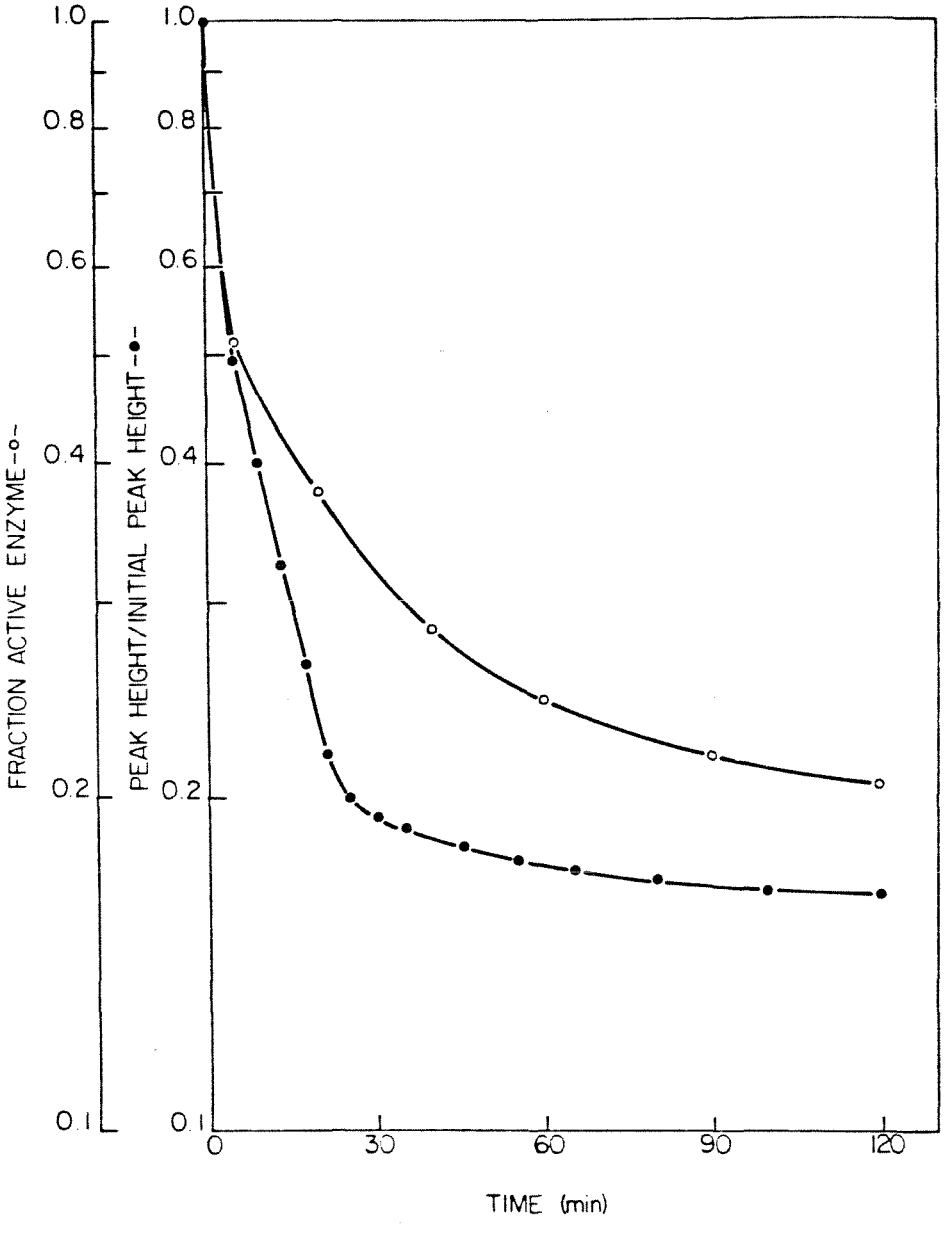
1.0
0.8
0.6
0.4
0.2
0.1
FRACTION ACTIVE ENZYME -o-
PEAK HEIGHT/INITIAL PEAK HEIGHT -●-
0
30
60
90
120
TIME (min)

FIGURE 5

CHAPTER 5: DEACTIVATION KINETICS OF IMMOBILIZED α-CHYMOTRYPSIN SUBPOPULATIONS

INTRODUCTION

The economic feasibility of many enzyme-catalyzed biotransformations hinges critically on the active lifetime of the enzyme catalyst. Despite substantial research, the mechanisms of enzyme deactivation in solution are poorly understood. Even more unknown are the deactivation processes which occur for immobilized enzymes. While many previous studies have reported alterations in deactivation kinetics as a result of enzyme immobilization, many of these investigations did not properly account for changing diffusion effects on observed activities. In these cases, it is not possible to define clearly whether or not immobilization actually has altered the intrinsic stability properties of the protein.

Many experimental studies have shown that the kinetics of enzyme deactivation in denaturing environments often differ substantially from first-order decay. A number of alternative mechanistic hypotheses and corresponding mathematical models have been proposed to describe such deactivation processes. These include the two-stage deactivation model in which an active enzyme form undergoes a reversible transition to an inactive form in the first stage transition, followed by a second stage transition of the reversibly inactived form to another inactive form via an irreversible step.[1] Alternate models have been formulated in which a distribution of states among the active enzyme molecules is hypothesized.[2] Then, assuming that different states deactivate at different rates, overall population deactivation differs significantly from first order.

Unfortunately, when the only experimental data available are the time trajectory of enzyme activity, there is a large set of

alternative deactivation models which can equally well fit the experimental data. In such circumstances, one must view models which successfully fit the data only as acceptable candidates and not as identified deactivation mechanisms. The ability to fit certain data with a given model in no way proves that the model is correct – only that the model is consistent, possibly among many possible consistent models. This aspect of modeling logic has been frequently overlooked in previous examinations of deactivation kinetics.

In this investigation, a variety of experimental methods have been applied in concert to characterize in detail deactivation kinetics of α-chymotrypsin-CNBr-Sepharose 4B conjugates. The most critical data in this investigation, which focus upon the parallel deactivation of different active forms of immobilized enzyme, are EPR spectroscopy. It has been shown previously that the motion of a spin label attached at a specific point in the active site of α-chymotrypsin, as manifested by the label's EPR spectrum, provides sensitive information on the molecular state and catalytic activity of the protein molecule.

In previous research on a variety of different preparations of immobilized α-chymotrypsin, it was shown that the immobilized enzyme consists of two different active forms, which will be designated here A and B.[3] The characteristic EPR spectra of the spin-labeled form of A and B immobilized enzyme have been defined, and this information has been used to determine the relative amounts of A and B forms resulting from different immobilization procedures and supports. Combining such information with catalytic activity measurements of these different supports, the initial intrinsic activity of each enzyme form has been

estimated. This analysis has shown that form A, in which the spin-label motion is much more constricted than in form B, possesses approximately 15 times less activity than does form B. This is consistent with intuitive expectations on the relationship between active site structure and the efficiency of enzyme function, and is the first report of this type known to the authors for immobilized enzymes.

With this knowledge of the initial state of the system established and with access to extremely powerful tools for characterization of immobilized enzyme at the molecular level, this work explores the deactivation behavior of the A and B immobilized enzyme subpopulations in the presence of a solution containing 50% n-propanol. It has been shown previously that, in this environment, globular proteins in solution exist in unfolded and/or ordered helical forms, presumably because of interference with intramolecular hydrophobic interactions.

MATERIALS AND METHODS

Materials and methods for preparation of α-chymotrypsin-Sepharose 4B conjugates, for assay of enzyme catalytic activity, for determination of the quantity of active enzyme, and for spin labeling the enzyme with spin label m-IV[4] and with an organophosphate spin label[5] have been previously described.[6,7]

Two new procedures were implemented in this work in order to apply EPR spectroscopy to analysis of subpopulation responses to deactivation. In order to examine perturbations in active site structure of active enzyme caused by deactivation, the following

procedure was applied: 0.20 grams of immobilized enzyme catalyst were exposed to 10 ml of 50% n-propanol (pH 7.2). Intermittently, 0.10 gram samples of immobilized enzyme samples were withdrawn from the deactivation reactor and reacted with spin label m-IV as previously described. However, a modified washing procedure was then employed; the labeled enzyme was continuously flushed with 9% v/v acetonitrile in 1 mM acetic acid for 5 min. After this washing, the sample was transferred to the EPR spectrometer (Varian E-Line Century Series interfaced to a Digital Equipment Corp. PDP-8/A minicomputer) and the EPR spectrum of the sample was recorded intermittently.

A somewhat different procedure, based in part on the results of the previous experiment, was applied in order to estimate the fractions of A and B enzyme forms remaining active after different exposure times to n-propanol solution. Samples withdrawn from the deactivation reactor were labeled as previously described and washed for 16 hours. EPR spectra were then recorded and decomposed into A and B components by the previously described method,[3] the spectrum of either the A or the B form identified in previous studies of the initial immobilized enzyme preparation was subtracted from the overall spectrum until the difference spectrum showed no features indicative of two populations and also no physically unreasonable features. As noted previously[3], this procedure, while apparently somewhat subjective, is quite sensitive and offers estimates of the active A and B fractions without significant ambigiuity.

A CONCEPTUAL VIEW OF DEACTIVATION

Earlier investigation of chymotrypsin covalently attached to CNBr-Sepharose provided clear evidence of the existence of two different active forms of immobilized enzyme. Further evidence is now available based upon EPR measurements of α-chymotrypsin in solution and immobilized chymotrypsin, both labeled with a different stable nitroxide. In previous work with spin-label m-IV, it was necessary to add indole, a competitive inhibitor of the enzyme, to the spin-labeled enzyme sample in order to provide clear resolution of multiple population features in the immobilized enzyme spectrum. As shown in Fig. 1, these differences are clearly manifested without the addition of indole for the organophosphate spin label. The upper spectrum is typical of a relatively homogeneous population of immobilized-enzyme active site environments and corresponding spin-label motions, while the lower spectrum for the immobilized enzyme exhibits features clearly indicative of at least two forms of immobilized enzyme.

Since the immobilized enzyme catalyst before deactivation contains two different active enzyme forms, the simplest representation of the deactivation process involves four parallel steps indicated in Fig. 2. Both enzyme forms may undergo a transition to a completely inactive form. In parallel, both enzyme forms may be perturbed into altered forms which, although still catalytically active, possess reduced activity relative to the initial enzyme state. It should be noted that, given the potentially diverse nature of the population of immobilized enzyme molecules and their potentially complex, multistep responses to denaturing environments, this view is likely extremely oversimplified. However, it has only proven possible

in research to date to provide experimental data at a level of resolution compatible with the conceptual view shown in Fig. 2.

SUBPOPULATION DEACTIVATION KINETICS

Applying methods described above, it is possible to spin label immediately after some interval of exposure of n-propanol the enzyme subpopulations which are catalytically active at that point. While direct demonstration of the correspondence between ability to label an enzyme molecule and its ability to catalyze substrate conversion has not been proven conclusively for deactivated immobilized enzymes, there is substantial evidence in favor of this correspondence for the enzyme in solution.[8] Investigations of α-chymotrypsin immobilized on CNBr-Sepharose 4B prior to deactivation support the validity of this correspondence for the immobilized enzyme. For a number of different preparations possessing different contents of active enzyme, the quantity of catalytically active enzyme as detemined by active site titration is directly proportional in each case with the quantity of spin-labeled enzyme determined by double integration of the EPR spectrum. Accordingly, it is reasonable to apply this hypothesis to immobilized enzyme after exposure to denaturing conditions.

After a relatively short wash to remove unattached spin label, the spin-labeled immobilized enzyme was transferred to the EPR spectrometer and the spectrum was recorded after different times. The results, presented in Fig. 3, contain a number of interesting features. The line shape in the neighborhood of the mode labeled A, characteristic of enzyme form A, does not change significantly. However, the other mode characteristic of enzyme form B is

substantially accentuated immediately after the wash. This may be a direct observation of the altered active site configuration of a modified form of immobilized enzyme B which, although retaining ability to react with the label, allows significantly greater label mobility, expected for a partially unfolded active site, than does the initial form of immobilized enzyme chymotrypsin-B. As time proceeds, the sharply perturbed B mode relaxes, approaching after twelve hours a lineshape closely approximating that of enzyme form B initially.

This result suggests a strategy for estimating the relative quantities of immobilized chymotrypsin-A and immobilized chymotrypsin-B remaining active after different intervals of deactivation. Since the EPR spectra of form A and form B in the initial state are known from previous studies, one can extract a sample from the denaturing environment and apply spin label so as to label only the A and B enzyme remaining active at that point in time. Then, by washing that spin-labeled preparation for twelve hours or longer, the spectra components contributed by forms A and B will relax to the known spectra characteristic of the initial enzyme forms. Spectral decomposition methods may then be applied to determine the amount of A and B forms which were spin labeled after sampling.

Fig. 4 shows the indole EPR spectra of α-chymotrypsin-Sepharose 4B conjugates obtained by this method. The exposure times to 50% n-propanol prior to sampling and spin labeling are indicated on the figure. Visual examination of this data clearly shows that the relative quantities of active chymotrypsin-A and active chymotrypsin-B change as a result of exposure to alcohol with the relative quantity of the B-form increasing with time.

Results indicating the success of the refolding procedure and the EPR spectral decomposition methodology are shown in Fig. 5. In this example, immobilized chymotrypsin after exposure to 50% n-propanol for 5 minutes was spin labeled, washed extensively, and analyzed on the EPR spectrometer. The EPR spectrum of enzyme form B in its initial state, which is the same as the indole EPR spectrum of the enzyme in solution, was subtracted from the overall sample spectrum until the specified criteria were satisfied. Fig. 5 shows the residual spectrum obtained in this way along with the spectrum of enzyme form A in its initial state. While not exact, the correspondence between the two spectra is excellent considering the complexity of these measurements. This result and others like it for different exposure times to n-propanol support the applicability and validity of the applied methodology.

By means of this procedure, the fractions of active immobilized chymotrypsin-A and immobilized chymotrypsin-B (α_A and α_B, respectively) were determined as a function of exposure time to denaturing conditions. Combined with active site titration data providing the total quantity of active enzyme at the same times, the catalyst content of active form A and active form B, e_A and e_B, respectively, have been determined. These results are listed in Table I. Caution should be exercised in inferring from these results that the A and B forms deactivate by different kinetics. As shown in the Appendix, shifts in the active form distribution may occur in many cases in which each subpopulation has the same deactivation kinetics.

The specific activity based upon total active enzyme, v(t), may be written at time t in the form

$$\alpha_A(t)v_A(t) + \alpha_B(t)v_B(t) = v(t) \quad . \tag{1}$$

With the addition of intrinsic catalytic activity measurements, this is a single equation in two unknowns, the specific activities of the A and B enzyme forms, at each time t. However, based upon other information, it is possible to make reasonable hypotheses which allow application of Eq. (1). It was observed in the EPR data shown in Fig. 3 that exposure to alcohol, while preferentially completely inactivating some enzyme of form A, did not alter substantially the EPR spectrum of the chymotrypsin-A remaining active. Accordingly, as one plausible model, it may be assumed that the specific activity of enzyme form A is not substantially altered by exposure to alcohol, corresponding to the statement

$$v_A(t) = v_{A_0} \quad , \tag{2}$$

where v_{A_0} is the initial specific activity of enzyme form A. As an alternative, it might be assumed that both forms of active enzyme lose activity in constant proportion, giving rise to a second hypothesis,

$$v_A(t) = f(t)v_{A_0} \tag{3.1}$$

$$v_B(t) = f(t)v_{A_0} \tag{3.2}$$

Applying experimental data for v(t) and subpopulation fractions $\alpha_A(t)$ and $\alpha_B(t)$ from EPR analyses, the specific activities of enzyme forms A and B after different deactivation intervals may be estimated by applying Eq. (1) together with either Eq. (2) or Eq. (3). The results of such calculations are listed in Table II. While these

results must be viewed with some reservation because of the necessity of invoking certain hypotheses in determining these numbers, it is interesting to note that the important trends are the same for both of the hypothetical models represented by Eqs. (2) and (3). The activity of enzyme form B, by far the more active enzyme form, remains relatively constant during the initial 60 min. of deactivation but then decreases signficantly.

RELATIONSHIP BETWEEN IMMOBILIZATION AND DEACTIVATION SEQUENCE

In previous investigations in which different quantities of α-chymotrypsin were immobilized on CNBr-Sepharose, it was observed that the fraction of chymotrypsin-A increased as the quantity of enzyme affixed to the support increased. The present investigation shows a reverse effect. As enzyme activity is removed by deactivation, enzyme of form A deactivates completely more rapidly than does form B, causing an increase in the fraction of chymotrypsin-B as the quantity of active enzyme is reduced. This observation suggests the following interesting question: Is there a one-to-one relationship between the amount of active enzyme and the proportions of A and B forms independent of how one arrives at that amount of active enzyme?

This interesting possibility has been explored based upon the methods and data presented above. Two different immobilized enzyme conjugates possessing approximately the same quantity of active enzyme were prepared in two completely different ways first, by an immobilization process giving that quantity of active enzyme, and, second, by preparing a catalyst containing an initially greater amount of active enzyme which was then reduced by exposure to 50% n-propanol

to the same amount of active enzyme as the first preparation. These two preparations were then spin labeled and examined by EPR spectroscopy. The spectrum for each is shown in Fig. 6. The nearly identical lineshapes in the two cases strongly suggest that the distribution of A and B forms is a function of total active enzyme loading but not of the means of producing that loading.

Further evidence for a one-to-one correspondence between active enzyme content for a particular support and the fractions of A and B forms is contained in Fig. 7. Shown there are data based upon a number of different preparations with different initial loadings of active enzyme illustrating the relationship between the amount of active enzyme immobilized and enzyme-A fraction. Shown also are data obtained during the time course of deactivation of another immobilized enzyme preparation using a similar Sepharose material. While the latter points are consistently above the former, the similarity in the suggested functional relationship in the two quite different cases is surprising, considering the potential experimental error in the measurements.

DISCUSSION

EPR spectroscopy of spin-labeled enzyme, allied with associated measurements of catalytic activity and the quantity of active immobilized protein, has provided unprecedented insights into the deactivation events which occur when α-chymotrypsin-CNBr-Sepharose 4B conjugates are exposed to 50% n-propanol. The results provide a clear explanation for the counterintuitive experimental observation that the overall specific activity of active enzyme increases during the deactivation process. Based upon the information given in Tables I

and II, this behavior is clearly deciphered. While overall activity declines substantially as a result of exposure to alcohol, this is due primarily to complete inactivation during the initial 60 min. of forms A and B. Form B, which has much lower specific activity than form A, is preferentially deactivated. The result is a shift in the distribution of the two enzyme forms, resulting in an increase in the relative amount of the much more active form A. This result is proven by the direct EPR data itself (Fig. 4) and stands in spite of any possible reservations about the spectral decomposition calculations and subpopulations specific activity estimates.

Observation of a relationship between the quantity of active enzyme immobilized and the fraction of A and B active forms which applies both to preparation of the catalyst and to its deactivation offers some basis for hypotheses concerning the origin of the A and B forms and the identity of those enzyme subpopulations most labile in the presence of alcohol. The results summarized in Figs. 6 and 7 suggest that the last enzyme immobilized is the first enzyme to deactivate. This may occur because enzyme molecules binding to the surface initially occupy certain preferred sites which perturb the native enzyme structure relatively little (larger perturbations imply greater increases in free energy of the molecule) and that subsequent enzyme attachment to the surface occurs at different, less favorable sites which cause more substantial disruption of molecular structure. The greater tendency to immobilize enzyme in A form as more enzyme is attached may be due either to an *a priori* heterogeneity in the support material (different binding groups, binding group densities, gel structure) or due to induced heterogeneity because of interactions of

enzyme which attaches later with those protein molecules already established on the surface. These alternative mechanisms for heterogeneity in adsorption and chemisorption are well known for adsorption of gases and liquids on surfaces.[9]

Interestingly, this research has shown that the enzyme which immobilizes last has the most perturbed collection of active site environments and perhaps also the largest free energy increase relative to the native enzyme form in aqueous solution. These more perturbed molecular forms are apparently more vulnerable to further unfolding to inactive states in the presence of n-propanol.

In addition to providing detailed information on a particular immobilized enzyme catalyst, these studies demonstrate a powerful and potentially generalizable methodology for the study of immobilized enzyme systems. EPR spectroscopy, which can be applied to opaque samples and which provides sensitive information directly about the active site environment and perturbations of that environment, warrants significantly greater development and emphasis as a tool for characterization and eventually for optimization of immobilized enzyme catalysts.

ACKNOWLEDGEMENT

This work is supported by the National Science Foundation.

REFERENCES

1. R. Lumry and H. Eyring, J. Phys. Chem., **58**, 110 (1954).

2. Y. Kawamura, K. Nakanishi, R. Matsuno, and T. Kimikubo, Biotech. Bioeng., **23**, 1219 (1981).

3. D. S. Clark and J. E. Bailey, Biotechnol. Bioeng., in press.

4. L. J. Berliner and S. S. Wong, J. Biol. Chem., **249**, 1668 (1974).

5. J. D. Morrisett, C. A. Broomfield, and B. E. Hackley, Jr., J. Biol. Chem., **244**, 5758 (1969).

6. D. S. Clark and J. E. Bailey, Biotechnol. Bioeng., **25**, 1027 (1983).

7. D. S. Clark and J. E. Bailey, Biochim. Biophys. Acta, submitted.

8. S. S. Wong, K. Quiggle, C. Triplett, and L. J. Berliner, J. Biol. Chem., **249**, 1678 (1974).

9. J. N. Thomas and W. J. Thomas, Introduction to the Principles of Heterogeneous Catalysis (Academic Press, London, 1967).

10. V. W. Weekman, Jr., I&EC Process Design Develop., **7**, 90 (1968).

11. R. T. Struck, W. E. Clark, P. J. Dudt, W. A. Rosenhoover, C. W. Zielke, and E. Corin, I&EC Process Design Develop., **8**, 546 (1969).

12. F. H. Johnson, H. Eyring, and M. J. Polissar, The Kinetic Basis of Molecular Biology (John Wiley, New York, 1954).

13. J. P. Cardoso and A. N. Emery, Biotechnol. Bioeng., **20**, 1471 (1978).

14. Y. Kawamura, K. Nakanishi, R. Matsuno, T. Kamikubo, Biotechnol. Bioeng., **23**, 1219 (1981).

APPENDIX: ENZYME SUBPOPULATION DYNAMICS AND DEACTIVATION KINETICS

Studies of the overall kinetics of large sets of parallel reactions, often conducted previously in the context of hydrocarbon processing, have shown that both power law kinetics (e.g., second order)[10] and a weighted sum of decaying exponential functions[11] can usefully approximate overall composition -time trajectories. Since enzyme deactivation is conceptually similar to these reaction networks, the same types of kinetics are expected to be appropriate for describing overall activity decay, and, indeed, both kinetic models have been applied previously to describe enzyme deactivation.[12-14] Analysis of experimental data for active enzyme decay kinetics of α-chymotrypsin-CNBr Sepharose 4B conjugates in 50% n-propanol[7] shows reasonable approximation by

$$\frac{de}{dt} = -ke^N \qquad \text{(A1)}$$

where $k = 0.166\ (\mu mol/g)^{-2.23} min^{-1}$ and $N = 3.23$. While perhaps less appealing on a mechanistic basis (which actually has no sound foundation unless presumed intermediates are detected and monitored directly) than alternative models, this form of kinetics representation is advantageous for the following analysis.

Considering the change with time in the relative fractions of A and B active enzyme forms decribed above, it might be appealing to propose different deactivation kinetics for the two types of active enzyme. However, as will be shown next, shifts in the distribution of A and B forms are expected in many cases even when both A and B enzyme types deactivate with exactly the same power-law kinetics. To show this, assume that decay of enzyme-A and enzyme-B are described by

$$\frac{de_A}{dt} = -ke_A^N \quad ; \quad e_A(0) = e_{A_0} \tag{A2}$$

$$\frac{de_B}{dt} = -ke_B^N \quad ; \quad e_B(0) = e_{B_0} \tag{A3}$$

respectively.

For $N \neq 1$, the solution of these equations is

$$e_i(t) = e_{io}\left[1+(N-1)e_{io}^{N-1}kt\right]^{\frac{1}{1-N}} \quad ; \quad i = A,B \ . \tag{A4}$$

For $N<1$, this equation applies up to time $(1-N)^{-1}e_{io}^{1-N}k^{-1}$, after which $e_i = 0$. Based on the overall deactivation behavior observed for immobilized α-chymotrypsin, the case $N>1$ is of primary interest. For $N<1$, the analysis is restricted to times t sufficiently small so that both e_A and e_B are nonzero.

The fractions of active enzyme in forms A and B at time t are given by

$$\alpha_i(t) = \frac{e_i(t)}{e_A(t)+e_B(t)} \quad ; \quad i = A,B. \tag{A5}$$

The central objective of this analysis is to investigate the redistribution of the active enzyme forms as deactivation occurs. For this system with two active enzyme types, the redistribution can be characterized by the direction (sign) of the change with time of the ratio of α_A to α_B which is given by

$$\frac{d}{dt}\left(\frac{\alpha_A}{\alpha_B}\right) = \frac{d}{dt}\left(\frac{e_A}{e_B}\right) , \tag{A6}$$

where Eq. (A5) has been used to obtain the right-hand side.

Conducting the differentiation indicated on the right-hand side of Eq. (A6) and using Eqs. (A2) and (A3) to write the time derivatives of e_A

and e_B in terms of e_A and e_B yields

$$\frac{d}{dt}\left(\frac{\alpha_A}{\alpha_B}\right) = \left(\frac{ke_Ae_B}{e_B^2}\right)\left(e_B^{N-1} - e_A^{N-1}\right) \quad . \tag{A7}$$

Since the first term on the right-hand side of Eq. (A7) is never negative, it follows that

$$\text{sgn}\left[\frac{d}{dt}\left(\frac{\alpha_A}{\alpha_B}\right)\right] = \text{sgn}\left[e_B^{N-1} - e_A^{N-1}\right] \quad , \tag{A8}$$

where sgn (·) denotes the sign or signum function. Applying Eq. (A4), one obtains

$$e_B^{N-1} - e_A^{N-1} = \frac{e_{B_0}^{N-1} - e_{A_0}^{N-1}}{[1+(N-1)e_{B_0}^{N-1}kt][1+(N-1)e_{A_0}^{N-1}kt]} \quad . \tag{A9}$$

Since the denominator of the right-hand side of Eq. (A9) is always positive under the conditions of interest,

$$\text{sgn}\left(e_B^{N-1} - e_A^{N-1}\right) = \text{sgn}\left(e_{B_0}^{N-1} - e_{A_0}^{N-1}\right) \quad . \tag{A10}$$

Combining Eqs. (A8) and (A10) gives the final result

$$\text{sgn}\left[\frac{d}{dt}\left(\frac{\alpha_A}{\alpha_B}\right)\right] = \text{sgn}\left[e_{B_0}^{N-1} - e_{A_0}^{N-1}\right] \quad . \tag{A11}$$

This equation shows that the active enzyme distribution will change in many

cases throughout the deactivation process so long as both active forms coexist. Table AI summarizes the different possible situations as revealed by Eq. (A11)(a separate, straightforward analysis gives the N = 1 result). It is interesting that the sign of $d(a_A/a_B)/dt$ depends only on the kinetic order N and the <u>initial</u> concentrations of e_A and e_B. This implies that the a_A/a_B ratio changes in the same direction throughout the deactivation process. This analysis shows that observed shifts in the active subpopulation distribution do not necessarily imply different kinetics for subpopulation deactivation.

TABLE AI

Relationships among deactivation kinetics order N, initial active enzyme distribution, and the change in the active enzyme distribution ($\alpha_A/\alpha_B = e_A/e_B$) with time during deactivation based on the model described in the Appendix.

N	e_{A_0}/e_{B_0}	α^A/α^B
>1	>1	decreases
>1	<1	increases
any	1	constant
1	any	constant
<1	>1	increases
<1	<1	decreases

TABLE I

Influence of different exposure times to 50% n-propanol on the A and B immobilized enzyme active subpopulation content (e) and fractions (α) of chymotrypsin (CT)-Sepharose 4B conjugates

Exposure time to 50% n-propanol (min)	α_A	e_A $\frac{\mu mols\ active\ CT}{g\ catalyst}$	α_B	e_B $\frac{\mu mols\ active\ CT}{g\ catalyst}$
0	0.80	0.70	0.20	0.18
5	0.75	0.39	0.25	0.13
65	0.76	0.19	0.24	0.059
120	0.67	0.13	0.33	0.066

TABLE II

Specific activities ($\mu mol \cdot ATEE \cdot sec^{-1} \cdot (\mu mol\ active\ chymotrypsin)^{-1}$) of immobilized enzyme subpopulations after different exposure times to alcohol. Overall activities were measured at room temperature with 1 mM ATEE in 0.1 M phosphate buffer, pH 7.3, 1 M NaCl, and corrected for diffusion limitations as described in Clark and Bailey[6]

Exposure time to 50% n-propanol (min)	$v_B(t)^*$	$v_A(t)^\#$	$v_B(t)^\#$
0	144	8.3	144
5	134	7.8	135
65	136	7.9	137
120	104	6.2	108

*Assuming $v_A(t) = v_{A_0} = 8.3$.

#Assuming $v_A(t)/v_{A_0} = v_B(t)/v_{B_0}$.

FIGURE CAPTIONS

Figure 1 EPR spectra recorded at room temperature of α-chymotrypsin labeled with organophosphate spin label. Upper spectrum: spin labeled α-chymotrypsin in 1 mM acetic acid, 0.1 M KCl, pH 3.5. Lower spectrum: spin labeled α-chymotrypsin immobilized on CNBr-activated Sepharose 4B (0.97 μmols active chymotrypsin/g).

Figure 2 Conceptual view of immobilized enzyme deactivation consistent with available exerimental data.

Figure 3 Time sequence (arrows indicate increasing time) of EPR spectra recorded in 10 mM indole (indole spectra) at four-hour intervals. Immobilized α-chymotrypsin was spin labeled with m-IV after exposure to 50% n-propanol for 120 min. The spectral features indicated, representative of active yet perturbed immobilized enzyme, decay with time and after 12 hours closely coincide with the EPR spectrum of enzyme recorded before deactivation.

Figure 4 Indole spectra of immobilized α-chymotrypsin labeled with m-IV after different exposure times to 50% n-propanol. The exposure times (in minutes) prior to sampling and spin labeling are indicated to the right of each spectrum.

Figure 5 Comparison of the EPR spectrum of enzyme form A in its initial state (top) with the spectrum obtained by decomposing the EPR spectrum of immobilized chymotrypsin

spin labeled and extensively washed after a 5 min. exposure to 50% n-propanol (bottom).

Figure 6 EPR indole spectra of two different immobilized enzyme conjugates possessing approximately the same quantity of active enzyme but prepared in different ways. Top spectrum: active immobilized chymotrypsin loading of 0.19 μmols/g obtained by appropriate choice of initial enzyme concentration for the immobilizing solution. Bottom spectrum: active enzyme loading of 0.18 μmols/g obtained by exposing chymotrypsin-CNBr Sepharose 4B conjugate (initial loading of active enzyme, 1.0 μmol/g) to 50% n-propanol for 120 min.

Figure 7 Relationship between amount of active enzyme and fraction of enzyme-A for preparations with different initial loadings of active immobilized chymotrypsin (○), and samples taken after various exposure times of an immobilized enzyme conjugate to 50% n-propanol (□).

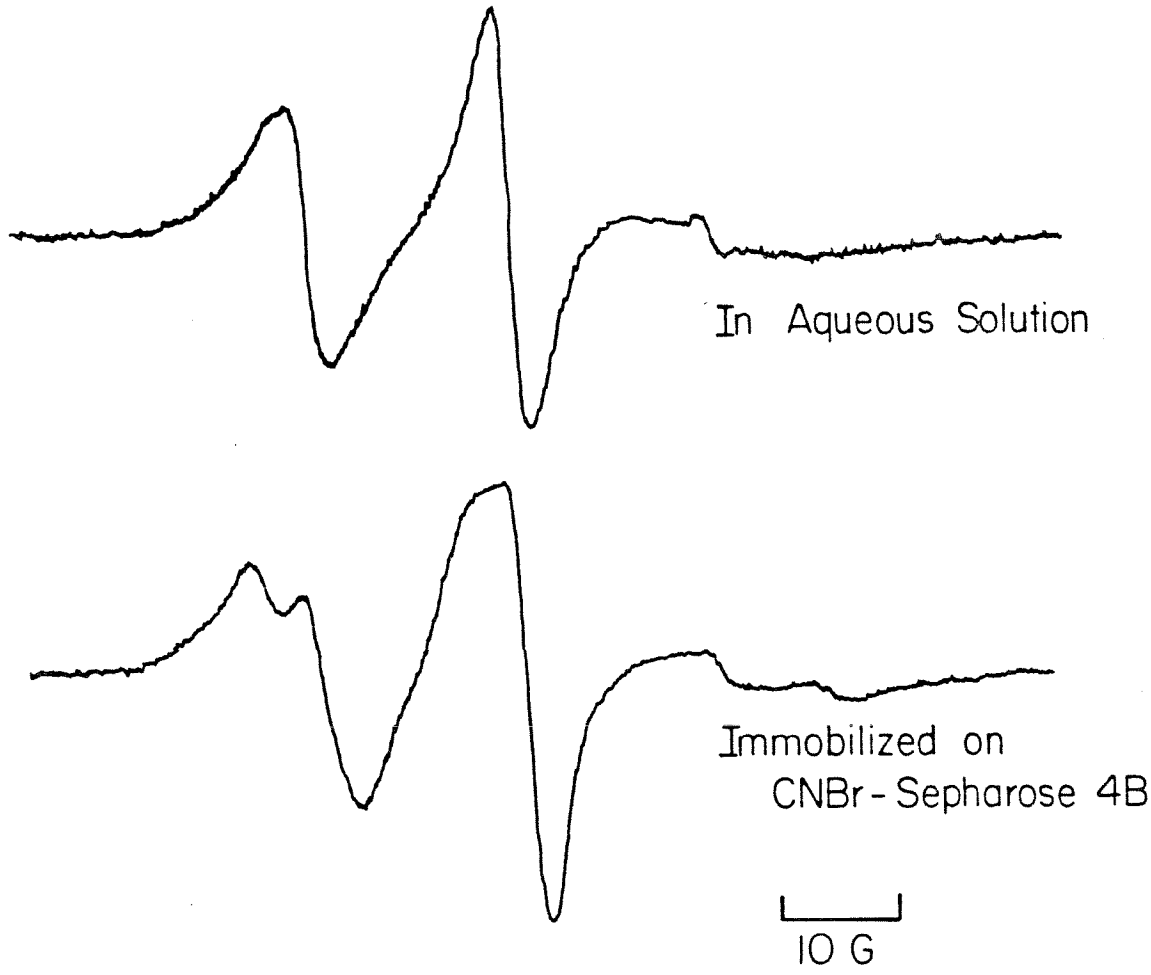

FIGURE 1

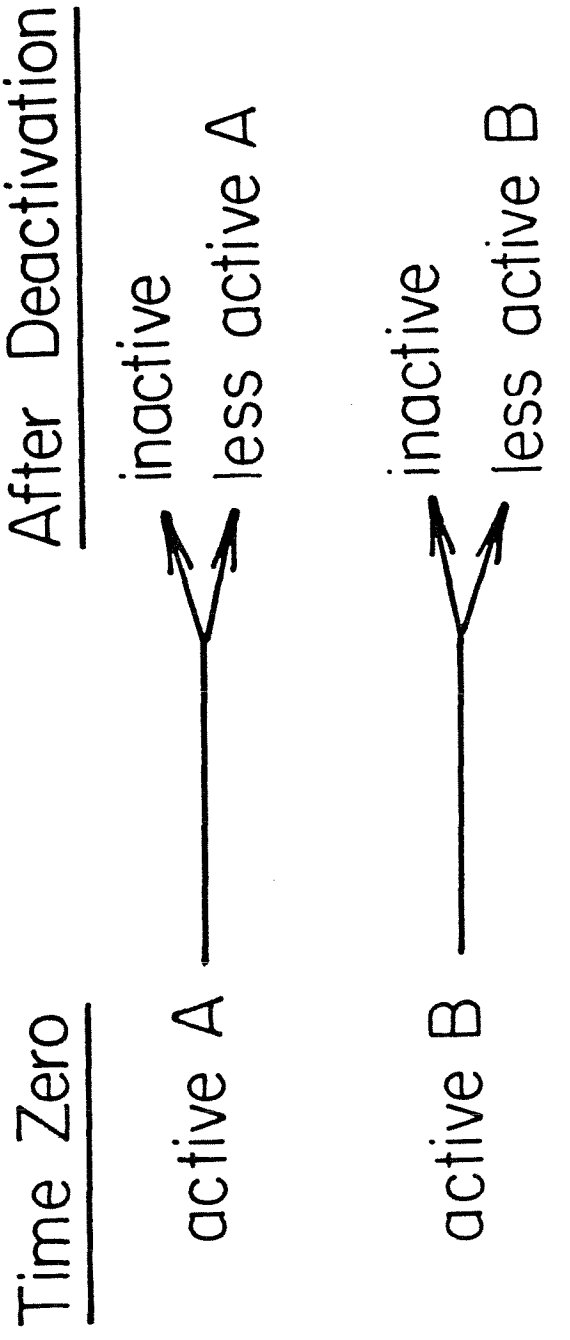
Time Zero
After Deactivation
active A
inactive
less active A
active B
inactive
less active B

FIGURE 2

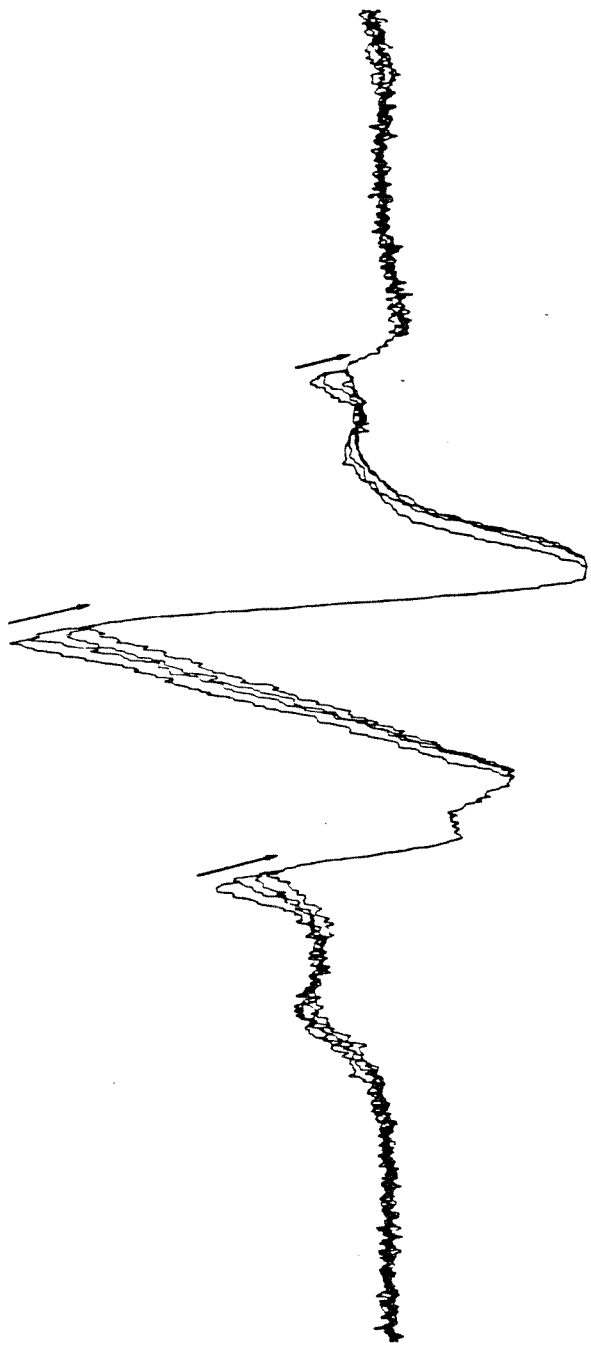

FIGURE 3

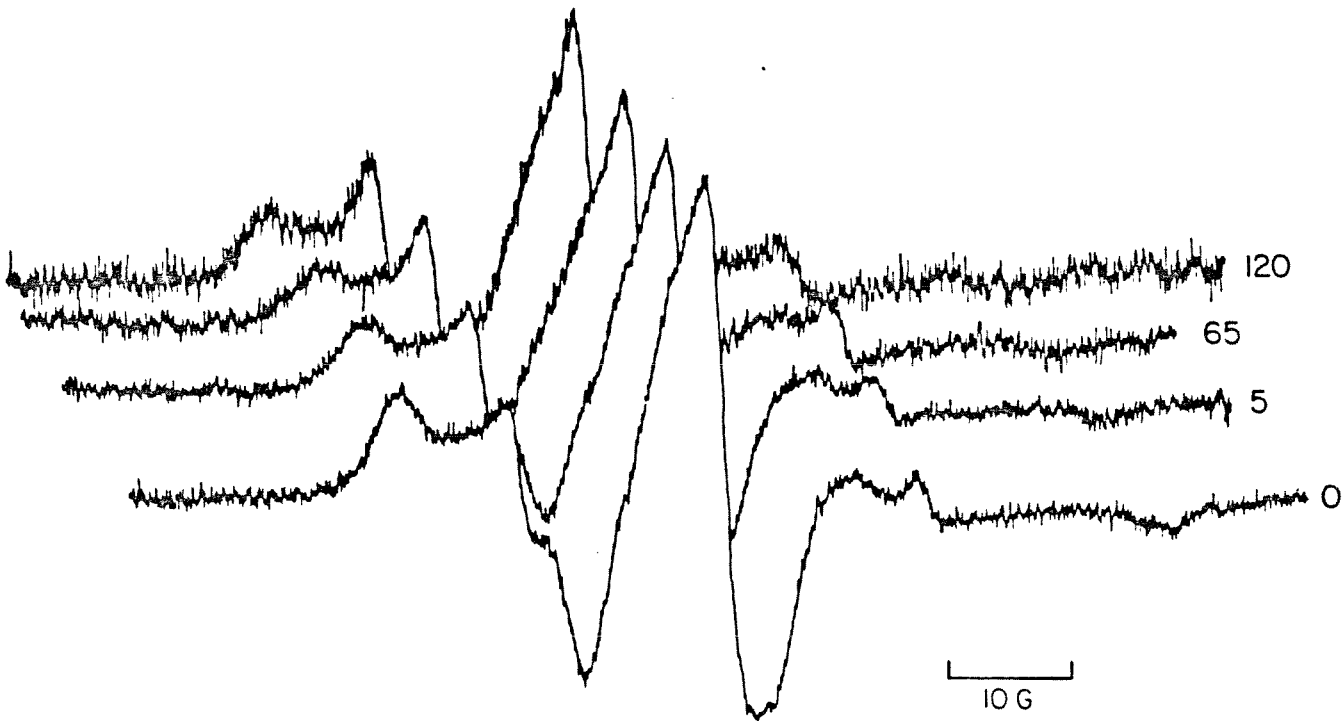

FIGURE 4

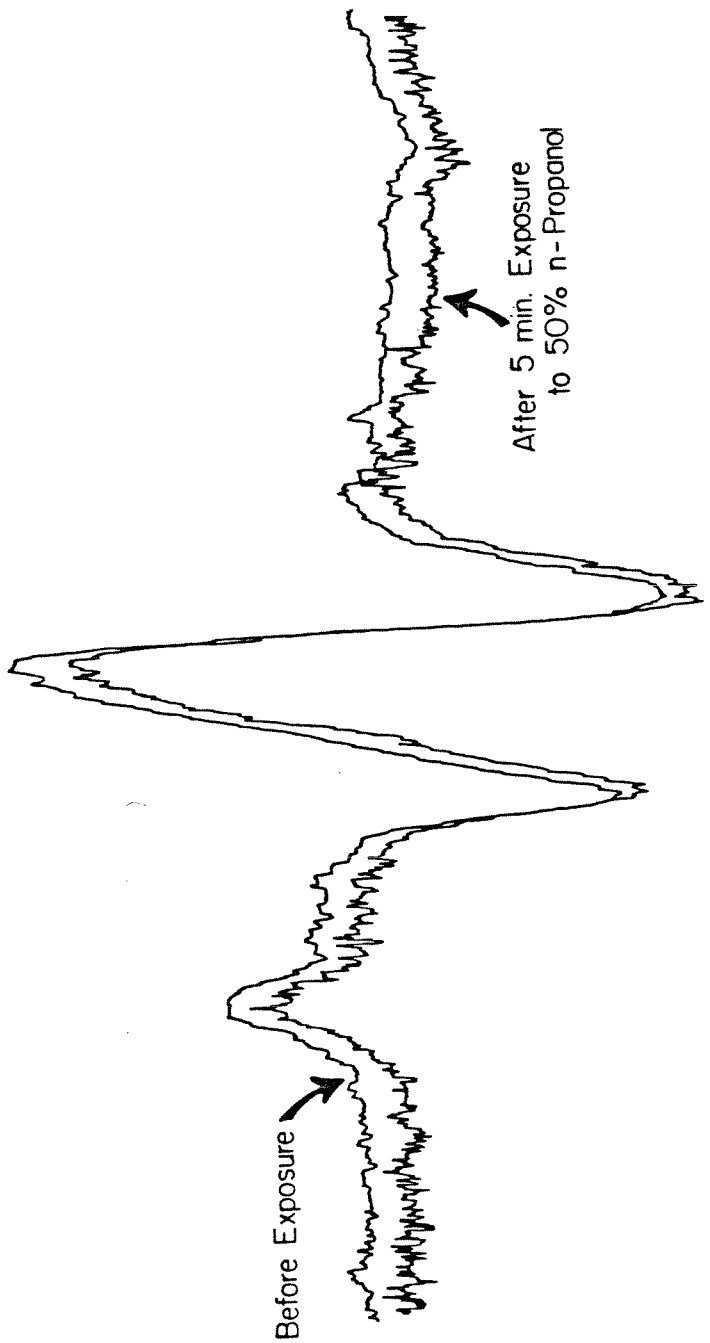

FIGURE 5

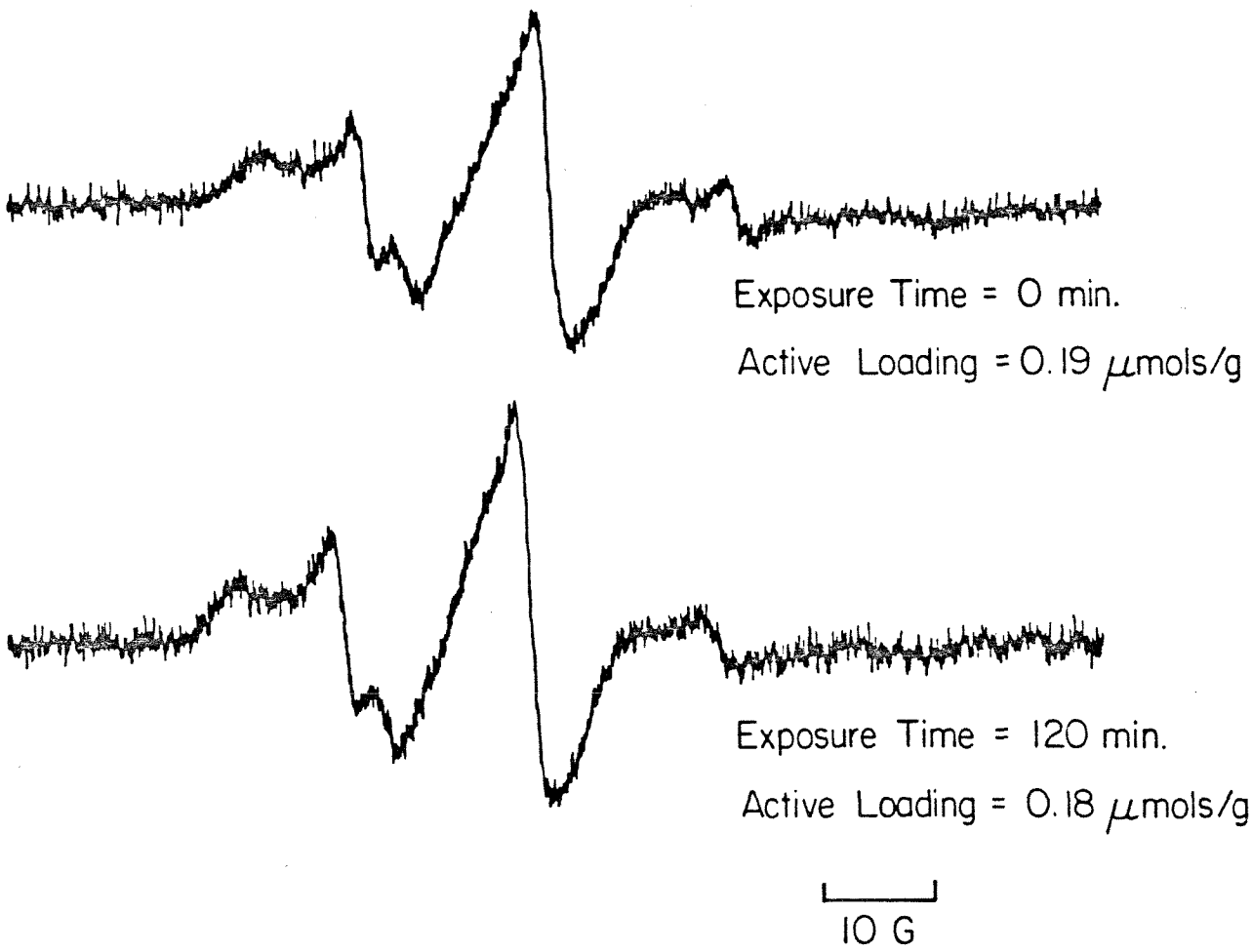
Exposure Time = 0 min.
Active Loading = 0.19 μmols/g
Exposure Time = 120 min.
Active Loading = 0.18 μmols/g
10 G

FIGURE 6

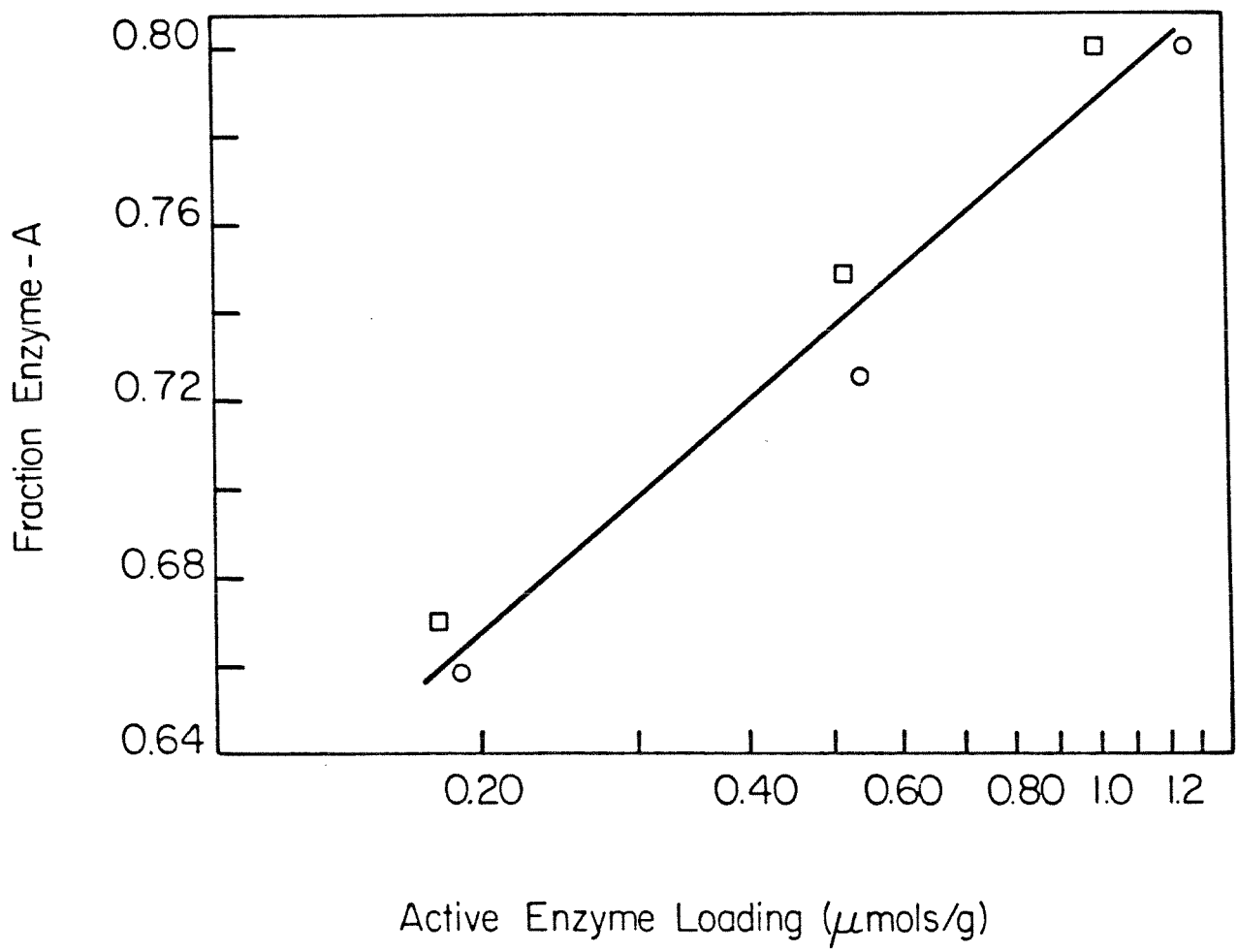
0.80
0.76
0.72
0.68
0.64
Fraction Enzyme - A
0.20
0.40
0.60
0.80
1.0
1.2
Active Enzyme Loading (μmols/g)

FIGURE 7

PART III: THEORY OF ENZYME IMMOBILIZATION IN POROUS MATERIALS

CHAPTER 6 MODELING ENZYME IMMOBILIZATION IN POROUS SOLID SUPPORTS

Introduction

Immobilized enzyme catalysts with high activities per unit volume may be prepared by adsorbing or covalently coupling enzymes to the interior surfaces of porous solid particles. Sephadex, Sepharose, activated carbon, cellulose, ceramics, and glass are some of the porous materials which have been used as immobilized enzyme supports.[1-8] By using supports with sufficiently large pores, substrates with molecular dimensions comparable to those of the enzyme can be converted on these supported catalysts in contrast to the situation with entrapped enzymes.

Catalysts consisting of enzymes immobilized within porous solid supports are usually prepared by contacting the porous solid, perhaps after chemical treatment to activate binding groups on its internal surfaces, with enzyme solution. During this immobilization process, enzyme diffuses into the porous solid matrix and is attached to the internal surfaces, while concurrently enzyme concentration in the immobilizing solution decreases. The time required to reach the final loading state and in some instances the final spatial distribution of immobilized enzyme within the porous particles depends on all of the physiochemical parameters which characterize the complex coupled transport and immobilization processes occurring during catalyst preparation.

As will be clearer by the end of this presentation, the overall activity per amount of enzyme immobilized and deactivation properties of the porous supported enzyme catalyst may depend strongly on the design and operation of the immobilization reactor as well as on the support and

enzyme properties. Mathematical modeling of the immobilization process serves to organize the interacting factors and corresponding parameters involved in a coherent structure and to identify major qualitative features and sensitivities of the process. Recognition of the immobilization process itself as a practically important problem in biochemical reaction engineering has been limited to date.

Carleysmith *et al.*[9] have analyzed the special case in which the enzyme entering the pores of the support is irreversibly attached at a rate much greater than the intraparticle diffusion rate. Under these circumstances, the immobilized enzyme is deposited in a zone on the outer periphery of the pellet, with a sharp front between the outer zone which is completely saturated with immobilized enzyme and a central core which contains no enzyme. Modeling of this immobilization situation then reduces to determination of the front position and shape as a function of time. The former problem was solved for spherical pellets under reasonable assumptions about pellet capacities and enzyme effective diffusivity by Carleysmith *et al.*;[9] similar analyses have also been performed in the context of fluid-solid heterogeneous reactions.[10-11] A recent analysis employing matched asymptotic expansions also yields a description of front structure and its development.[12]

A recent theoretical treatment has analyzed enzyme immobilization in porous particles during the initial period in which the support surfaces' capacity for enzyme is not closely approached anywhere within the particle.[13] One significant result from that analysis is a method for determining the intrinsic local immobilization rate constant from

the experimentally observable time trajectory of enzyme concentration in the immobilizing solution. In the present study, more general local immobilization kinetics are considered which include support surface saturation with enzyme and the possibility of a reversible immobilization reaction. Thus, this investigation is concerned with the entire time course of enzyme immobilization by reversible adsorption or irreversible covalent bonding within porous solid supports. An immobilization model which included reversible kinetics was formulated and solved for one particular case by Buchholz[14] this work extends greatly the parameter combinations examined and also presents new numerical and approximate analytical approaches to the problem.

FORMULATION OF THE MATHEMATICAL MODEL

In this investigation, the porous support particles will be presumed spherical (radius R). A particle will be modeled as a pseudohomogeneous solid with transport and kinetic parameters appropriately adjusted to reflect the solid's pore network characteristics.[15] Of interest here is a batch immobilization process in which a total mass m_p of the support particles are immersed in a well-mixed bath of enzyme solution with initial enzyme concentration e_{bo}. Several equivalent physical realizations exist for this situation, including fixed-bed recirculation systems with low conversion per pass. It is assumed that the pores of the support particles are filled initially with the solvent so that there is no fluid convection into the particles when the immobilzation process is initiated.

Enzyme molecules are transported from the bulk immobilizating solution to the exterior surface of the particles (mass transfer coefficient h_e) where they diffuse into the particle; the effective diffusion coefficient D_e is presumed for the moment to be constant. Immobilization

proceeds at a local rate v_i which depends upon the local concentrations of enzyme in the pore fluid and immobilized on the support surface. Since the available internal surface area far exceeds the external particle surface area for the porous materials of interest, it is assumed that the enzymes attach only to the pore interior surfaces which contain a uniform distribution of functional groups.

The material balances for enzyme in the immobilizing solution, immobilized on the support surfaces, and in solution within the support pores are given by

$$V_e \frac{de_b(t')}{dt'} = h_e \frac{3m_p}{\rho_p R}\left[\frac{e(R,t')}{P_e} - e_b(t')\right] \; ; \; e_b(0) = e_{bo} \tag{1}$$

$$\frac{\partial e_s(r,t')}{\partial t'} = v_i \; ; \quad e_s(r,0) = 0 \tag{2}$$

and

$$\frac{\partial e(r,t')}{\partial t'} = \frac{D_e}{r^2}\frac{\partial}{\partial r}\left(r^2\frac{\partial e(r,t')}{\partial r}\right) - v_i \; , \tag{3.1}$$

$$D_e \frac{\partial e(R,t')}{\partial r} = h_e\left[e_b(t') - \frac{e(r,t')}{P_e}\right] \; , \tag{3.2}$$

$$\frac{\partial e(0,t')}{\partial r} = 0 \; ; \quad e(r,0) = 0 \; , \tag{3.3}$$

respectively. The local rate of immobilization v_i will be assumed to have the form

$$v_{ih} = k_i e\left(1 - \frac{e_s}{e_{sm}}\right) - k_d\left(\frac{e_s}{e_{sm}}\right) , \tag{4}$$

where e_{sm} denotes the maximum possible immobilized enzyme concentration.

Parametric influences on the immobilization process are best summarized by recasting the above model in dimensionless form. Introducing the following dimensionless variables and parameters:

$$E_b = \frac{e_b}{e_{bo}} , \quad E = \frac{e}{e_{bo}P_e} , \quad E_s = \frac{e_s}{e_{sm}} \tag{5.1}$$

$$x = \frac{r}{R} , \quad t = \frac{D_e t'}{R^2} \tag{5.2}$$

$$\phi^2 = \frac{R^2 k_i}{D_e} , \quad \theta = \frac{k_d}{(k_i e_{bo} P_e)} , \quad \psi = \frac{e_{bo}P_e}{e_{sm}} \tag{5.3}$$

$$Bi = \frac{h_e R}{D_e P_e} , \quad \nu = \frac{m_p P_e}{V_e \rho_p} , \tag{5.4}$$

the model becomes

$$\frac{dE_b(t)}{dt} = -3\nu Bi\left[E_b(t) - E(1,t)\right] ; \quad E_b(0) = 1 , \tag{6.1}$$

$$\frac{\partial E_s(x;t)}{\partial t} = \psi\phi^2\left\{E(x,t)\left[1 - E_s(x,t)\right] - \theta E_s(x,t)\right\} , \tag{6.2}$$

$$E_s(x,0) = 0 , \tag{6.3}$$

$$\frac{\partial E(x,t)}{\partial t} = \frac{1}{x^2}\frac{\partial}{\partial x}\left[x^2 \frac{\partial E(x,t)}{\partial x}\right] - \frac{1}{\psi}\frac{\partial E_s(x,t)}{\partial t} , \tag{7.1}$$

$$\frac{\partial E(1,t)}{\partial x} = -\frac{1}{3\nu}\frac{dE_b(t)}{dt} , \tag{7.2}$$

$$\frac{\partial E(0,t)}{\partial x} = 0 ; \qquad E(x,0) = 0 . \tag{7.3}$$

It is worthwhile to point out here the physical meaning of the dimensionless parameters involved. First, the square of the Thiele modulus ϕ^2 is the ratio of a characteristic immobilization rate to a characteristic diffusion rate. The parameter θ denotes the ratio of desorption to adsorption characteristic rates. The ratio (ν/ψ) is the solid support capacity for immobilized enzyme relative to the amount of enzyme available in the immobilizing solution, ν is P_e times the total support volume divided by the immobilizing solution volume, and the Biot number Bi is a characteristic external mass transfer rate divided by a characteristic diffusion rate.

ANALYSIS OF THE IMMOBILIZATION MODEL

Analysis of the immobilization process for very large times; that is, after steady state has been achieved, is relatively straightforward. In this connection the following overall material balance is useful:

$$E_b(t) + 3\nu \int_0^1 x^2 E(x,t)\,dx + \frac{3\nu}{\psi}\int_0^1 x^2 E_s(x,t)\,dx = 1 . \tag{8}$$

For irreversible immobilization kinetics ($\theta = 0$), immobilization proceeds until either the surface is saturated with enzyme [$E_s^o(x) = 1$, superscript o denotes steady-state value] or until all of the enzyme in the immobilizing solution is exhausted ($E_b^o = 0$). From Equation (8) it follows that saturation occurs if $\nu/\psi \leq 1$ and incomplete loading occurs if $\nu/\psi > 1$.

If immobilization is reversible ($\theta \neq 0$), $E^o = E_b^o$, and the internal profiles of enzyme in the pore and on the pore surfaces will be spatially uniform and at equilibrium

$$E_s^o = \frac{E^o}{(E^o + \theta)} \quad . \tag{9}$$

Using these relationships in Equation (8), it follows that

$$E^o = E_b^o = -A + \sqrt{A^2 + \frac{\theta}{1 + \nu}} \tag{10.1}$$

where

$$A = \left[\theta(1 + \nu) - 1 + \frac{\nu}{\psi}\right] \Big/ 2(1 + \nu) \quad . \tag{10.2}$$

In most immobilization processes, the volume of enzyme solution is much larger than the total volume of the support particles ($\nu << 1$). This implies that, except for a very short initial transient period, the quasi-steady state approximation may be applied to intraparticle diffusion processes. Then, it can be shown using multiple time scale perturbation analysis[13] that after the short induction time the immobilization model above may be written in the following dimensionless form:

$$\frac{1}{x^2}\frac{\partial}{\partial x}\left(x^2\,\frac{\partial E(x,\tau)}{\partial x}\right) - \phi^2\left[E(x,\tau)\left\{1 - E_s(x,\tau)\right\} - \theta E_s(x,\tau)\right] = 0\ , \qquad (11.1)$$

$$\frac{\partial E_s(x,\tau)}{\partial \tau} = \left(\frac{\psi}{\nu}\right)\phi^2\left[E(x,\tau)\left\{1 - E_s(x,\tau)\right\} - \theta E_s(x,\tau)\right]\ , \qquad (11.2)$$

$$\frac{1}{3}\frac{dE_b(\tau)}{d\tau} = -\frac{\partial E(1,\tau)}{\partial x} = Bi\left[E(1,\tau) - E_b(\tau)\right]\ , \qquad (11.3)$$

and

$$E_b(0) = 1; \quad E(x,0) = E_s(x,0) = \frac{\partial E(0,\tau)}{\partial x} = 0\ , \qquad (11.4)$$

where the slow time τ is defined by

$$\tau = \nu t\ . \qquad (12)$$

The material balance corresponding to this approximate model is obtained by neglecting the second term on the left-hand side of Equation (8); the corresponding steady-state values of E^o and E_s^o for reversible immobilization are obtained by neglecting ν with respect to unity in Equation (10). These results are consistent with the $\nu << 1$ condition which justifies the quasi-steady state model.

An effective computational algorithm has been developed to effect numerical solution of the coupled nonlinear partial differential equations required to simulate transient behavior for the model described in Equation (11). This method involves application of a finite integral transform in the dimensionless spatial coordinate x to yield a set of coupled ordinary differential equations in dimensionless time τ which are then integrated numerically. Details of this solution technique are provided in the Appendix.

In addition to numerical simulations based upon the complete model, it is useful to consider approximate approaches and limiting cases for which analytical treatments are available. These provide algebraic results which may be applied directly in certain situations, and they also provide a means of checking the numerical approach and its implementation.

A common strategy for approximate analysis of diffusion-reaction problems called lumping analysis involves replacing variables which depend on x by an effective average value[16] or by a value at one particular internal position.[17] Simultaneously, the Laplacian operator is replaced by a constant times the difference between the immobilizing solution concentration and the characteristic intraparticle concentration. If the particular approach to lumping suggested by Frank-Kamenetskii[16] is applied to the model above, there results

$$\xi_o^2[E_b^*(\tau) - E^*(\tau)] - \phi^2\{E^*(\tau)[1 - E_s^*(\tau)] - \theta E_s^*(\tau)\} = 0 \qquad (13.1)$$

$$\frac{dE_s^*(\tau)}{d\tau} = \left(\frac{\psi}{\nu}\right)\phi^2\{E^*(\tau)[1 - E_s^*(\tau)] - \theta E_s^*(\tau)\} \qquad (13.2)$$

$$\frac{dE_b^*(\tau)}{d\tau} = -\left(\frac{\nu}{\psi}\right)\frac{dE_s^*(\tau)}{d\tau}\ , \qquad (13.3)$$

$$E_b^*(0) = 1;\ E_s^*(0) = E^*(0) = 0,$$

where ξ_o satisfies Equation (A13.2; n = 0) and where superscript * denotes results based on the lumping treatment.

Using Equations (13) to eliminate E^* and E_s^*, the following ordinary differential equation for E_b^* is obtained

$$\frac{dE_b^*}{d\tau} = -\xi_o^2\phi^2\left(\frac{\psi}{\nu}\right)\left[\frac{E_b^{*2} + E_b^*\left(\frac{\nu}{\psi} - 1 + \theta\right) - \theta}{\xi_o^2 + \phi^2\left(1 - \frac{\psi}{\nu}\right) + \phi^2\frac{\psi}{\nu}E_b^*}\right] , \tag{14}$$

for which the solution is

$$\alpha\ell n\left(\frac{E_b^* - E_1}{1 - E_1}\right) + \beta\ell n\left(\frac{E_b^* - E_2}{1 - E_2}\right) + \xi_o^2\phi^2\left(\frac{\psi}{\nu}\right)\tau = 0 , \tag{15}$$

$$\alpha = \frac{A' + BE_1}{E_1 - E_2} , \tag{16.1}$$

$$\beta = \frac{A' + BE_2}{E_2 - E_1} , \tag{16.2}$$

$$A' = \xi_o^2 + \phi^2(1 - \frac{\psi}{\nu}) , \tag{16.3}$$

$$B = \frac{\phi^2\psi}{\nu} , \tag{16.4}$$

$$E_{1,2} = -\frac{1}{2}\left(\frac{\nu}{\psi} - 1 + \theta\right) \pm \left[\frac{1}{4}\left(\frac{\nu}{\psi} - 1 + \theta\right)^2 + \theta\right]^{\frac{1}{2}} . \tag{16.5}$$

Once $E_b^*(\tau)$ is evaluated from Equation (15), E_s^* and E^* are given by

$$E_b^*(\tau) + \frac{\nu}{\psi}E_s^*(\tau) = 1 , \tag{17}$$

and

$$E^*(\tau) = \frac{\xi_o^2 E_b^*(\tau) + \theta\phi^2 E_s^*(\tau)}{\xi_o^2 + \phi^2\left(1 - E_s^*(\tau)\right)} , \tag{18}$$

respectively. These equations may be used to estimate the time required for achievement of a given degree of enzyme loading with the support particles. Notice that, since the spatial dependences of E and E_s have

been neglected in this treatment, lumping analysis provides no information on the intraparticle profile of immobilized enzyme.

SIMULATION RESULTS

The model given in Equation (11) which includes the quasi-steady state approximation for diffusion into the particles has been solved numerically for several different combinations of parameter values. Shown in Figure 1 (solid lines) are the time trajectories for the dimensionless enzyme concentration in the immobilizing solution for several cases involving irreversible immobilization of enzyme ($\theta = 0$).

The lower portion of the figure includes results for several different values of the parameter ψ. In all of these simulations, the Thiele modulus ϕ is equal to unity, indicating that diffusional resistance is relatively mild. Following the earlier remarks about the asymptotic value of E_b in terms of the ratio $\frac{\nu}{\psi}$, the immobilizing solution enzyme concentration approaches a constant nonzero value for ψ larger than ν. For smaller values of ψ, E_b eventually reaches zero before the enzyme has been completely loaded to its saturation value.

It is interesting to note that all of the curves in the lower portion of Figure 1 have the same slope at time zero. This is an important observation, since the situation with ψ much smaller than ν can be shown by perturbation analysis arguments to be identical to the case in which the surface is presumed to have unbounded capacity for loading enzyme. Thus, the results for very small ψ correspond to the case considered in a previous publication in which a method was described for estimating the intrinsic

immobilization rate constant, k_i, from the initial slope of the E_b time trajectory.[13] The results in Figure 1 are consistent with the intuitive notion that the finite capacity of the support for immobilized enzyme does not influence the initial loading trajectory, indicating that the method described earlier is satisfactory for real systems in which the particle capacity for immobilizing enzyme is limited.

The upper portion of Figure 1 illustrates the effect of increasing Thiele modulus ϕ on the change with time in the immobilizing solution enzyme concentration. Clearly, larger values correspond to more rapid loading. Because of the other parameters used in these calculations, the particle is completely loaded when $E_b = 0.504$ so that this common asymptotic value is observed in all situations considered.

The dotted lines in Figure 1 were calculated using the lumping approximation result of Equation (15). These trajectories very closely approximate those calculated using the distributed model of Equation (11). While the lumping approximation cannot be used to compute intraparticle conditions, it is a very powerful shortcut method for evaluating $E_b(t)$.

Figure 2 illustrates the changes with time in the internal profiles of dimensionless concentration of enzyme in the fluid in the porous particle (E) and the dimensionless concentration of immobilized enzyme (E_s).

The following parameters were employed in this calculation

$$\theta = 0, \quad \phi = 1.0, \quad \nu = 0.05, \quad Bi = 500, \quad \psi = 0.1 \tag{18}$$

The Thiele modulus is again not large, which results in very flat profiles of enzyme loading and progressively flatter profiles of pore fluid enzyme concentration. The time intervals between the different lines in Figure 2 are equal to 0.25 slow time (τ) units. In this case, which is expected to result for other relatively small values of Thiele modulus, the loading profile within the particle is always relatively uniform. If different parameter values are considered such that the immobilizing solution's supply of enzyme is exhausted, the results look essentially as in Figure 2, with again a quite uniform loading of enzyme, although with a final value smaller than unity.

A much different situation obtains for larger Thiele modulus as is illustrated clearly in Figure 3. Now the initial profiles of both pore fluid enzyme concentration and immobilized enzyme concentration are relatively steep, with no enzyme present in either phase near the center of the particle. In this case, in which there is sufficient enzyme in the immobilizing solution eventually to saturate all of the pellets' capacity for enzyme, the loading profile becomes more and more uniform as time progresses, with similar trends evident in the pore fluid enzyme concentration. If, on the other hand, a smaller amount of enzyme is available in the immobilizing solution, the enzyme loading profile within the particle at the conclusion of the immobilization will be quite steep for large Thiele modulus (see Figure 4, bottom frame). The corresponding

enzyme concentration in the intraparticle fluid now eventually decays everywhere to zero as all enzyme in all fluid phases is ultimately attached to the interior surfaces of the porous support particles.

Changes with time of the immobilizing solution enzyme concentration for $\phi = 10$ and several values of Bi are illustrated in Figure 5. The effect of external mass transport as characterized by Bi is not significant for Bi values in the range of 20 or greater. However, distinctly different trajectories occur for smaller Bi values. The curve for Bi = 2 corresponds to particles in stagnant fluid.[18] This situation is also closely approximated when the support particles are very small and hence have small velocities relative to the surrounding fluid.

Qualitatively different results are obtained for reversible immobilization kinetics ($\theta \neq 0$). Two cases corresponding to small and large Thiele modulus values are illustrated in Figures 6 and 7. In both instances, the intraparticle fluid phase enzyme concentration initially has a nonuniform distribution whcih eventually approaches a constant value given by Equation (10.1). Interesting, however, are the differences between the enzyme loading profiles and their time development. In the case of large Thiele modulus, the loading profiles are initially nonuniform and eventually relax towards the asymptotic constant value given by Equation (9). In this situation, immobilized enzyme is redistributed from the outside to the-inside of the particle by coupled reversible interactions with the surface locally and diffusion within the particle. Corresponding immobilizing solution enzyme concentrations at different times after initiation of the immobilization process are depicted in Figure 8, where again solid curves denote results from Equation (11) and dotted are results from lumping approximation Equation (15).

DISCUSSION

In addition to determining the time required for completion of immobilization, the mathematical modeling studies reported above also allow, through simulation, insight into the evolution with time of the internal distribution of immobilized enzyme within the porous particle. To appreciate the practical significance of knowledge of this loading profile, consider the subsequent application of the immobilized enzyme catalyst for conversion of substrate to product. Now a different diffusion reaction problem arises, in which substrate diffuses into the catalyst particles and undergoes reaction locally at the immobilized enzyme active site.

Computational studies for diffusion and reaction in porous catalytic pellets have shown clearly that the overall reaction rate for such pellets is strongly influenced by the distribution of catalytic sites within the particle.[19-22] That is, for a given total amount of supported catalyst, the overall reaction rate is often largest when the catalyst is located near the external surface of the particle rather than being uniformly distributed. This conclusion, originally demonstrated for first order kinetics, is most likely valid for any kinetics of ordinary form; that is, kinetics, which exhibit a decrease in reaction rate for a decrease in substrate concentration. Michaelis-Menten kinetics are ordinary in this sense and substrate-inhibited Michaelis-Menten kinetics are not. New theoretical approaches for calculating effectiveness factors for catalyst particles with nonlinear local kinetics including Michaelis-Menten have been described recently.[22] Experimental investigations which demonstrate the greater overall activity of immobilized enzyme catalysts in which the enzyme is localized near the external surface have been reported by Lasch for leucine aminopeptidase immobilized on Sepharose 6B,[23] and claimed by Borchert and Buchholz[8] for trypsin immobilized on porous glass and porous copolymer

particles.

Not yet demonstrated experimentally for immobilized enzymes but anticipated by previous simulations are the influences of internal enzyme distribution on the deactivation properties of the immobilized enzyme catalyst.[20] When the enzyme is more concentrated near the external surface of the particle, if the deactivation process uniformly lowers local enzyme activity at all points within the catalyst, the nonuniformly loaded catalyst will appear from an overall reaction rate viewpoint to deactivate more rapidly than a uniformly loaded catalyst. A similar trend will be observed if the enzyme deactivation occurs in a shell progressive manner, moving inwards from the external surface of the particle as might be caused by an external poison. In this case as well, the more uniformly loaded catalyst will appear to be more stable than the nonuniformly loaded one. Thus, there is a trade-off in terms of design of the internal loading profile between higher initial activity, which is favored by concentrating the immobilized enzyme near the pellet's outer surface, and a slower apparent rate of deactivation, which is favored by uniform internal loading of the immobilized enzyme. This parallels the situation between free and immobilized enzymes in which the latter, while often less active on a specific enzyme basis, also exhibit slower apparent rates of loss of enzymatic activity than the enzyme in solution.[23-25] The catalyst loading profile can also influence selectivity if multiple reactions occur.[20] Similar effects may be expected for multiple immobilized enzyme systems.

According to the model employed above for penetration and local attachment of enzyme within a porous support, uniform loading will ultimately result in all cases involving reversible immobilization kinetics. Also, if there

is sufficient enzyme in the immobilizing solution to saturate the support capacity, uniform loading will also occur for irreversible immobilization kinetics. If the Thiele modulus is of the order of unity or smaller, the final loading profile will be approximately uniform even in situations where the immobilizing solution becomes depleted of enzyme before saturation of the support. If, on the other hand, the immobilizing solution does not contain enough enzyme to saturate the support and the Thiele modulus is large, sharply nonuniform internal loading profiles of immobilized enzyme may result as seen in Figure 4 above.

Since intentional nonuniform loading of the enzyme might be of interest for some applications, it is useful to consider other situations in which nonuniform loading may be obtained. One of these is interruption of the loading process for a high Thiele modulus system. Considering the calculated internal profiles for loading in Figure 3, suppose that at dimensionless time $\tau = 0.05$, the immobilized enzyme particles are separated from immobilizing solution and suspended in buffer. This will freeze the loading profile in approximately the nonuniform configuration shown in Figure 3 for $\tau = 0.05$. Thus, by varying the time of contact between immobilizing solution and porous support, a wide spectrum of loading profiles may be obtained providing the Thiele modulues for immobilization is large. It is very interesting in this context that Lasch was able to obtain more nonuniform loading by pretreating Sepharose particles longer with activating CNBr.[23] Presumably, this longer activation increases the density of reacting groups for immobilization, thereby providing both greater capacity and a higher local rate of immobilization. His experimental

results are therefore qualitatively consistent with the trends expected based upon the above model.

It should be noted, however, that the model described here requires refinement in order to simulate certain enzyme immobilization processes. Experiments in this laboratory have shown that in some cases immobilization ceases although the support particles are not completely saturated and although the immobilizing solution still contains enzyme. The final loading of enzyme in these experiments is nonuniform and is localized towards the outer surface of the particles. This situation, not encompassed by the above model, is the subject of current research.

It should be noted also that the mathematical models given above can be used to describe washing of the immobilized enzyme pellets; that is, the suspension of the particles after immobilization in buffer solution in order to remove enzyme in the internal pore fluid. Clearly in the case of reversibly attached enzyme, the ultimate effect of this process will be complete removal of enzyme from the particle. However, the rate of removal may be sufficiently slow to permit practical use of the reversibly immobilized enzyme. Also, after some modification of the fluid phase part of the model, such a mathematical description may also be useful in describing slow leaching of strongly held yet reversibly immobilized enzymes during onstream process application for conversion of substrate.

Acknowledgment

This work was supported by the National Science Foundation.

Nomenclature

A	defined in Equation (10.2)
A'	defined in Equation (16.3)
B	defined in Equation (16.4)
Bi	Biot number, defined in Equation (5.4)
D_e	effective diffusivity
e	enzyme concentration in pore fluid
e_b	enzyme concentration in the bath
e_{bo}	initial enzyme concentration in the bath
e_s	immobilized enzyme concentration
e_{sm}	maximum immobilized enzyme surface concentration
E	nondimensional enzyme concentration in pore fluid
$E_{1,2}$	defined in Equation (16.5)
E_b	nondimensional enzyme concentration in the bath
E_s	nondimensional immobilized enzyme concentration
$\overline{E_s}$	defined in Equation (A12)
h_e	mass transfer coefficient
k_d	rate constant for desorption
k_i	rate constant for immobilization
K_n	kernel of integral transform, defined in Equation (A13.1)
K_j	defined in Equation (A7)
m_p	total mass of support
P_e	partition coefficient
r	radial coordinate
R	particle radius

t nondimensional time, defined in Equation (5.2)

t' dimensional time

v_i local rate of enzyme immobilization, defined in Equation (4)

V_e bath volume

x nondimensional radial coordinate, defined in Equation (5.2)

Greek Symbols

α defined in Equation (16.1)

α_n defined in Equation (A5)

β defined in Equation (16.2)

ν defined in Equation (5.4)

ρ_p apparent density of solid support

τ nondimensional time, defined in Equation (12)

θ defined in Equation (5.3)

ϕ^2 Thiele modulus, defined in Equation (5.3)

ψ defined in Equation (5.3)

ε_n eigenvalue

Superscripts

$\hat{}$ scaling transform, defined in Equation (A1.1)

$*$ effective average

o steady-state value

References

1. R. Axén and S. Ernback, Eur. J. Biochem. 18, 351 (1971).
2. J. Porath, K. Aspberg, H. Drevin and R. Axén, J. Chromatogr. 86, 53 (1973).
3. Y. K. Cho and J. E. Bailey, Biotechnol. Bioeng. 21, 461 (1979).
4. Y, K. Cho and J. E. Bailey, Biotechnol. Bioeng. 20, 1651 (1978).
5. M. Singh, P. Vasudevan, A. R. Ray and S. K. Guha, Makromol. Chem. 181, 2433 (1980).
6. H. H. Weetall, Science 166, 615 (1969).
7. B. R. Allen, M. Charles, and R. W. Coughlin, Biotechnol. Bioeng. 21, 689 (1979).
8. A. Borchert and K. Buchholz, Biotechnol. Lett. 1, 18 (1979).
9. S. W. Carleysmith, M. B. L. Eames and M. D. Lilly, Biotechnol. Bioeng. 22, 957 (1980).
10. J. Szekely, J. W. Evans and H. Y. Sohn, Gas-Solid Reactions (Academic, New York, 1976), pp. 66ff.
11. E. Kawasaki, J. Sanscrainte and T. J. Walsh, AIChE J. 8, 48 (1963).
12. D. D. Do and R. H. Weiland, Ind. Eng. Chem. Fundam. 20, 48 (1981).
13. D. D. Do and J. E. Bailey, Chem. Eng. Commun., 1981 (in press).
14. K. Buchholz, Biotechnol. Lett. 1, 451 (1979).
15. A. Wheeler, Adv. Cat. 3, 249 (1951).
16. D. A. Frank-Kamenetskii, Diffusion and Heat Exchange in Chemical Kinetics (Plenum, New York, 1969), Second Edition.

17. J. Villadsen and M. L. Michelsen, Solution of Differential Equation Models by Polynomial Approximation (Prentice-Hall, Englewood Cliffs, N.J., 1978).

18. R. B. Bird, W. E. Stewart and E. N. Lightfoot, Transport Phenomena (John Wiley & Sons, New York, 1960) p. 409.

19. J. Shadman-Yazdi and E. E. Petersen, Chem. Eng. Sci. 27, 227 (1972).

20. W. E. Corbett and D. Luss, Chem. Eng. Sci. 29, 1473 (1974).

21. J. B. Wang and A. Varma, Chem. Eng. Sci. 35, 613 (1980).

22. D. D. Do and J. E. Bailey, Chem. Eng. Sci., 1981 (in press).

23. J. Lasch, Fed. Eur. Biochem. Soc. Proc. 52, 495 (1979).

24. H. H. Weetall, Biochem. Biophys. Acta 212, 1 (1970).

25. O. Zaborsky, Immobilized Enzymes (CRC Press, Cleveland, 1973), pp. 57-60.

26. D. D. Do and R. H. Weiland, Ind. Eng. Chem. Fundam., 1980 (submitted).

27. D. D. Do and J. E. Bailey, Chem. Eng. Sci., 1981 (in press).

APPENDIX

An algorithm based on finite integral transforms has been developed for numerical solution of the immobilization model. A scaling integral transform is defined as follows

$$\hat{E}_n(\tau) = (E,K_n)/(1,K_n) \quad , \tag{A1.1}$$

where

$$(E,K_n) = \int_0^1 x^2 E(x,\tau) K_n(x;\xi_n)\,dx \quad , \tag{A1.2}$$

and where the transform kernel $K_n(x;\xi_n)$ is the solution of the associated eigenproblem

$$\frac{1}{x^2}\,\frac{d}{dx}\left(x^2 \frac{dK_n}{dx}\right) + \xi_n^2 K_n = 0 \quad , \tag{A2.1}$$

$$x = 0 \; ; \quad dK_n/dx = 0 \quad ,$$

$$x = 1 \; ; \quad K_n + \frac{1}{Bi}\frac{dK_n}{dx} = 0 \quad . \tag{A2.3}$$

Applying the scaling transform (A1) to Equations (11), there results

$$\xi_n^2(E_b - \hat{E}_n) - \phi^2\left[\hat{E}_n(1 - \hat{E}_{s_n}) - \theta\hat{E}_{s_n}\right] = 0 \quad , \tag{A3.1}$$

$$\frac{d\hat{E}_{s_n}}{d\tau} = \frac{\psi}{\nu}\,\phi^2\left[\hat{E}_n(1 - \hat{E}_{s_n}) - \theta\hat{E}_{s_n}\right] \quad , \tag{A3.2}$$

$$\frac{1}{3}\frac{dE_b}{d\tau} = -\frac{\partial E(1,\tau)}{\partial x} \quad , \tag{A3.3}$$

in which a previously proposed approximation formulae in transform space has been applied.[22,26]

The solution for enzyme concentration in the pore fluid is best represented as a combination of a boundary term and a series term.[27] It is given by

$$E = E_b - \sum_{n=0}^{\infty} (E_b - \hat{E}_n)\, \alpha_n K_n(x;\xi_n) \quad , \tag{A4}$$

where

$$\alpha_n = (1,K_n)/(K_n,K_n) \quad . \tag{A5}$$

Differentiating Equation (A4) with respect to x, evaluating at x = 1 and substituting into Equation (A3.3) yields

$$\frac{dE_b}{d\tau} = -3 \sum_{j=0}^{\infty} (E_b - \hat{E}_j)\xi_j^2 \alpha_j (1,K_j) \quad , \tag{A6}$$

in which the relationship

$$K_j'(1,\xi_j) = -\xi_j^2 (1,K_j) \quad . \tag{A7}$$

has been employed. Eliminating $\hat{E}_n$ from Equations (A3.1), (A3.2) and A6) gives

$$\frac{d\hat{E}_{s_n}}{d\tau} = \frac{\psi}{\nu}\, \phi^2 \xi_n^2\, \frac{\left[E_b(1 - \hat{E}_{s_n}) - \theta \hat{E}_{s_n}\right]}{\xi_n^2 + \phi^2(1 - \hat{E}_{s_n})} \quad , \tag{A8.1}$$

$$\frac{dE_b}{d\tau} = -3\phi^2 \sum_{j=0}^{\infty} \frac{\left[E_b(1 - \hat{E}_{s_j}) - \phi\hat{E}_{s_j}\right]}{\xi_j^2 + \phi^2(1 - \hat{E}_{s_j})} \xi_j^2 \alpha_j(1,K_j) \quad , \tag{A8.2}$$

and

$$\hat{E}_n = \frac{\xi_n^2 E_b + \theta\phi^2 \hat{E}_{s_n}}{\xi_n^2 + \phi^2(1 - \hat{E}_{s_n})} \quad . \tag{A8.3}$$

Combining Equations (A8.1) and (A8.2), and integrating with respect to time, a relationship between E_b and the sequence $\left\{\hat{E}_{s_j}\right\}$ at any time τ may be obtained as follows

$$E_b = 1 - \frac{3\nu}{\psi} \sum_{j=0}^{\infty} \hat{E}_{s_j} \alpha_j(1,K_j) \quad . \tag{A9}$$

Substituting Equation (A9) into Equation (A8.1), an infinite set of ordinary differential equations in terms of the sequence $\hat{E}_{s_n}$ is developed

$$\frac{d\hat{E}_{s_n}}{d\tau} = \frac{\psi}{\nu} \phi^2 \xi_n^2 \frac{\left\{(1 - \hat{E}_{s_n})\left[1 - \frac{3\nu}{\psi} \sum_{j=0}^{\infty} \hat{E}_{s_j} \alpha_j(1,K_j)\right] - \theta\hat{E}_{s_n}\right\}}{\left[\xi_n^2 + \phi^2(1 - \hat{E}_{s_n})\right]}$$

$$\text{for } n = 0,1,2,\cdots \quad . \tag{A10}$$

For practical computation, one considers only the first N ordinary differential equations of Equation (A10). In the results given above, N = 50 was used. Changing N to 20 or to 10 did not affect the simulation results significantly. Once the sequence $\left\{\hat{E}_{s_n}\right\}$ is determined, the enzyme concentration E_b in the

immobilizing fluid is obtained from Equation (A9), the enzyme concentration E in the pores is obtained using Equation (A4) where $\hat{E}_n$ is given in Equation (A8.3), and the enzyme loading E_s is given by

$$E_s(x,\tau) = \bar{E}_s(\tau) - \sum_{j=0}^{\infty}\left(\bar{E}_s(\tau) - \hat{E}_{s_j}\right)\alpha_j K_j(x;\xi_j) \quad , \tag{A11}$$

when $\bar{E}_s(\tau)$ is determined from

$$\frac{d\bar{E}_s}{d\tau} = \frac{\psi}{\nu}\,\phi^2\left\{(1 - \bar{E}_s)\left[1 - \frac{3\nu}{\psi}\sum_{j=0}^{\infty}\hat{E}_{s_j}\alpha_j(1,K_j)\right] - \theta\bar{E}_s\right\} . \tag{A12}$$

The kernel, eigenvalue equation, and other quantities useful for these calculations are listed below for spherical porous support particles:

$$K_n(x;\xi_n) = \frac{\sin(\xi_n x)}{x} \tag{A13.1}$$

$$\xi_n\cos\xi_n = (1 - Bi)\sin\xi_n \tag{A13.2}$$

$$(1,K_n) = Bi\,\sin\xi_n/\xi_n^2 \tag{A13.3}$$

$$\alpha_n = \frac{2Bi\,\sin\xi_n}{\xi_n^2}\left(1 + \frac{\cos^2\xi_n}{Bi - 1}\right)^{-1} \tag{A13.4}$$

Figure Captions

Fig 1: Dimensionless bulk enzyme concentration (E_b) versus dimensionless time (τ) obtained with the integral transform method (solid lines) and lumping analysis (squares). (Top) Different trajectories correspond to different values of ϕ (from top to bottom, ϕ = 0.5, 1.0, 2.0, 10. For all of these cases, θ = 0, Bi = 500, ν = 0.05, ψ = 0.1). (Bottom) Results for various ψ values (0.5, 0.2, 0.1, 0.05, 0.01 and 0.005 from top to bottom. Remaining parameters θ = 0, ϕ = 1.0, Bi = 500, ν = 0.05).

Fig. 2: (Top) Sequence of dimensionless intraparticle fluid enzyme concentration profiles (E) for various times τ. (Bottom) Variation of dimensionless immobilized enzyme concentration (E_s) with dimensionless distance and time (dimensionless time τ increases as indicated in steps 0.25n, n = 1, 2, 3, ... θ = 0, ϕ = 1, ν = 0.05, Bi = 500, ψ = 0.10).

Fig. 3: (Top) Dimensionless immobilized enzyme concentration profiles (E_s) for various dimensionless times, given by τ = 0.005, 0.010, 0.010n, n = 2, 3, 4, ... (Bottom) Profiles of dimensionless enzyme concentration in the pore fluid (E) for increasing times τ. (Values of τ, in direction of arrow, are τ = 0.005n, n = 0, 1, 2, ... θ = 0, ϕ = 10, ψ = 0.1, ν = 0.05, Bi = 500.)

Fig. 4: (Top) Internal profiles of dimensionless enzyme concentration (E) in the fluid within the porous support (θ = 0.025n, n = 0, 1, 2, ...). (Bottom) Loading profiles of dimensionless immobilized enzyme concentration (E_s) (θ = 0.025n, n = 1, 2, 3, ..., θ = 0, ϕ = 10, ψ = 0.01, ν = 0.05, Bi = 500).

Fig. 5: Effect of Bi on the dimensionless time dependence of the bulk enzyme concentration (E_b). (Integral transform solutions (solid lines) from top: Bi = 2, 5, 20, 50, 500. Lumping analysis (squares) from top: Bi = 2, 500. $\theta = 0$, $\phi = 10$, $\nu = 0.05$, $\psi = 0.10$.)

Fig. 6: (Top) Plots of dimensionless pore fluid enzyme concentration (E) against dimensionless distance for times $\tau = 0$, 0.10, 0.25, 0.25n, n = 2, 3, 4, ... (Bottom) Radial dependence of immobilized enzyme loading (E_s) for times $\tau = 0.25n$, n = 1, 2, 3, ... ($\theta = 1$, $\phi = 1$, $\nu = 0.05$, $\psi = 0.1$, Bi = 500).

Fig. 7: (Top) Distribution of internal fluid enzyme concentration (E) with radial distance for times $\tau = 0.01n$, n = 0, 1, 2, ... (Bottom) Dimensionless loading of immobilized enzyme (E_s) as a function of dimensionless distance for times $\tau = 0.01n$, n = 1, 2, 3, ... ($\theta = 1$, $\phi = 10$, $\nu = 0.05$, $\psi = 0.1$, Bi = 500).

Fig. 8: (Top) The time dependence of the dimensionless bulk enzyme concentration for (E_b). (From top) $\phi = 1$, 2, 10. As in Figure 1, solid lines are the result of the integral transform technique, squares computed using lumping analysis ($\theta = 1$, $\nu = 0.05$, $\psi = 0.1$, Bi = 500). (Bottom) Dimensionless enzyme concentration in the bath (E_b) as a function of time for different values of θ. (θ, from top to bottom: 2.0, 1.0, 0.5, 0.1, 0.0. The other parameters are $\phi = 1.0$, $\nu = 0.05$, $\psi = 0.1$, Bi = 500.)

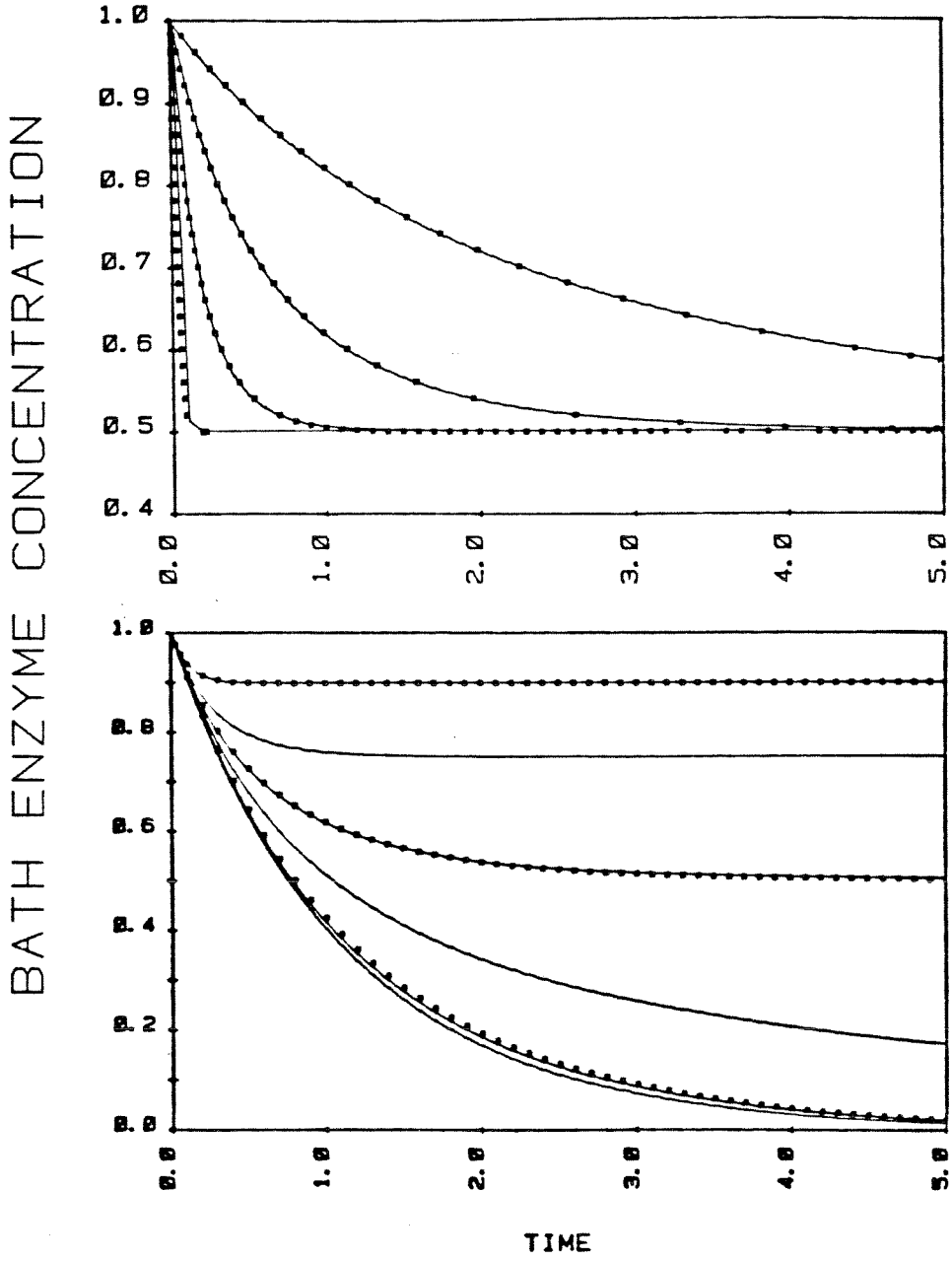
BATH ENZYME CONCENTRATION
1.0
0.9
0.8
0.7
0.6
0.5
0.4
0.0
1.0
2.0
3.0
4.0
5.0
TIME

FIGURE 1

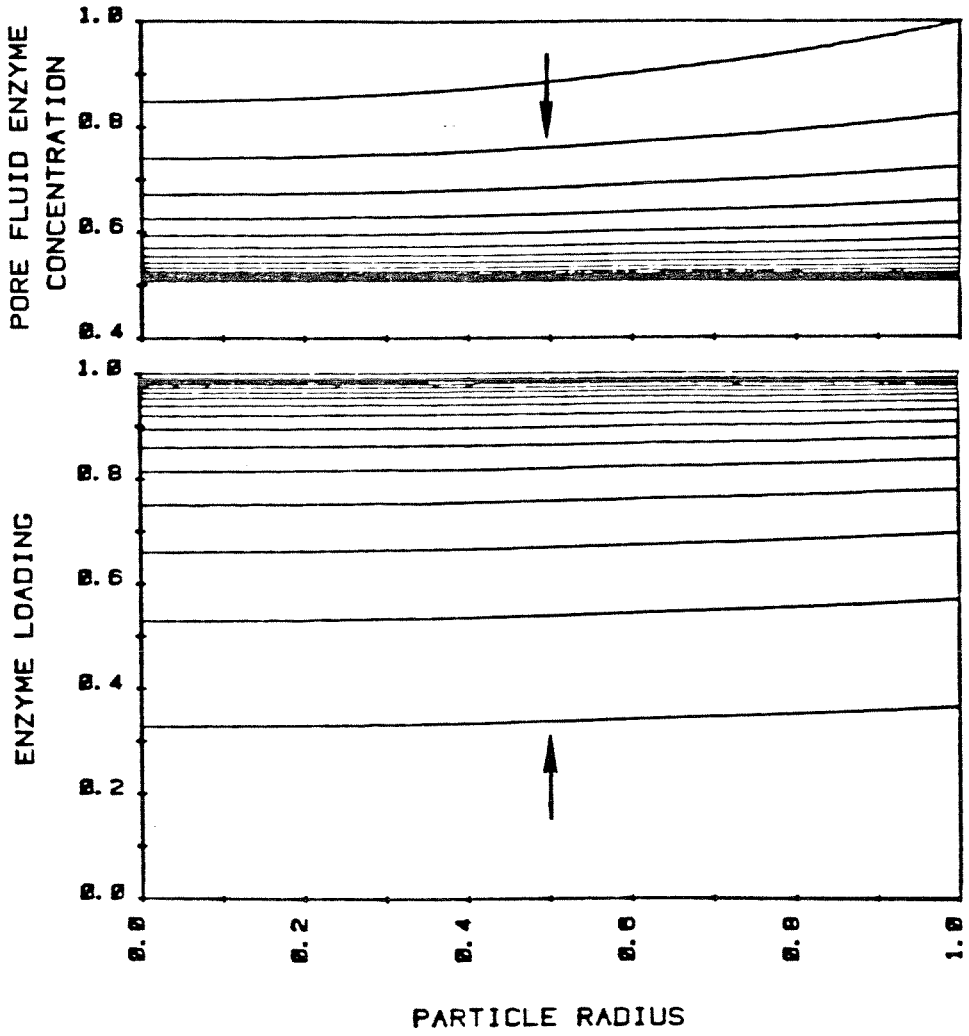
PORE FLUID ENZYME CONCENTRATION
1.0
0.8
0.6
0.4
ENZYME LOADING
1.0
0.8
0.6
0.4
0.2
0.0
0.0
0.2
0.4
0.6
0.8
1.0
PARTICLE RADIUS

FIGURE 2

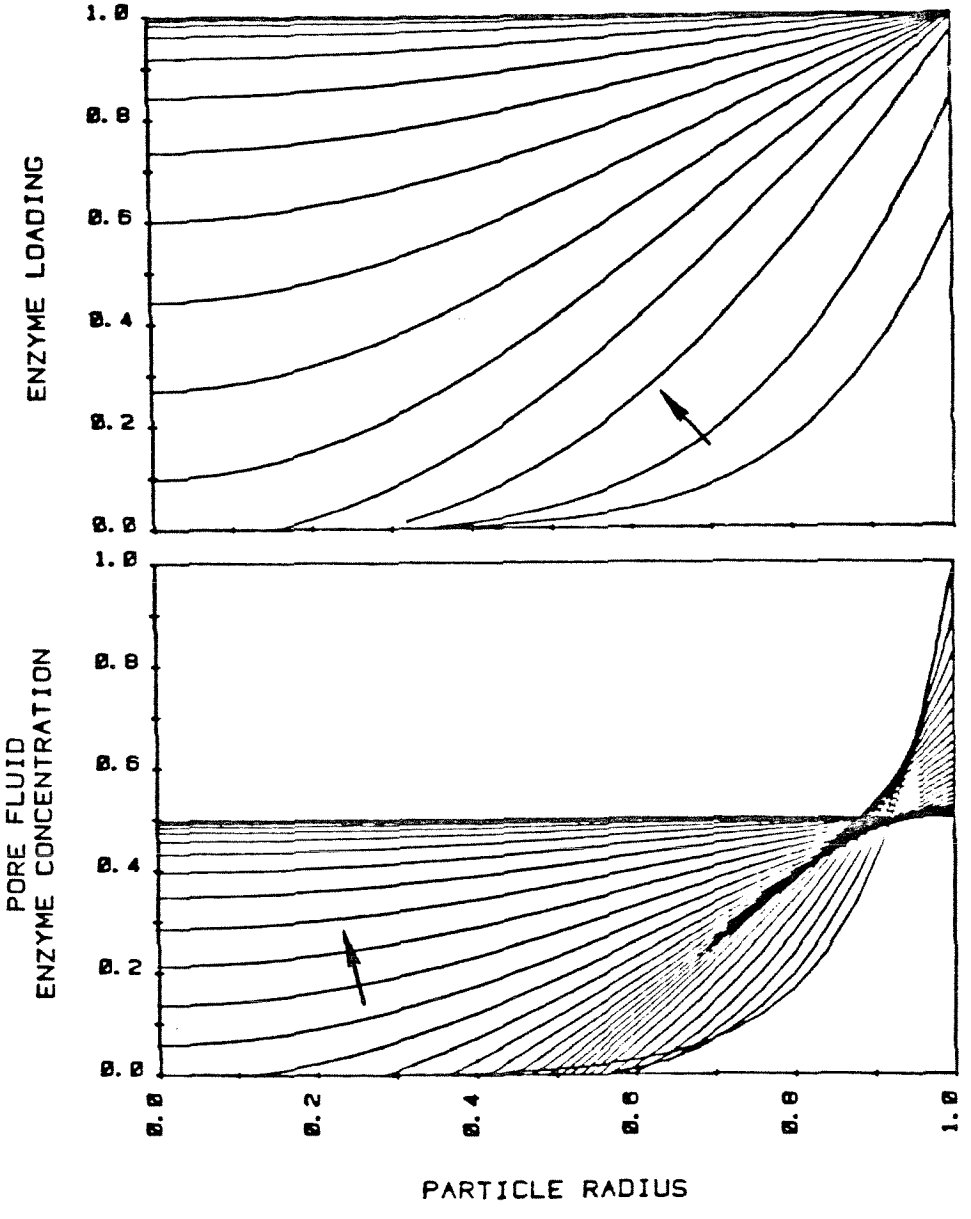
ENZYME LOADING
1.0
0.8
0.6
0.4
0.2
0.0
PORE FLUID
ENZYME CONCENTRATION
1.0
0.8
0.6
0.4
0.2
0.0
0.0
0.2
0.4
0.6
0.8
1.0
PARTICLE RADIUS

FIGURE 3

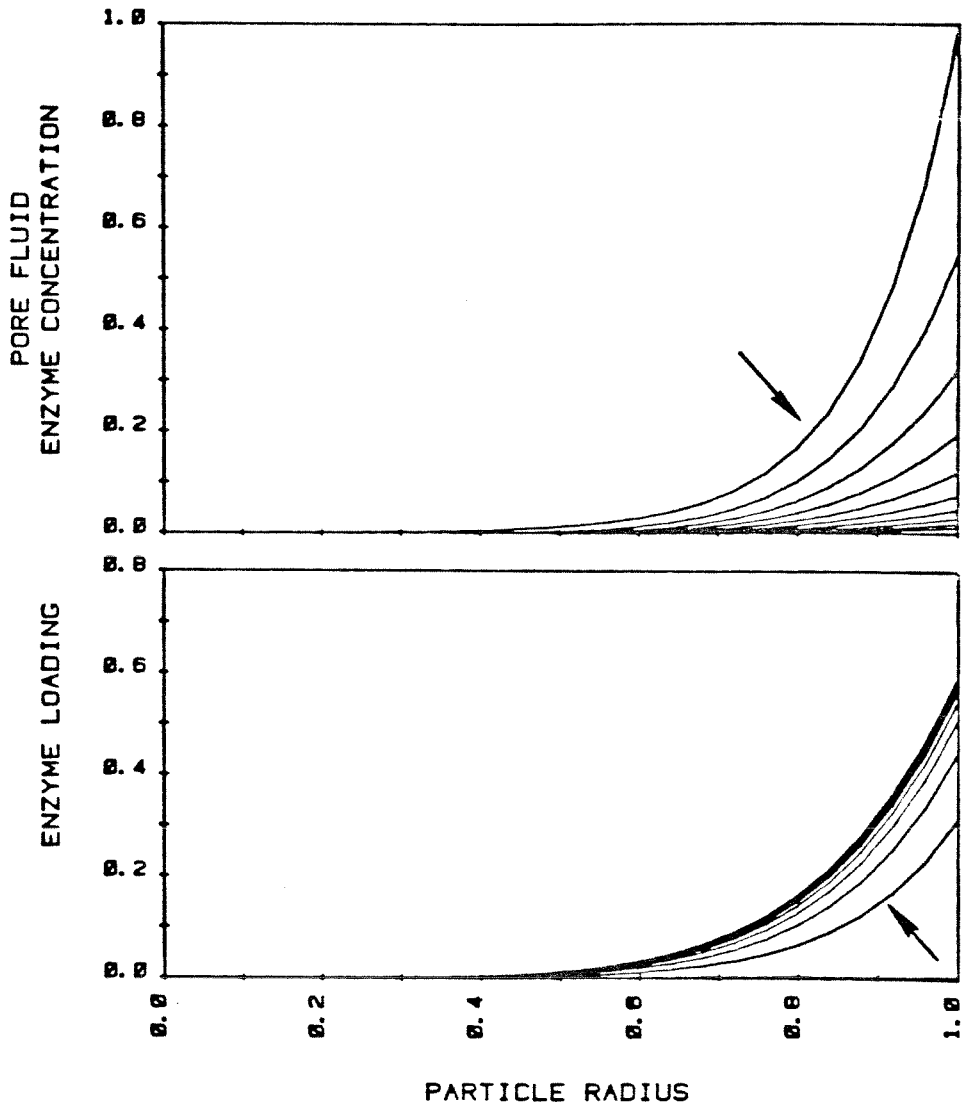
PORE FLUID
ENZYME CONCENTRATION
1.0
0.8
0.6
0.4
0.2
0.0
ENZYME LOADING
0.8
0.6
0.4
0.2
0.0
0.0
0.2
0.4
0.6
0.8
1.0
PARTICLE RADIUS

FIGURE 4

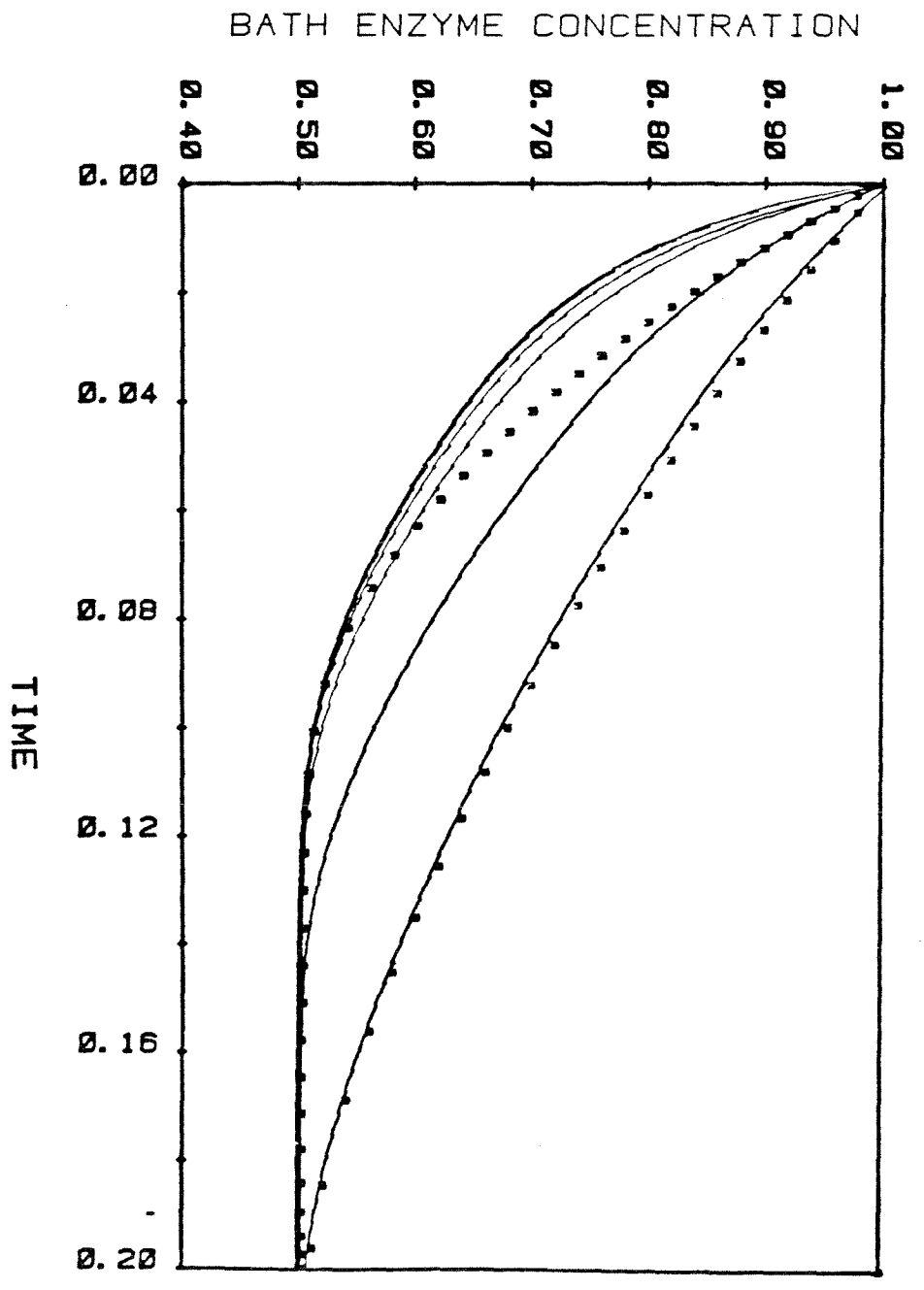
BATH ENZYME CONCENTRATION
0.40
0.50
0.60
0.70
0.80
0.90
1.00
0.00
0.04
0.08
0.12
0.16
0.20
TIME

FIGURE 5

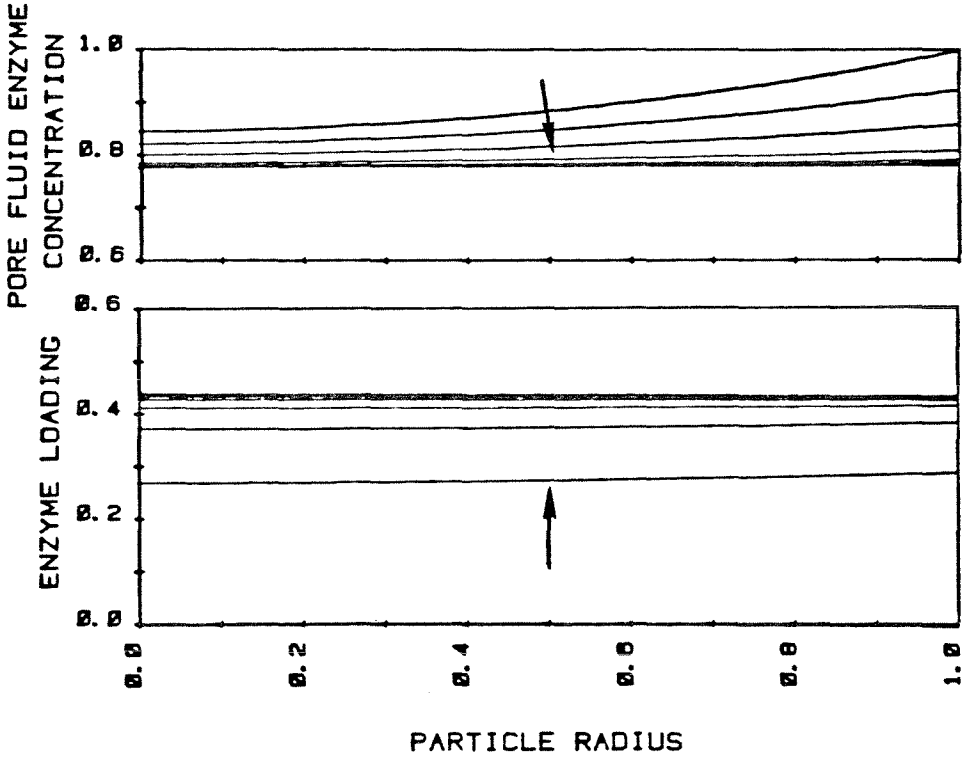
PORE FLUID ENZYME CONCENTRATION
1.0
0.8
0.6
ENZYME LOADING
0.6
0.4
0.2
0.0
0.0
0.2
0.4
0.6
0.8
1.0
PARTICLE RADIUS

FIGURE 6

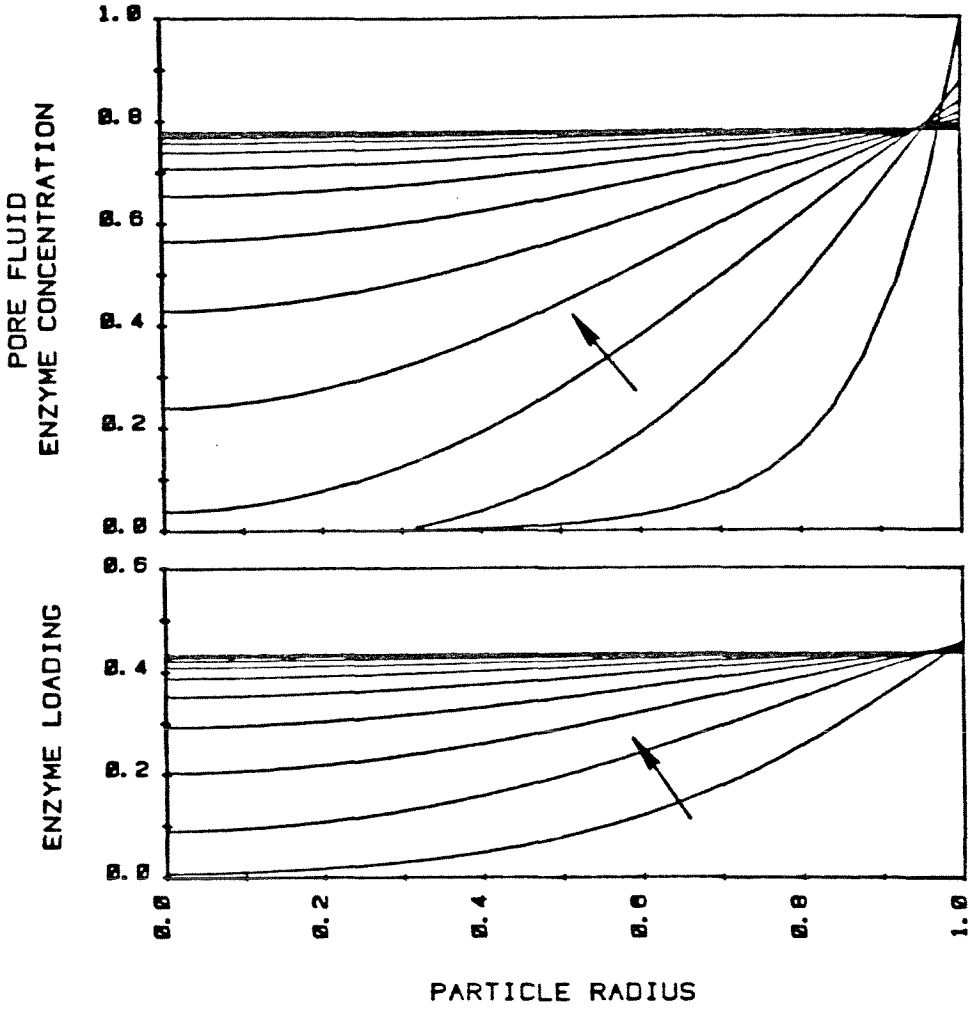
PORE FLUID
ENZYME CONCENTRATION
1.0
0.8
0.6
0.4
0.2
0.0
ENZYME LOADING
0.6
0.4
0.2
0.0
0.0
0.2
0.4
0.6
0.8
1.0
PARTICLE RADIUS

FIGURE 7

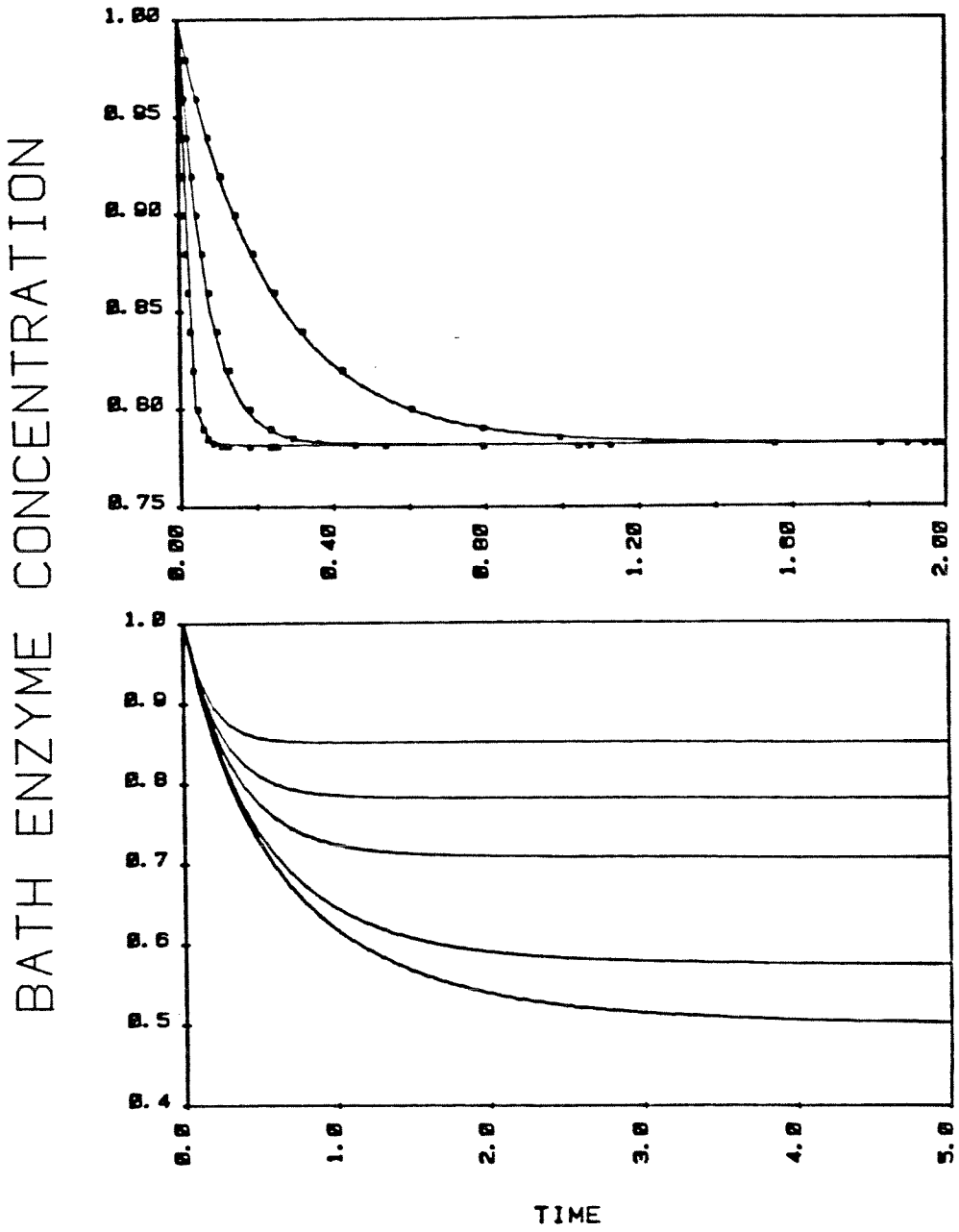
BATH ENZYME CONCENTRATION
1.00
0.95
0.90
0.85
0.80
0.75
0.00
0.40
0.80
1.20
1.60
2.00
1.0
0.9
0.8
0.7
0.6
0.5
0.4
0.0
1.0
2.0
3.0
4.0
5.0
TIME

FIGURE 8

CHAPTER 7 A MATHEMATICAL MODEL FOR RESTRICTED DIFFUSION EFFECTS ON MACROMOLECULE IMPREGNATION IN POROUS MATERIALS

INTRODUCTION

Enzymes, antibodies, antigens, and nucleic acids are commonly attached to the surfaces and internal structures of insoluble materials. In order to maximize the activity of the immobilized catalyst or sorbent per unit process volume, a high active surface area to unit volume ratio is desirable. If the catalyst or sorbent is to be continuously contacted with a fluid stream, which is commonly the desired configuration, the insoluble support materials must exceed a certain minimal size to avoid difficulties in support-effluent fluid stream separation. Then, use of a porous support is desirable to maximize active surface areas.

The catalyst or adsorbent particles may be formulated by entrapping the macromolecule of interest within a gel or polymer matrix provided the substrate or adsorbate molecules are significantly smaller than the macromolecule. This rules out, for example, use of entrapment for immobilization of enzymes which act on macromolecular substrates and for immobilization of antibodies for affinity separations of large proteins or other antigens. Further, entrapment formulations may provide relatively large diffusional resistances even in cases where the substrate/adsorbate molecule is able to permeate the support matrix.

The alternative in such situations is to impregnate the desired macromolecule within a porous solid. In such systems, the pore structure employed is a compromise among surface areas accessible to the active molecule to diffuse into the pore structure during the impregnation process, and mechanical properties of the support.

Commonly employed porous support materials include cellulose, glass, ceramics, activated carbon, agarose, Sepharose, Sephadex, and other polysaccharides. To streamline the text of the following discussion, impregnation of enzymes in porous materials will be considered; analogous treatments apply to impregnation of other macromolecules for other applications.

Several previous investigations have explored and discussed the pore size requirements for enzyme impregnation.[1,2] Recently reported experiments show a new phenomenon.[3] Enzyme initially penetrates the pore structure of the support, but, later, entry of enzyme into the support essentially stops before the particle is completely impregnated. In these cases, the immobilized enzyme is nonuniformly distributed within the porous support. All of the immobilized enzyme occupies a layer adjacent to the exterior surface of the support, with no enzyme immobilized in the central core of the particle. Understanding this phenomenon is important in practice since it is well-established that the internal distribution of supported catalyst can significantly influence its overall activity and stability.[3-5]

It has been suggested that restricted diffusion phenomena may interact with the immobilization process to cause nonuniform impregnation of enzymes in porous supports. The purpose of this paper is formulation and computer solution of a mathematical model which considers simultaneous restricted diffusion and surface binding reaction of enzyme within a porous support material. A key feature of this model is accentuation of diffusion restrictions during immobilization due to local reduction in the effective pore cross

section caused by accumulation of immobilized enzyme on the pore walls.

MATHEMATICAL MODEL

The pore structure of the support is represented in this model by a collection of parallel, nonintersecting, cylindrical pores as proposed by Wheeler.[6] The initial pore radius is R_o. However, because the effective radius of the enzyme molecules attaching to the pore walls during immobilization is frequently of the same order of magnitude as R_o, the void pore cross-sectional area and effective pore radius R decrease at a particular depth within the pore due to enzyme immobilization at that position. Figure 1 provides a conceptual view of the immobilization process within a single pore and some of the key variables and parameters of this model.

Enzyme molecules have radii (r_e) in the 50-200 Å range and are frequently impregnated in supports with pore radii (R_o) in the range of 1000 Å. When the size of the solute is not very much less than the pore size, solute diffusion is restrictred by hydrodynamic drag and by solute inaccessibility to the entire pore volume.[7-9] Analysis of diffusion under these circumstances is complicated even for the simple case of spherical particles in a straight cylindrical pore. There is no available theory which describes diffusion of nonspherical macromolecules in a complex porous structure in which reaction occurs with simultaneous change in the local voidage structure of the support material. In the absence of such theoretical guidance a simplified model based on the pore centerline restricted diffusion analysis for spheres in a cylindrical pore has been formulated. The objective of

the present model is initial assessment of the qualitative effects of coupled restricted diffusion and enzyme immobilization. Predictive simulation models for enzyme impregnation may well require a more detailed treatment of intrapellet diffusion processes.

Accordingly, the molar flow rate of enzyme in the pore in the positive z-direction, F_e, is presumed to be given by

$$F_e(z) = -A_e(z)D(z)\frac{de(z)}{dz} \quad , \tag{1}$$

where D is the restricted diffusion coefficient, e is the concentration of enzyme molecular centers in the central region of the pore occupied by those centers, and A_e is the cross-sectional area of this pore core region. A_e and D are in general functions of z because the concentration of enzyme immobilized on the pore walls, which reduces the void cross-sectional area, is a function of z.

Assuming the diffusing macromolecules are spheres of radius r_e, the void cross-sectional area at position z with local immobilized enzyme concentration $e_s(z)$ is given by

$$A(z) = A_o\left[1-4\lambda_o(1-\lambda_o)\frac{e_s(z)}{e_{sm}}\right] \quad . \tag{2}$$

where e_{sm} is the immobilized enzyme concentration at monolayer coverage. A_o $(=\pi R_o^2)$ is the initial cross-sectional area of the pore, and λ_o is the ratio of enzyme to initial pore diameter:

$$\lambda_o = \frac{r_e}{R_o} \quad . \tag{3}$$

Assuming that the void cross section is approximately circular, the local effective pore radius is given by

$$R(z) = \frac{1}{\pi}\sqrt{A(z)}, \quad . \tag{4}$$

This is of course an approximation given the potentially complicated arrangements of attached enzyme molecules around the pore periphery. Centers of the enzyme molecules cannot reach radial positions beyond $R(z) - r_e$. Consequently, the pore core area which contains enzyme molecule centers is

$$A_e(z) = A(z)\left[1 - \lambda(z)\right]^2 \tag{5}$$

where

$$\lambda(z) = r_e/R(z) \quad . \tag{6}$$

Because A_e is employed in flow rate formula (1), the so-called "partition coefficient" is included in that term. The restricted diffusion coefficient may therefore be written as the product of D_∞, the diffusion coefficient of an infinitesimal solute in the porous support, and K_r, a hydrodynamic resistance factor:

$$D(z) = D_\infty K_r\left(\lambda(z)\right) \quad . \tag{7}$$

In general K_r is an average of complicated radially varying resistances.[7-9] Here an approximation is introduced by using the centerline formula developed by Pappenheimer, Renkin, and Borrero[10]

$$K_r\left(\lambda(z)\right) = 1 - 2.1044\lambda(z) + 2.089\lambda^3(z) - 0.948\lambda^5(z) \quad . \tag{8}$$

This formula is suitable at the centerline for $\lambda < 0.4$. Its application here to evaluate the average resistance introduces some

error but is consistent with the objectives of this study. The calculations of Anderson and Quinn[7] suggest that use of Eq. (8) overestimates the restricted diffusion coefficient and thus underestimates the influence of restricted diffusion on enzyme transport into the pore.

The local rate of immobilization r_{imm} (moles enzyme/unit pore surface area/unit time) is presumed here to be proportional to the product of the local enzyme concentration in the fluid and the vacant surface area:

$$r_{imm} = k_{imm}\, e(z) \left[1 - \frac{e_s(z)}{e_{sm}} \right] \tag{9}$$

This is a reasonable kinetic form for irreversible covalent enzyme attachment. Different kinetics should be used to simulate reversible adsorptive immobilization.

Using these immobilization kinetics and the flow formula given in Eq. (1), the differential material balances on enzyme in solution and immobilized in the pore are given by

$$\frac{\partial \left[A_e \cdot e \right]}{\partial t} = \frac{\partial}{\partial z} \left[A_e \cdot D \cdot \frac{\partial e}{\partial z} \right] - 2\pi R_o\, k_{imm}\, e \left[1 - \frac{e_s}{e_{sm}} \right] \tag{10}$$

$$\frac{\partial e_s}{\partial t} = k_{imm}\, e \left[1 - \frac{e_s}{e_{sm}} \right] . \tag{11}$$

Introducing the dimensionless parameters and variables listed in the Nomenclature, these equations may be rewritten in the form

$$\frac{\partial}{\partial \tau}(g E) = \frac{\partial}{\partial x}\left(f \frac{\partial E}{\partial x}\right) - \phi^2 E\left(1 - E_s\right) \tag{12}$$

$$\frac{\partial E_s}{\partial \tau} = \psi \phi^2 E\left(1 - E_s\right) \quad . \tag{13}$$

The Thiele modulus ϕ is the ratio of characteristic immobilization rate to characteristic enzyme diffusion rate. The parameter ψ, defined by

$$\psi = \frac{e_{bo} R_o}{2 e_{sm}} \quad , \tag{14}$$

is the ratio of enzyme concentration in the immobilizing solution compared to the maximum immobilized enzyme concentration. Under conditions of practical interest, this parameter is significantly smaller than unity. This means that E_s changes on a time scale significantly longer than the time scale for E changes, suggesting that the quasi-steady state approximation may be applied to E. This may be rigorously justified under these circumstances by perturbation theory.[11]

Accordingly, for dimensionless times of order ψ and longer, the impregnation process may be adequately described by the approximate model

$$\frac{d}{dx}\left[f \frac{dE}{dx}\right] - \phi^2 E\left(1 - E_s\right) = 0 \tag{15.1}$$

$$\frac{\partial E_s}{\partial \tau} = \psi\phi^2 E\left(1 - E_s\right) \quad . \tag{15.2}$$

$$f \triangleq A_e D / A_o D_\infty \quad . \tag{15.3}$$

$$f = K_r(\lambda) \cdot (1 - \lambda)^2 \cdot \left[1 - 4\lambda_o\left(1 - \lambda_o\right) E_s\right] \tag{15.4}$$

In these calculations it will be assumed that the amount of enzyme in the immobilizing solution reservoir is much greater than the maximum immobilized enzyme content of the covered support so that the enzyme concentration e_{bo} in the fluid surrounding the support particles does not change significantly during immobilization. Assuming also that contacting between support particles and immobilizing solution provides negligible external resistance to enzyme transport to the pellet exterior,

$$e(L,t) = e_{bo} \Rightarrow E(1,\tau) = 1 \quad . \tag{16.1}$$

The other required boundary conditions derive from symmetry about the center of the particle and zero initial immobilized enzyme loading:

$$\frac{dE(0,\tau)}{dx} = 0 \tag{16.2}$$

$$E_s(x,0) = 0 \quad . \tag{17}$$

SOLUTION METHOD

The quasi-steady state approximate model was solved numerically by alternating solution of the nonlinear spatial boundary value problem posed by Eqs. (15.1), (16.1) and (16.2) with integration in time of the immobilized enzyme material balance (15.2) with initial condition (17). Using E_s given by Eq. (17), the corresponding quasi-steady state E profile was obtained by a shooting method. In this procedure, Eq. (15.1) is rewritten as an equivalent pair of first-order ordinary differential equations which are treated as an initial value problem with dE/dx at x=0 given by Eq. (16.2) and E at x=0 an assumed value. The ordinary differential equations were then integrated from x=0 to x=1 using a variable step-length Runge-Kutta algorithm which provides dependent variable values at uniformly-spaced positions internal to the [0,1] interval. The value of E at x=1 so calculated was compared with the value prescribed in Eq. (16.1), and a bisection method was applied to search for the appropriate centerline E value consistent with boundary condition (16.1).

Then, using this E profile, the E_s equations were integrated from $\tau=0$ to $\tau=\Delta\tau$ applying Euler's method. The $E_s(x,\Delta\tau)$ profile so obtained was then used in the next round of $E(x,\Delta\tau)$ calculations using the shooting method as described. The solutions for $E_s(x,\tau)$ and $E(x,\tau)$ were then advanced in time through steps of size $\Delta\tau$ by cycling through these alternating procedures. The total amount of immobilized enzyme at dimensionless time τ has been determined by evaluating the integral

$$E_{s,total}(\tau) = \int_0^1 E_s(x,\tau)\,dx \qquad (18)$$

numerically using Simpson's rule.

SIMULATION RESULTS

Each frame in Figure 2 shows immobilized enzyme profiles at different times ($E_s(x,\tau)$ versus x at different values of τ). The results in different frames correspond to different values of λ_o, the ratio of the enzyme molecule radius to the initial pore radius. Thus, the parameter λ_o characterizes the magnitude of the restricted diffusion influence, with larger λ_o values corresponding to greater diffusion restriction.

As expected, when diffusion is unrestricted ($\lambda_o = 0$; top frame in Figure 2), enzyme loading, while initially somewhat nonuniform, becomes spatially uniform at monolayer coverage as contacting time with immobilizing solution increases. However, for the restricted diffusion cases shown, the internal distribution of immobilized enzyme remains distinctly nonuniform at all times considered. Loading near the pore mouth (the catalyst particle exterior; x=1) achieves monolayer coverage, but the particle center (x=0) contains little or no immobilized enzyme.

The influence of increasing the immobilization reaction rate relative to the enzyme diffusion rate may be seen by comparing Figure 2, calculated for Thiele modulus value $\phi = 3$, and Figure 3, which shows analogous results computed for $\phi = 5$. These figures show that for each value of λ_o considered, the loading profiles of immobilized enzyme for $\phi = 5$ are steeper than the loading profiles at corresponding times for $\phi = 3$. When $\lambda_o = 0$, enzyme immobilization proceeds until the particle is saturated for $\phi = 5$ as it does for $\phi = 3$, but for the larger ϕ value immobilized enzyme is localized more toward the outer portion of the support throughout the loading

process. The same is true for the much slower penetration of the particle by enzyme observed for $\lambda_o = 0.2$. A higher Thiele modulus therefore leads to more nonuniform loading profiles of immobilized enzyme when diffusion is restricted as well as when diffusion is unrestricted, where here again the term "restricted" indicates that diffusion of unbound enzyme is influenced by the large size of the enzyme compared to the accessible cross-sectional area of the support's pores.

Figure 4 displays the calculated changes with immobilization time τ of the total amount of immobilized enzyme $E_{s,total}$ for the cases considered in Figures 2 and 3. These results show that the quantity of enzyme which can be immobilized after a given time decreases significantly as restricted diffusion effects become more pronounced. When diffusion is unrestricted i.e., when $\lambda_o = 0$, a saturating concentration of immobilized enzyme throughout the particle is established more rapidly on the same dimensionless time scale for $\phi = 5$ than for $\phi = 3$. This is not unexpected given the faster immobilization reaction rate relative to diffusion rate which prevails at the larger value of ϕ. Somewhat surprising, however, is the crossover of calculated loading trajectories that occurs with $\phi = 5$ and $\phi = 3$ for $\lambda_o = 0.2$. Here the immobilization rate determined from the slope of the loading curve is initially higher for $\phi = 5$ than for $\phi = 3$. At times greater than $\tau = 2$, however, the opposite situation occurs, at least for the calculated values included in Figure 4. This is particularly interesting considering that a similar crossover of immobilization trajectories has been reported for enzymes immobilized on porous activated carbon in a recirculation reactor.[3]

DISCUSSION

Model simulations for reasonable parameter ranges mimic well some of the phenomena observed in previous experimental studies. A large protein such as glucoamylase effectively stops impregnation of CNBr-Sepharose 6B although the internal loading is incomplete and nonuniformly distributed, while BSA, a smaller protein, impregnates the entire porous particle with an internally uniform immobilized protein distribution. Simulation results show the same trend.

Earlier impregnation models[11,12] which did not include restricted diffusion and reduction in void pore cross section could not simulate effective cessation of immobilization with nonuniform internal loading. Success of the present model in this regard derives from inclusion here of the interaction of immobilization reactions, which cause local increase in bound macromolecule concentration, and reduced enzyme flows to pore surfaces deeper in the pore. While more sophisticated descriptions of intraparticle transport may be desirable for quantitative design of supports and impregnation processes, the relatively simplified description employed here is sufficient for qualitative purposes.

Interactions of enzyme impregnation in porous supports with time-varying immobilizing solution enzyme concentrations may influence the amount and internal distribution of immobilized enzyme. Research is currently in progress on models and simulations which include this feature. Since the activities and stabilities of immobilized biomolecules depend on the quantity and the intraparticle distribution of the active immobilized species, further experimental and modeling

studies aimed at understanding, simulating, and predicting impregnation processes should contribute to improved methods and practices for biocatalyst and biosorbent manufacture.

Acknowledgement

This research was supported by the National Science Foundation.

NOMENCLATURE

A_e	cross-sectional area of pore region that contains enzyme molecule centers
A_o	initial cross-sectional area of the support's pores
D	restricted diffusion coefficient
D_∞	bulk phase diffusion coefficient
e	concentration of enzyme molecule centers in central region of pore
e_{bo}	immobilizing solution enzyme concentration at the exterior surface of the particle (time invariant)
e_s	local immobilized enzyme concentration
e_{sm}	immobilized enzyme concentration at monolayer coverage
E	dimensionless concentration of enzyme molecule centers in central region of pore (= e/e_{bo})
E_s	local immobilized enzyme dimensionless concentration (e_s/e_{sm})
$E_{s,total}$	total amount of immobilized enzyme (dimensionless), defined in Eq. (18)
f	function defined in Eq. (15.3)
F_e	molar flow rate of enzyme in z-direction of pore
g	dimensionless cross-sectional area of pore region containing enzyme centers (=A_e/A_o)
k_{imm}	rate constant for immobilization
K_r	hydrodynamic resistance factor, defined in Eq. (8)
L	pore length
r_e	radius of diffusing enzymes
R	effective pore radius
R_o	initial pore radius
x	dimensionless axial coordinate (= z/L)
z	axial coordinate

Greek symbols

λ	ratio of enzyme to effective pore diameter
λ_o	ratio of enzyme to initial pore diameter
ψ	defined in Eq. (14)
τ	dimensionless time
ϕ	Thiele modulus $\left(= L(2k_{imm}/D_\infty R_o)^{\frac{1}{2}}\right)$

REFERENCES

1. R. A. Messing, Biotechnol. Bioeng., **16**, 897 (1974).

2. R. A. Messing, in Immobilized Enzymes for Industrial Reactors, R. A. Messing, Ed. (Academic, New York, 1975), pp. 63-78.

3. K. E. Dennis, D. S. Clark, J. E. Bailey, Y. K. Cho, and Y. H. Park, Biotechnol. Bioeng., in press.

4. W. E. Corbett, Jr., and D. Luss, Chem. Eng. Sci., **29**, 1473 (1974).

5. S. H. Park, S. B. Lee, and D. D. Y. Ryu, Biotechnol. Bioeng., **23**, 2591 (1981).

6. A. Wheeler, Adv. Catalysis, **3**, 249 (1951).

7. J. L. Anderson and J. A. Quinn, Biophys. J., **14**, 130 (1974).

8. H. Brenner and P. M. Bungay, Fed. Proc., **30**, 1565 (1971).

9. H. Brenner and L. J. Gaydos, J. of Colloid and Interface Science, **58**, 312 (1977).

10. J. R. Pappenheimer, E. M. Renkin, and L. M. Borrero, Am. J. Physiol., **167**, 13 (1951).

11. D. D. Do and J. E. Bailey, Chem. Eng. Commun., **12**, 221, (1981).

12. D. D. Do, D. S. Clark and J. E. Bailey, Biotechnol. Bioeng., **24**, 1527 (1982).

FIGURE CAPTIONS

Figure 1 Schematic diagram illustrating the major features and rate processes of the single pore model of enzyme immobilization described in the text.

Figure 2 Dimensionless immobilized enzyme concentration profiles (E_s) at various dimensionless times given by $\tau = 0.80n$, $n = 1, 2, \ldots, 7$, for $\phi = 3$ and three different values of λ_o, shown at the lower right of each plot.

Figure 3 Loading profiles of dimensionless immobilized enzyme concentration E_s for $\phi = 5$, $\tau = 0.80n$, and $\lambda_o = 0.0$, $n = 1$–8 (top), and $\lambda = 0.20$, $n = 1$–4 (bottom).

Figure 4 Time dependence of $E_{s,total}$, the total amount of immobilized enzyme (dimensionless), for $\phi = 3$, $\phi = 5$, and various values of λ_o, as marked.

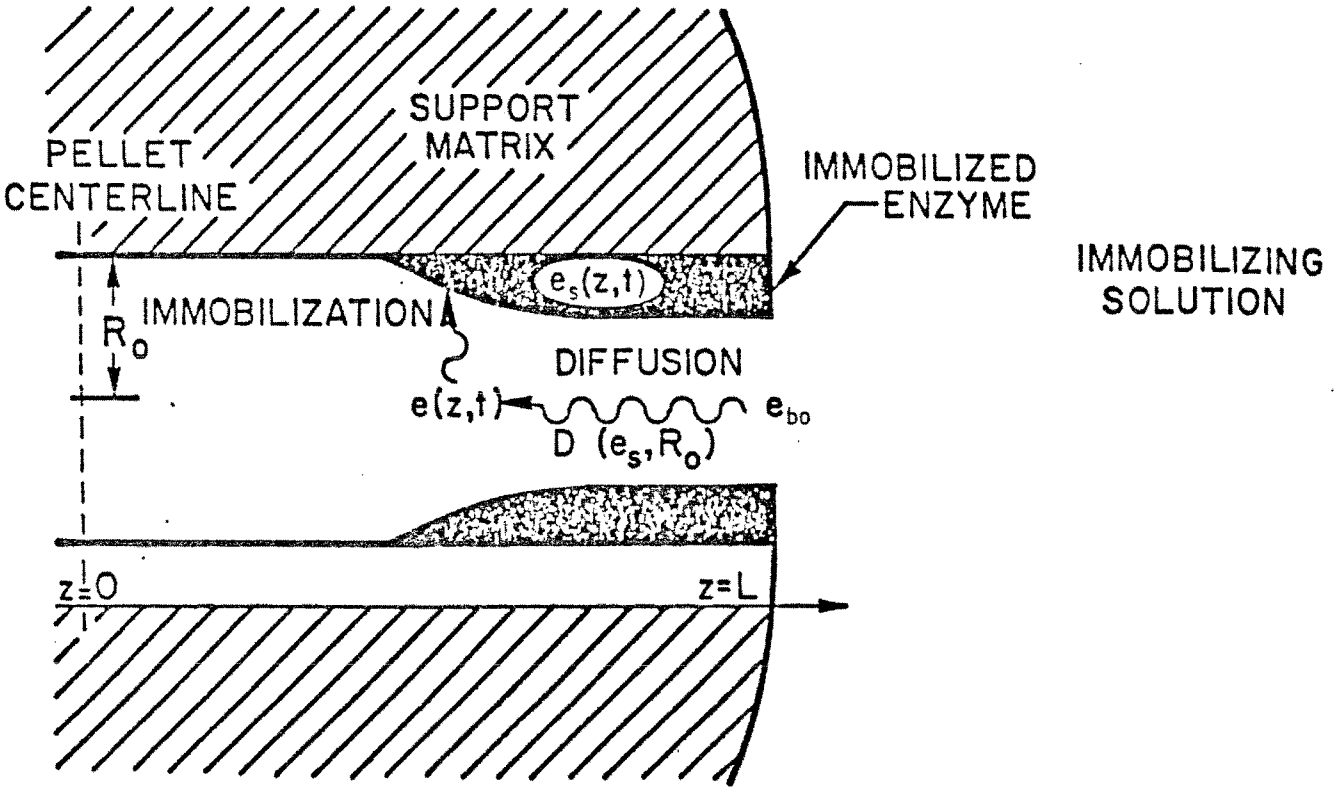
PELLET
CENTERLINE
SUPPORT
MATRIX
IMMOBILIZED
ENZYME
IMMOBILIZING
SOLUTION
$e_s(z,t)$
R_o
IMMOBILIZATION
DIFFUSION
$e(z,t)$
e_{bo}
$D\ (e_s, R_o)$
z=0
z=L

FIGURE 1

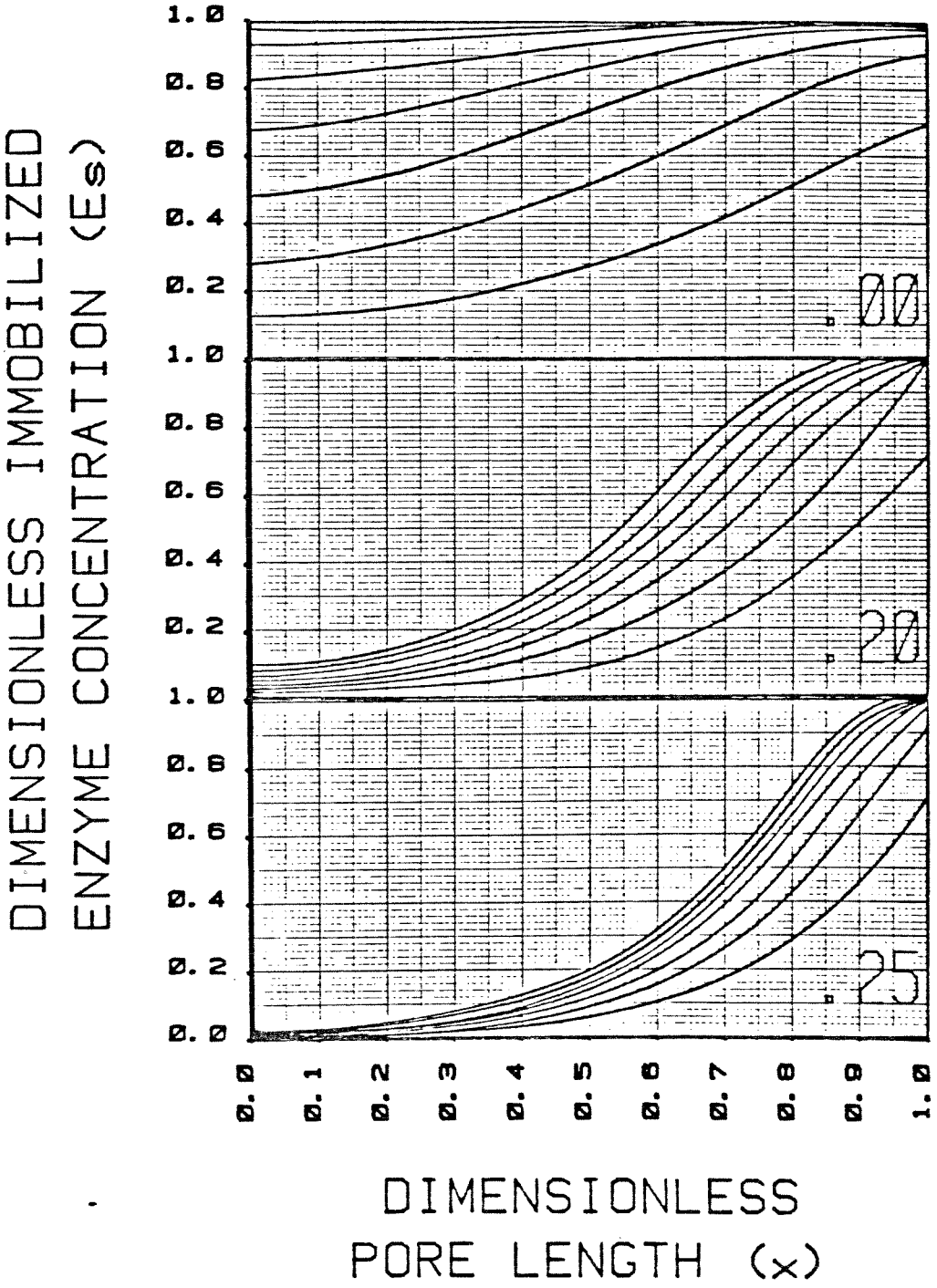
DIMENSIONLESS IMMOBILIZED ENZYME CONCENTRATION (Es)
1.0
0.8
0.6
0.4
0.2
1.0
0.8
0.6
0.4
0.2
1.0
0.8
0.6
0.4
0.2
0.0
.00
.20
.25
0.0 0.1 0.2 0.3 0.4 0.5 0.6 0.7 0.8 0.9 1.0
DIMENSIONLESS PORE LENGTH (x)

FIGURE 2

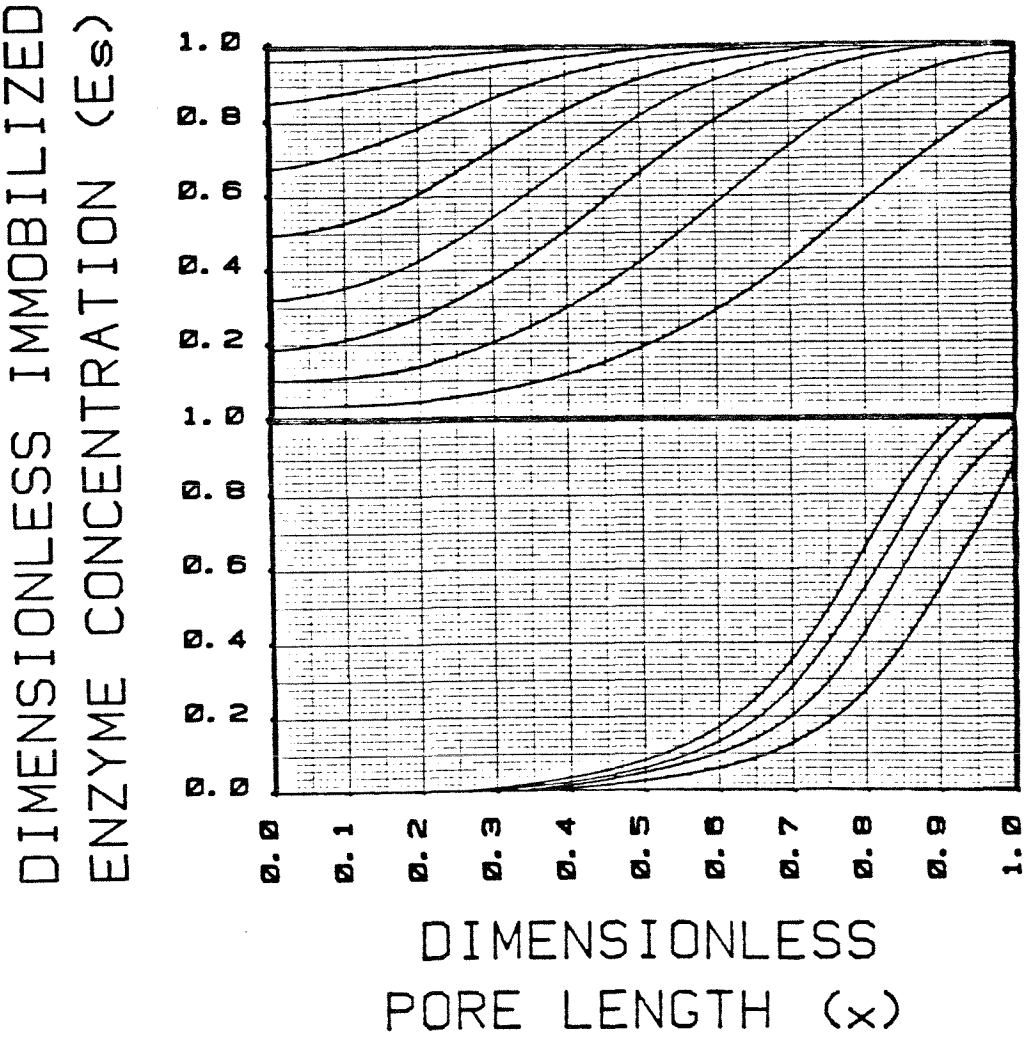
DIMENSIONLESS IMMOBILIZED ENZYME CONCENTRATION (Es)
1.0
0.8
0.6
0.4
0.2
1.0
0.8
0.6
0.4
0.2
0.0
0.0
0.1
0.2
0.3
0.4
0.5
0.6
0.7
0.8
0.9
1.0
DIMENSIONLESS PORE LENGTH (x)

FIGURE 3

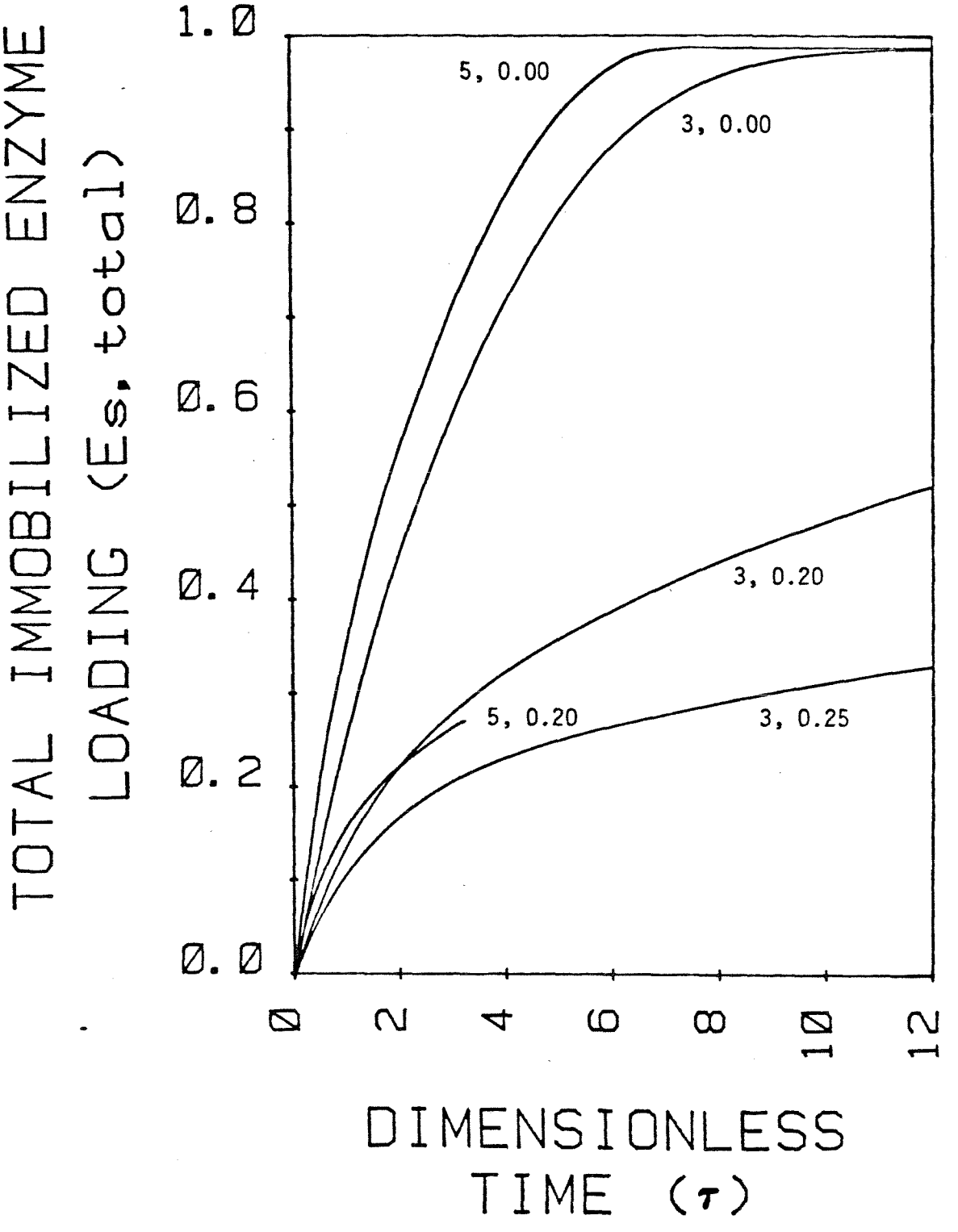
TOTAL IMMOBILIZED ENZYME LOADING (Es, total)
1.0
0.8
0.6
0.4
0.2
0.0
5, 0.00
3, 0.00
3, 0.20
5, 0.20
3, 0.25
0
2
4
6
8
10
12
DIMENSIONLESS TIME (τ)

FIGURE 4

CONCLUDING DISCUSSION

Several important conclusions concerning the preparation and properties of immobilized α-chymotrypsin can be drawn from this research. Before focusing on these, however, it is appropriate to emphasize an important consideration that was recognized early in this study: the vast complexity of immobilized enzyme systems practically ensures that several measurements using a variety of physiochemical methods are required to obtain significant understanding of immobilized enzyme behavior. The approaches taken by many investigators often oversimplify the phenomena under study and are consequently inadequate. For example, it is not uncommon to immobilize an enzyme and then measure the catalyst's activity under conditions where it is unclear how much enzyme is active and accessible to substrate, whether substrate partitioning by the support matrix is occurring, if internal or external diffusion effects are significant, and so forth. Results obtained in this fashion are often so confusing and so misleading it is doubtful they are useful at all. Care has been taken here to avoid such pitfalls, and, as a result, unparalleled insights into immobilized enzyme behavior have been obtained. This in itself is a significant conclusion of this research.

More specific conclusions can be summarized as follows:

* Polymeric conjugates consisting of polyacrolein particles (20-30 nm O.D.) radiation-grafted to larger polymethylmethacrylate microspheres (1.2 or 6.5 μm O.D.) serve as adequate supports for α-

chymotrypsin immobilization, and presumably for other enzymes as well.

* Magnetic microspheres of polystyrene polymerized with magnetite (10 μm O.D.) strongly adsorb α-chymotrypsin. Pretreatment of this material with polyacrolein microparticles produces very small loading enhancement and increases diffusional resistance.

* A mathematical description of simultaneous reaction and diffusion within a spherical immobilized enzyme catalyst accurately interprets the measured reaction rates of α-CT-CNBr Sepharose 4B conjugates.

* The specific activity of α-chymotrypsin immobilized on CNBr-activated Sepharose 4B decreases with increasing enzyme loading.

* α-Chymotrypsin immobilized using a six-carbon spacer arm exhibits greater specific activity than directly coupled enzyme.

* The observed activity changes of α-chymotrypsin due to immobilization are accompanied by active site structural alterations revealed by EPR spectroscopy. Specifically, the mobility of attached spin label becomes more restricted as the specific activity decreases.

* The existence of two subpopulations of immobilized α-chymotrypsin on CNBr-Sepharose 4B has been indicated by two different spin labels. EPR measurements in the presence of indole in conjunction with activity assays and active site titrations reveal that the two subpopulations of immobilized chymotrypsin have specific activities that differ by a factor of fifteen.

* The relative amounts of each enzyme subpopulation vary with the active enzyme loading. As more enzyme is immobilized, the relative amount of the less active subpopulation increases.

* Immobilization to CNBr-Sepharose 4B significantly improves the stability of α-chymotrypsin in high concentrations of n-propanol and t-butanol.

* Deactivation of immobilized α-chymotrypsin in solutions of aliphatic alcohols differs significantly from first-order. In 50% n-propanol, the first 120 minutes of immobilized chymotrypsin deactivation can be described fairly well by Nth-order kinetics, N = 3.23.

* Deactivation in aliphatic alcohols of immobilized α-chymotrypsin is accompanied by severe structural distortion of the active site that follows similar kinetics as the loss of active enzyme.

* The specific activity of active immobilized chymotrypsin increases slightly with increasing exposure to 50% n-propanol. This counterintuitive phenomenon is due to a redistribution of active immobilized enzyme subpopulations favoring the more active form. Data are only available for contact times of 120 minutes or less.

* A mathematical model of enzyme immobilization in porous supports predicts that nonuniform loading of immobilized enzyme will occur under certain conditions. The distribution of enzyme within the support matrix can influence the overall activity and stability of an immobilized enzyme catalyst.

* Computer simulation of enzyme immobilization in porous materials indicates that accumulation of immobilized enzyme in the support's pores, and restricted diffusion of unattached enzyme, can combine to reduce significantly the overall rate of immobilization and result in nonuniform loading profiles of enzyme through the support.

Many of the above findings can serve as starting points for further research. Particularly interesting is the heterogeneity of immobilized α-chymotrypsin molecules revealed directly by EPR spectroscopy. Possible causes for the occurrence of multiple enzyme subpopulations will most likely be elucidated by direct efforts to influence or control the distribution of enzyme forms on various supports. Using CNBr-Sepharose 4B as one model system, possible experiments along these lines include immobilizing enzyme in the presence of small and large inhibitors to better preserve the enzyme's active site conformation and limit the orientations that enzyme can assume on the support surface, and performing the immobilization reaction at low temperatures for short times to determine if one enzyme subpopulation results before the other and can be isolated in its pure form. In addition, better characterization of the support material, which may possess heterogeneous binding sites and/or local microstructures, can be obtained by titrating the reactive surface groups (see reference 14, Chapter 3) or by spin labeling the support directly (see reference 15, Chapter 3). These experiments should improve understanding of how and why immobilization affects the properties and constitution of enzyme molecules that exist in solution as a homogeneous population. This information will lead to greater

precision and versatility in the formulation and utilization of immobilized enzyme catalysts.

Finally, the enormous contributions that EPR spectroscopy has made to his research should again be emphasized. No other single technique has provided as much information at the molecular level about the structure and function of an immobilized enzyme system. It is therefore anticipated that EPR spectroscopy will play an expanded role in future studies of immobilized enzymes, especially as greater emphasis is placed on enlarging the range of enzyme systems suitable for study by EPR techniques. At present, active site directed spin labels such as those used in this study are available only for serine proteases and enzymes that contain sulfhydryl or methionyl groups in or around their active sites. Further research is needed to develop spin labels for enzymes beyond these relatively limited categories, and to develop more general and versatile methods for labeling enzyme active sites. Future studies directed toward these objectives are strongly recommended.

APPENDIX

The following is a double precision Fortran program, RESDIF, that solves the mathematical model of enzyme immobilization presented in Chapter 7.

```
      PROGRAM RESDIF

C     THIS IS A DOUBLE PRECISION PROGRAM TO SIMULATE ENZYME IM-
C     MOBILIZATION IN A POROUS PARTICLE. THE IMMOBILIZED ENZYME
C     MATERIAL BALANCE IS INTEGRATED IN INCREMENTS OF DTAU BY
C     EULER'S APPROXIMATION. THE QUASI-STEADY STATE MASS BAL-
C     ANCE FOR THE CONCENTRATION OF ENZYME MOLECULE CENTERS IN
C     THE SUPPORT'S PORES IS THEN SOLVED BY A SHOOTING METHOD
C     FOR EACH VALUE OF THE IMMOBILIZED ENZYME CONCENTRATION.
C     FOR FURTHER DETAILS OF THIS SOLUTION METHOD, SEE D.S.
C     CLARK, J.E. BAILEY, AND D.C. DC, "A MATHEMATICAL MODEL
C     FOR RESTRICTED DIFFUSION EFFECTS ON MACROMOLECULE IM-
C     PREGNATION IN POROUS MATERIALS", BIOTECHNOL. BIOENG.,
C     SUBMITTED (1983). THE PRIMARY FEATURES OF THIS SINGLE
C     PORE MODEL ARE: FIRST ORDER, IRREVERSIBLE REACTION KINETICS
C     BETWEEN ENZYME AND SUPPORT; RESTRICTED DIFFUSION OF ENZYME
C     THROUGH THE SUPPORT - RENKIN'S EQUATION IS USED TO RELATE
C     THE EFFECTIVE DIFFUSIVITY OF ENZYME TO LAMBDA ZERO, THE
C     RATIO OF THE ENZYME RADIUS TO THE INITIAL PORE RADIUS;
C     LINEAR DEPENDENCE BETWEEN THE AVAILABLE CROSS-SECTIONAL
C     AREA OF THE PORE (AREA) AND MONOLAYER COVERAGE OF ENZYME
C     ON THE INTERNAL SURFACE OF THE PORE.


      IMPLICIT DOUBLE PRECISION (A-H,O-Z)
      REAL*8 LAM,LAMB

      DIMENSION E(100),ES(100),YDOT(2),Y(2),
     $ EX(11),S(50),BOUND(50),YC(2),YEND(100),
     $ SES(100),DES(100),LAMB(100),AREA(100),
     $ DEFF(100),DLAM(100),DOT(100),RENK(100),
     $ DREAK(100)


      COMMON F,ES,THIELE,PSI,EN,TAU,DTAU,KI,M,SES,
     $ DES,LAM,LAMB,AREA,CAREA,DEFF,DOT,RENK,DLAM
      COMMON /EPCOM9/ NUSED,NCUSED,NSTEP,NFE,NJE

      DATA EX/0.0,0.1,0.2,0.3,0.4,0.5,0.6,0.7,0.8,0.9,1.0/

C     SPECIFY INPUT DATA:
C     THIELE = THIELE MODULUS OF IMMOBILIZATION REACTION,
C     PSI = RATIO OF ENZYME CONCENTRATION IN IMMOBILIZING
C     SOLUTION TO MAXIMUM IMMOBILIZED ENZYME CONCENTRATION,
C     DTAU = STEPSIZE OF DISCRETIZED DIMENSIONLESS TIME
C     FOR EULER'S APPROXIMATION,
C     TAUMAX = MAXIMUM TIME OF THE IMMOBILIZATION REACTION,
C     LAM = LAMBDA ZERO, THE RATIO OF ENZYME RADIUS TO THE
C     INITIAL PORE RADIUS.

      THIELE = 5.0D0
      PSI = 0.1D0
      DTAU = 0.02D0
      TAUMAX = 15.0D0
      LAM=0.25D0

      DAREA=(-4.0D0*LAM*(1.0D0-LAM))

C     INITIALIZE IMMOBILIZED ENZYME CONCENTRATION THROUGHOUT
C     100 GRID POINTS IN PARTICLE, AND SELECT INITIAL GUESS,
C     YC(1), FOR THE PORE ENZYME CONCENTRATION AT THE CENTER
C     OF THE PARTICLE.

      DO 5 J=1,100
    5 ES(J) = 0.0D0
      N=2
      YC(1) = 0.05D0

C     INTRODUCE THE FOLLOWING COUNTING INDECES:
C     M - SERVES AS A COUNTER TO INDICATE A) IF
C     THE OUTER BOUNDARY VALUE HAS BEEN CALCULATED AT LEAST
C     TWICE, AND B) HOW MANY BISECTIONS HAVE BEEN MADE;
C     NN - AN INDEX TO INDICATE IF TWO CONSECUTIVE CALCU-
C     LATED OUTER BOUNDARY VALUES LIE ON OPPOSITE SIDES
C     OF 1.0. IF SO ( E.G. NN > 0, SEE LINE 72 ) THEN THE
C     BISECTION METHOD IS INITIATED TO DETERMINE A NEW IN-
C     ITIAL GUESS FOR THE CENTERLINE BOUNDARY VALUE.

C     SET THE FIRST DERIVATIVE OF THE ENZYME LOADING PROFILE
C     AT THE CENTER OF THE PARTICLE, YC(2), EQUAL TO ZERO.

      IF (TAU .EQ. 0.0D0) GO TO 30
   29 YC(1) = S(M)
      M = 0
```

```
      NN=0
 30   TO = 0.0D0
      YO(2) = 0.0D0

      M = M+1
      S(M) = YO(1)

      EPS = 0.0001D0
      HO = 0.0000D0
      MF = 22
      INDEX = 1
      IERROR=1

      IF (M .GT. 1) GO TO 33

C     SOLVE THE MASS BALANCE FOR THE IMMOBILIZED ENZYME CON-
C     CENTRATION, ES, USING EULER'S APPROXIMATION AND DISCRETIZED
C     TIME ELEMENT DTAU, AND DEFINE THE PARAMETERS THAT FOLLOW.

      DO 9 K=1,100
      ES(K)=ES(K)+(DTAU*PSI*(THIELE**2.0D0))*E(K)
     $ *(1.0D0-ES(K))
      DES(K)=(1.0D0-LAM/DSQRT(1.0D0-4.0D0*LAM*
     $ (1.0D0-LAM)*ES(K)))

      LAMB(K)=1.0D0-DES(K)

      AREA(K)=1.0D0-4.0D0*LAM*(1.0D0-LAM)*ES(K)

      DLAM(K)=DSQRT(1.0D0-4.0D0*LAM*(1.0D0-LAM)*ES(K))

      DERF(K)=(2.0D0*(1.0D0-
     $ LAM)*(LAM**2.0D0))/(DLAM(K)**3.0D0)

      DRENK(K)=-2.1044D0*6.267D0*(LAMB(K)**2.0D0)
     $ -4.74D0*(LAMB(K)**4.0D0)

      RENK(K)=1.0D0-2.1044D0*LAMB(K)+2.089D0*
     $ (LAMB(K)**3.0D0)-0.948D0*(LAMB(K)**5.0D0)

      DDT(K)=((DES(K)**2.0D0)*DRENK(K)-2.0D0*
     $ DES(K)*RENK(K))

C     DIVIDE THE PARTICLE INTO INCREMENTS OF 0.01, AND USE
C     FINITE DIFFERENCES TO CALCULATE SES, THE DERIVATIVE OF
C     THE IMMOBILIZED ENZYME PROFILE AT EACH INTEGRATION ENDPOINT.

   9  XEND(K)=DFLOAT(K)/100.0D0

      SES(1)=(ES(2)-ES(1))/(XEND(2)-XEND(1))
      DO 11 K=2,99

  11  SES(K)=(ES(K+1)-ES(K-1))/(XEND(K+1)-XEND(K-1))

      SES(100)=(ES(100)-ES(99))/(XEND(100)-XEND(99))

 33   DO 10 K=1,100
      KI=K

C     SET ENDPOINTS (TOUT) FOR RUNGE KUTTA NUMERICAL INTEGRATION OF
C     QUASI-STEADY STATE MASS BALANCE OF E, THE ENZYME CONCENTRATION
C     IN PARTICLE'S PORES. CALL DRIVE, A ROUTINE WITHIN THE
C     PROGRAM "EPISODE". EPISODE IS A DIFFERENTIAL EQUATION
C     SOLVING PROGRAM PACKAGE THAT MUST BE LINKED WITH RESDIF
C     TO CREATE A FUNCTIONAL PROGRAM (I.E. THE EXECUTE FILE
C     RESDIF.EXE).

      TOUT = (DFLOAT(K))/100.0D0
      CALL DRIVE(N,TO,HO,YO,TOUT,EPS,IERROR,MF,INDEX)

  10  E(K) = YO(1)

C     THE FOLLOWING SECTION USES THE BISECTION METHOD TO CHOOSE
C     CENTERLINE ENZYME CONCENTRATION THAT RESULTS IN AN ENZYME
C     CONCENTRATION AT THE SURFACE OF THE PARTICLE OF 1.0 +/- 0.01.

      BOUND(M) = YO(1)-1.0D0
      ABOUND = DABS(BOUND(M))

      IF (ABOUND .LT. 0.01D0) GO TO 25
      IF (M .GT. 50) GO TO 25

      IF (NN .GT. 0) GO TO 88
```

```
      IF (M .GT. 1) GO TO 190
   70 IF (YO(1)-1.0D0) 24,25,26
C     INCREASE INITIAL GUESS FOR CENTERLINE BOUNDARY VALUE, IF
C     NECESSARY (THIS IS DONE ONLY IF NN = 0).
   24 YO(1) = S(M) + 0.1D0

      GO TO 30
C     DECREASE INTIAL GUESS FOR CENTERLINE BOUNDARY VALUE, IF
C     NECESSARY (THIS IS DONE ONLY IF NN = 0).
   26 YO(1) = S(M) - 0.1D0

      GO TO 30
C     CHECK TO SEE IF LAST TWO CALCULATED OUTER BOUNDARY VALUES
C     LIE ON OPPOSITE SIDES OF 1.0. IF SO, INITIATE BISECTION
C     METHOD.
  190 IF (BOUND(M)*BOUND(M-1)) 72,25,70
   72 NN=NN+1
      A=BOUND(M)
      B=BOUND(M-1)
      AS=S(M)
      BS=S(M-1)
      YO(1)=(AS+BS)/2.0D0

      GO TO 30

   88 IF (BOUND(M)*A) 80,25,90
   80 B=BOUND(M)
      BS=S(M)
      YO(1)=(AS+BS)/2.0D0

      GO TO 30

   90 A=BOUND(M)
      AS=S(M)
      YO(1)=(AS+BS)/2.0D0

      GO TO 30
C     RETURN TO 30 TO RECALCULATE EXTERNAL ENZYME CONCENTRATION USING
C     NEW VALUE OF CENTERLINE ENZYME CONCENTRATION, YO(1). THIS PRO-
C     CESS IS REPEATED UNTIL ACCUPACY CRITERION OF 0.01 IS MET.

C     USE SIMPSON'S RULE TO CALCULATE EST, THE TOTAL AMOUNT OF ENZYME
C     IMMOBILIZED IN THE PORE.
   25 SUM=0.0D0
      SUM1=0.0D0

      DO 200 K=2,98,2
  200 SUM=SUM+(4.0D0*ES(K))

      DO 250 K=3,99,2
  250 SUM1=SUM1+(2.0D0*ES(K))

      EST=(0.01D0/3.0D0)*(ES(1)+SUM+SUM1+ES(100))

      RATE=(EST-REST)/DTAU

      REST=EST

      IF (TAU .EQ. 0.0D0) GO TO 39

      IF (MN .NE. 20) GO TO 55
```

```
      IF (TAU. NE. 0.0D0) GO TO 40

   39 WRITE (6,300) THIELE,LAM,DTAU
  300 FORMAT (3X,'THE THIELE MODULUS IS:',1X,F3.1,2X,
     $ 'LAMDA ZERO IS:',1X,F4.2,1X,'DTAU IS:',
     $ 1X,F5.3,/)

      WRITE (6,45) (EX(I), I=2,11)
   45 FORMAT (3X,4HTIME,2X,10(F6.3),2X,7HLOADING,/)


   40 WRITE (6,50) TAU,(E(I), I=10,100,10),EST
      WRITE (6,51) (ES(I), I=10,100,10)
      WRITE (6,52) RATE


   50 FORMAT (2X,F5.2,1X,10(F6.3),3X,F5.3,/)
   51 FORMAT (9X,10(F6.3),/)
   52 FORMAT (10X,'THE REACTION RATE IS:',1X,F5.3,//)
      MN=0

   55 TAU=TAU+DTAU
C     WRITE(6,70) NSTEP,NFE,NJE
C  70 FORMAT(//21H PROBLEM COMPLETED IN,I5,6H STEPS/
C     $       21X,I5,14H F EVALUATIONS/
C     $       21X,I5,14H J EVALUATIONS//)

C     WRITE (6,71) INDEX,HUSED,NQUSED
C  71 FORMAT(//,'THE VALUE OF INDEX IS:',1X,I3,/,
C     $        'THE LAST STEP SIZE USED WAS:',E7.5,/,
C     $        'THE ORDER LAST USED WAS:',I5//)


      MN=MN+1

      IF (EST .EQ. 0.000) RATE=1.000
      IF (RATE .LT. 0.0000100) GO TO 888

      IF (TAU .LE. TAUMAX) GO TO 29
  888 STOP



  666 WRITE (6,901)
  901 FORMAT (3X,'SECANT METHOD FAILED TO CONVERGE FOR B.C.')
      STOP
      END

C     DEFINE SUBROUTINE DIFFUN TO CONTAIN THE MASS BALANCE EQUATION
C     FOR E, THE ENZYME CONCENTRATION WITHIN THE PORE.

      SUBROUTINE DIFFUN(N,T,Y,YDOT)

      IMPLICIT DOUBLE PRECISION (A-H,O-Z)
      REAL*8 LAM,LAMB

      DIMENSION E(100),ES(100),YDOT(2),Y(2),EX(11),
     $ S(50),BOUND(50),YS(2),XEND(100),SES(100),DES(100),
     $ LAMB(100),AREA(100),DEFF(100),DLAM(100),DOT(100),
     $ RENK(100),DRENK(100)

      COMMON E,ES,THIELE,PSI,EN,TAU,DTAU,KI,P,SES,DES,
     $ LAM,LAMB,AREA,DAREA,DEFF,DOT,RENK,DLAM




      YDOT(1)=Y(2)

      IF (ES(KI) .EQ. 0.000) GO TO 105

      YDOT(2)=(1.000/((DES(KI)**2.000*RENK(KI))*AREA(KI)))*
     $ (-Y(2)*SES(KI)*(AREA(KI)*DEFF(KI)*DOT(KI)+(DES(KI)
     $ **2.000)*RENK(KI)*DAREA)
     $ +(THIELE**2.000)*(1.000-ES(KI))
     $ *Y(1))
```

```
      GO TO 106

105   YDOT(2)=((THIELE**2.0D0)*(1.0D0-ES(KI))*Y(1))
     $ /(((1.0D0-LAM)**2.0D0)*(1.0D0-2.1644D0*LAM+
     $ 2.0D0*(LAM**3.0D0)-0.94D0*(LAM**5.0D0)))

106   RETURN
      END


      SUBROUTINE FEDERV(N,T,Y,PD,NC)
      IMPLICIT DOUBLE PRECISION (A-H,O-Z)

      RETURN
      END
```